AD-A121 076 MODELING OF HUMAN JOINT STRUCTURES(U) OHIO STATE UNIV 1/2
COLUMBUS DEPT OF ENGINEERING MECHANICS
A E ENGIN ET AL. SEP 82 AFAMRL-TR-81-117
UNCLASSIFIED F33615-78-C-0510 F/G 6/19 NL

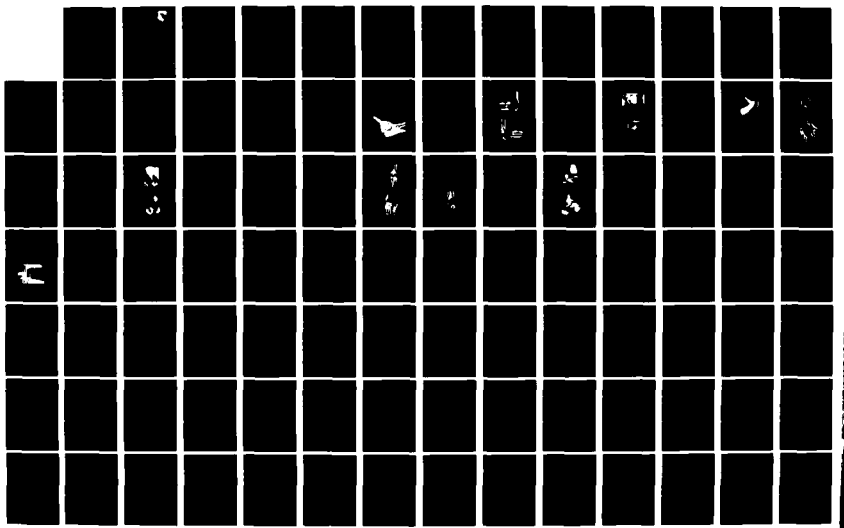

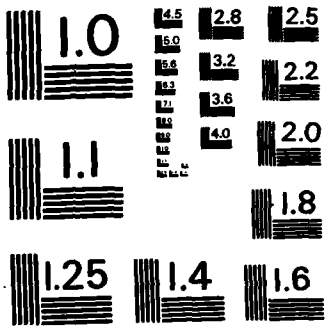

AFAMRL-TR-81-117

MODELING OF HUMAN JOINT STRUCTURES

ALI ERKAN ENGIN
MANSSOUR H. MOEINZADEH

THE OHIO STATE UNIVERSITY
COLUMBUS, OHIO 43210

SEPTEMBER 1982

Approved for public release; distribution unlimited.

AIR FORCE AEROSPACE MEDICAL RESEARCH LABORATORY
AEROSPACE MEDICAL DIVISION
AIR FORCE SYSTEMS COMMAND
WRIGHT-PATTERSON AIR FORCE BASE, OHIO 45433

NOTICES

When US Government drawings, specifications, or other data are used for any purpose other than a definitely related Government procurement operation, the Government thereby incurs no responsibility nor any obligation whatsoever, and the fact that the Government may have formulated, furnished, or in any way supplied the said drawings, specifications, or other data, is not to be regarded by implication or otherwise, as in any manner licensing the holder or any other person or corporation, or conveying any rights or permission to manufacture, use, or sell any patented invention that may in any way be related thereto.

Please do not request copies of this report from Air Force Aerospace Medical Research Laboratory. Additional copies may be purchased from:

National Technical Information Service
5285 Port Royal Road
Springfield, Virginia 22161

Federal Government agencies and their contractors registered with Defense Technical Information Center should direct requests for copies of this report to:

Defense Technical Information Center
Cameron Station
Alexandria, Virginia 22314

TECHNICAL REVIEW AND APPROVAL

AFAMRL-TR-81-117

This report has been reviewed by the Office of Public Affairs (PA) and is releasable to the National Technical Information Service (NTIS). At NTIS, it will be available to the general public, including foreign nations.

This technical report has been reviewed and is approved for publication.

FOR THE COMMANDER

Henning E. von Gierke

HENNING E. VON GIERKE, Dr Ing
Director
Biodynamics and Bioengineering Division
Air Force Aerospace Medical Research Laboratory

SECURITY CLASSIFICATION OF THIS PAGE *(When Data Entered)*

REPORT DOCUMENTATION PAGE		READ INSTRUCTIONS BEFORE COMPLETING FORM
1. REPORT NUMBER AFAMRL-TR-81-117	2. GOVT ACCESSION NO. A121076	3. RECIPIENT'S CATALOG NUMBER
4. TITLE *(and Subtitle)* MODELING OF HUMAN JOINT STRUCTURES		5. TYPE OF REPORT & PERIOD COVERED FINAL REPORT January 1978 - June 1981
		6. PERFORMING ORG. REPORT NUMBER
7. AUTHOR(s) Ali Erkan Engin Manssour H. Moeinzadeh		8. CONTRACT OR GRANT NUMBER(s) F33615-78-C-0510
9. PERFORMING ORGANIZATION NAME AND ADDRESS Department of Engineering Mechanics The Ohio State University Columbus, Ohio 43210		10. PROGRAM ELEMENT, PROJECT, TASK AREA & WORK UNIT NUMBERS 61102F; 2312-V3-06
11. CONTROLLING OFFICE NAME AND ADDRESS Air Force Aerospace Medical Research Laboratory, Aerospace Medical Div, Air Force Systems Command Wright-Patterson Air Force Base, OH 45433		12. REPORT DATE SEPTEMBER 1982 13. NUMBER OF PAGES 180
14. MONITORING AGENCY NAME & ADDRESS *(if different from Controlling Office)*		15. SECURITY CLASS. *(of this report)* UNCLASSIFIED 15a. DECLASSIFICATION/DOWNGRADING SCHEDULE

16. DISTRIBUTION STATEMENT *(of this Report)*

Approved for public release; distribution unlimited.

17. DISTRIBUTION STATEMENT *(of the abstract entered in Block 20, if different from Report)*

18. SUPPLEMENTARY NOTES

19. KEY WORDS *(Continue on reverse side if necessary and identify by block number)*

Biomechanics, elbow joint, knee joint, human joints, shoulder joint, ankle joint, joint models, hip joint, ligaments.

20. ABSTRACT *(Continue on reverse side if necessary and identify by block number)*

Dynamic simulation of the response of the total human body to external forces provides essential information for prediction of injury and subsequent design and development of crash protection systems.

[Continued on Reverse]

DD FORM 1 JAN 73 1473 EDITION OF 1 NOV 65 IS OBSOLETE

SECURITY CLASSIFICATION OF THIS PAGE *(When Data Entered)*

20. ABSTRACT (Continued)

The most sophisticated versions of the total-human-body models used for such simulations are articulated, multisegmented models which simulate the dynamics of all the major articulating joints and segments of the human body. The effectiveness of these multisegmented models to accurately predict live human response depends heavily on the proper biomechanical description and simulation of the articulating joints. The research program presented in this report is concerned with mathematical modeling of an articulating joint defined by the joint contact surfaces of two body segments and the joint ligaments.

A rather extended discussion of the articulations and anatomical descriptions of the elbow, shoulder, hip, knee and ankle joints are first presented, with special emphasis on the location and functional aspects of the major ligaments of each joint. This is followed by a description of the articulating surfaces and the development of a measurement technique for the determination of articulating surface equations for the elbow, hip, knee and ankle joints. Next, a constitutive equation representing ligament characteristics and behavior is presented and the attachment sites of the ligaments of the elbow, hip, knee and ankle joints are provided.

General two- and three-dimensional mathematical dynamic models of an articulating joint are then developed to determine the nature of motions and forces between two body segments. The governing equations for these models are a set of highly nonlinear equations and their numerical solutions are discussed in some detail. This is followed by a specific application to a two-dimensional dynamic model of the human knee joint. The numerical results from this model are presented to illustrate the effects of duration and shape of the dynamically applied loads on the response of the joint. Special attention has been given to the ligament and contact forces, the location of contact points, anterior-posterior displacements and the comparison between the internal and the external energy of the system. The results are compared with experimental data from the literature and the validity of the model is established.

PREFACE

The research work described in this report was performed for the Mathematics and Analysis Branch of the Aerospace Medical Research Laboratory at Wright-Patterson Air Force Base under Contract No. F33615-78-C-0510. The research was monitored by Mr. Ints Kaleps, the Chief of the Mathematics and Analysis Branch, and it was administered by the Ohio State University Research Foundation under Project No. 710961/784394.

The authors gratefully acknowledge the assistance provided by Dr. Nuri Akkaş of the Middle East Technical University, Ankara, Turkey. Dr. Akkaş served as a consultant on the numerical solution phase of the research program while he was in the U.S.A. as a visiting Fulbright Scholar.

The able assistance provided by the graduate research associates James L. Fry and Richard D. Peindl on various aspects of the research is also acknowledged by the authors.

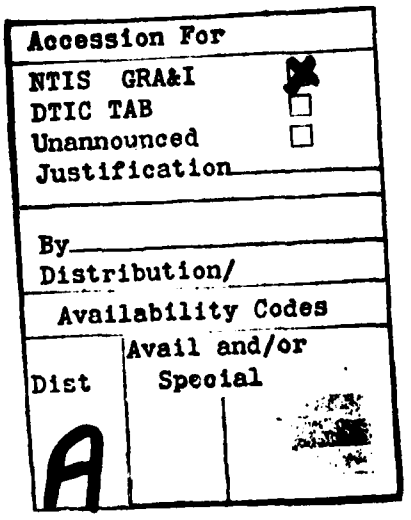

TABLE OF CONTENTS

TABLE OF CONTENTS (CONTINUED)

TABLE OF CONTENTS (CONTINUED)

TABLE OF CONTENTS (CONTINUED)

LIST OF ILLUSTRATIONS

LIST OF ILLUSTRATIONS (CONTINUED)

LIST OF ILLUSTRATIONS (CONTINUED)

LIST OF ILLUSTRATIONS (CONTINUED)

LIST OF ILLUSTRATIONS (CONTINUED)

LIST OF TABLES

INTRODUCTION

The mechanical behavior of the musculoskeletal system and the associated mathematical models have become an important area of biomedical research. In orthopaedics, developments in artificial replacements and reconstructive surgery have demanded greater knowledge of the mechanical functions of the major joints. In other disciplines such as sports medicine, crash protection, and Air Force related applications an increasing interest in the motions and forces in the human body is noted. This need for a better understanding of the complicated mechanical behavior of biological structures has led to the introduction of research methods and mathematical tools from the fields of life sciences as well as applied and theoretical mechanics.

In attempting to understand the biodynamic response of the human body subjected to expected and/or unexpected external load conditions, properly developed mathematical models can provide a sound basis for the design of support-restraint systems and vehicles as well. The most sophisticated versions of these mathematical models are the articulated and multisegmented total-human-body models which initially appeared in the crash victim simulation literature. These models simulate all the major articulating joints and segments of the human body. Representative references are McHenry [1963], Bartz and Butler [1972], Huston, Hessel and Passerelo [1974], Fleck, Butler and Vogel [1975] and Fleck [1975].

Currently, the Aerospace Medical Research Laboratory (AMRL) is in possession of an Articulated Total Body (ATB) model which is maintained and used in Air Force related applications, in particular, to study the pilot ejection problem. The ATB model has some special features which allow the capability of prescribing a) time-dependent forces on the body segments to simulate aerodynamic forces, b) joint torques which are functions of both flexure and azimuth angles, and

c) a generalized restraint belt subroutine which describes and simulates a typical Air Force harness system.

The effectiveness of these multisegmented models to accurately predict in-vivo response depends upon the bio-mechanical description and simulation of the articulating joints. This study, therefore, concerns with the analysis of the mechanical behavior of the major articulating joints and the development of mathematical models simulating their dynamic behavior. In general mathematical models are based on physical principles and consist of a set of mathematical relations among relevant parameters of the system. Assumptions and simplifications are introduced, ignoring elements assumed not to be relevant to the system's behavior. The relevant parameters of the system are defined and the relations are specified. This descriptive model is then expressed as a set of mathematical relations among the chosen parameters. The values assigned to the system's parameters are selected from the literature or determined by measurement. In some cases, the parameters cannot be measured and their values must be estimated.

Validation of a model is established when the model predictions correlate acceptably with data in the literature and, if available, with results of experiments. Within the framework of the present study, no validation experiments were conducted, so that model predictions could be compared only with experiments reported in the literature. Considering the conditions of the reported experiments are only partly known and owing to the variability between specimens, such a comparison should be viewed as an approximate one.

In this report, a rather extended discussion of the articulations and anatomical descriptions of the elbow, shoulder, hip, knee and ankle joints will be first presented, with special emphasis on the location and functional aspects of the major ligaments of each joint. This is followed by a

description of the articulating surfaces and the development of a measurement technique for the determination of articulating surface equations for the elbow, hip, knee and ankle joints. Next, a constitutive equation representing ligament characteristics and behavior is presented and the attachment sites of the ligaments of the elbow, hip, knee and ankle joints are provided.

General two- and three-dimensional mathematical dynamic models of an articulating joint are then developed to determine the nature of motions and forces between two body segments. The governing equations for these models are set of highly nonlinear equations and their numerical solutions are discussed in some detail. This is followed by a specific application to a two-dimensional dynamic model of the human knee joint. The numerical results from this model are presented to illustrate the effects of duration and shape of the dynamically applied loads on the response of the joint. Special attention has been given to the ligament and contact forces, the location of contact points, anterior-posterior displacements and the comparison between the internal and the external energy of the system. The results are compared with experimental data from the literature and the validation of the model is established. The report is concluded with a discussion of extensions of the model and its possible implications on future research.

ARTICULATION AND ANATOMICAL DESCRIPTION OF ELBOW, SHOULDER, HIP, KNEE AND ANKLE JOINTS

Realistic, accurate mathematical modelling of the major articulating joints of the human body requires a comprehensive knowledge and understanding of the physical behavior and the anatomical characteristics of each joint. In a previous report [Engin, 1979a] a survey was provided for various major human joint models including a single degree of freedom hinge

or revolute joint, a spherical joint limited to two degrees of freedom, three degrees of freedom planer joint, three degrees of freedom ball and socket joint, and a general six degrees of freedom. Passive and active force and moment response of major human joints, associated torques about the long-bone axes of these joints and some aspects of joint modeling were reported in the literature by the senior author in a series of articles [Engin, 1979b; Engin et al. 1979c; Engin, 1979d; Engin and Kaleps, 1980a; Engin, 1980b; Engin and Peindl, 1980c; Engin, Akkas and Kaleps, 1980d; Engin, 1981a&b; Engin and Moeinzadeh, 1981c]. The research works presented in these articles were performed with some obvious limitations on live subjects by means of specially designed experimental apparatus.

In the following paragraphs, descriptions of the essential anatomical and functional aspects of the elbow, shoulder, hip, knee and ankle joints will be presented. For each joint, the physical structure and the movements of the articulating segments are described and the ligaments having a significant contribution to the integrity and function of each joint are defined. A number of illustrative figures are presented for each joint with segments appropriately identified by the commonly accepted medical terminology. The anatomical and functional descriptions provided below were taken from various sources such as Gray [1973], Grant [1962], and Wells [1971].

ELBOW JOINT

The elbow joint is a uni-axial (hinge) joint. It is composed of, proximally, the trochlea and capitulum of the humerus, and distally, the trochlear notch of the ulna and the head of the radius. The trochlea of the humerus is convex, anteroposteriorly, and concave, side to side, fitting into the trochlear notch of the ulna. The spherical capitulum of the humerus fits into the concave head of the radius. The cavity of the elbow joint is continuous with the superior radio-ulnar joint where the head of the radius fits into the radial notch of the ulna.

Movements of the elbow consist of flexion and extension, determined by the shape of the trochlear surfaces: the medial portion of the trochlea projects, distally, further than the lateral portion. Flexion is limited by the soft tissues of the arm, whereas extension is limited by the olecranon of the ulna contacting the base of the olecranon fossa (Figure 1).

The capsule of the elbow joint is thin and covered by muscles, attaching anteriorly to the humerus slightly above the coronoid process and to the annular ligament around the head of the radius. Posteriorly, attachment is slightly above the capitulum of the humerus, to the olecranon fossa, the olecranon upper margins and to the capsule of the superior radio-ulnar joint.

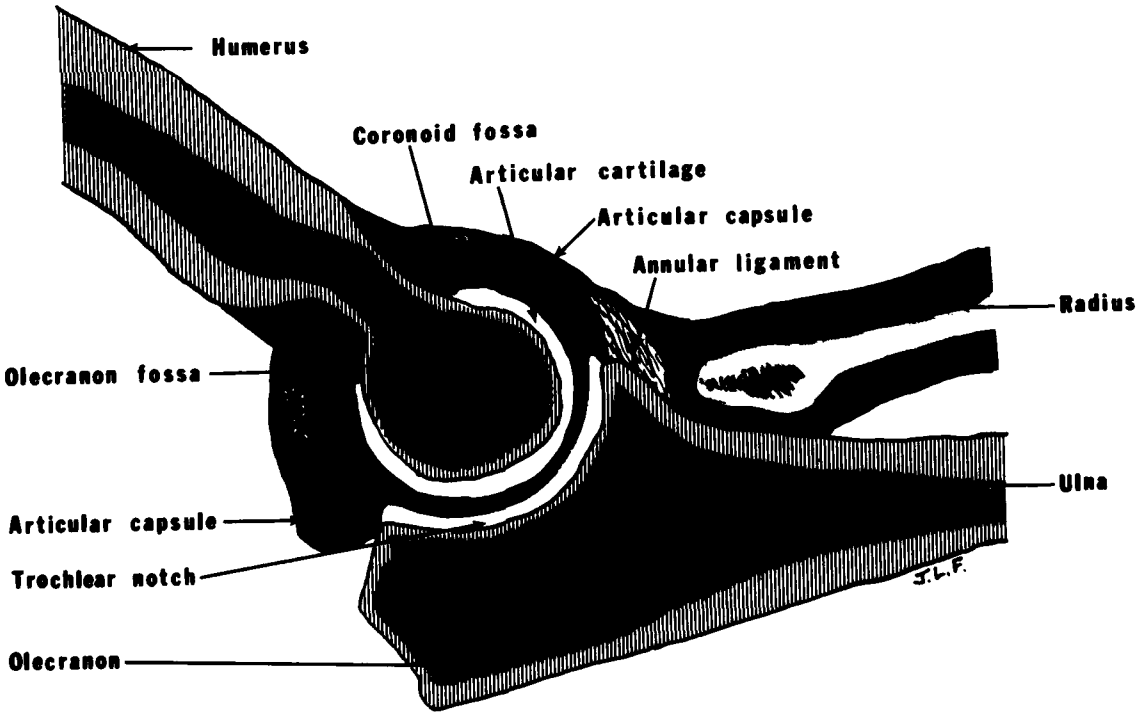

Figure 1. Anterior-posterior section of the right elbow joint.

The fibrous capsule is lined by a synovial membrane which extends into the coronoid, olecranon and radial fossae and between the ulna and radius, being continuous with the synovial membrane of the superior radio-ulnar joint. Pads of fat are present between the fibrous capsule and the synovial membrane. These fat pads fill the fossae: the olecranon fossa during flexion, and the coronoid and radial fossa during extension.

The capsule is strengthened by three ligaments:

1. ulnar collateral ligament (medial ligament);
2. radial collateral ligament (lateral ligament); and
3. annular ligament.

Ulnar Collateral Ligament

The ulnar collateral ligament is a roughly triangular thick band, composed of a strong anterior band and a weaker middle and transverse sheet (Figure 2). It extends from the medial epicondyle of the humerus to an attachment along the coronoid process and the olecranon of the ulna. The anterior portion is nearly a cord, being taut in extension. The posterior portion attaches to the distal and posterior of the medial epicondyle and to the medial margin of the olecranon. This portion of the ligament is a weaker sheet which is taut in flexion. An oblique band extends between the olecranon and the coronoid process, deepening the socket for the trochlea of the humerus.

Radial Collateral Ligament

This ligament is attached to the lateral epicondyle of the humerus, to the trochlear notch of the ulna and to the annular ligament. It does not attach directly to the radius so that rotation of the radius is permitted in pronation and supination of the forearm (Figure 3).

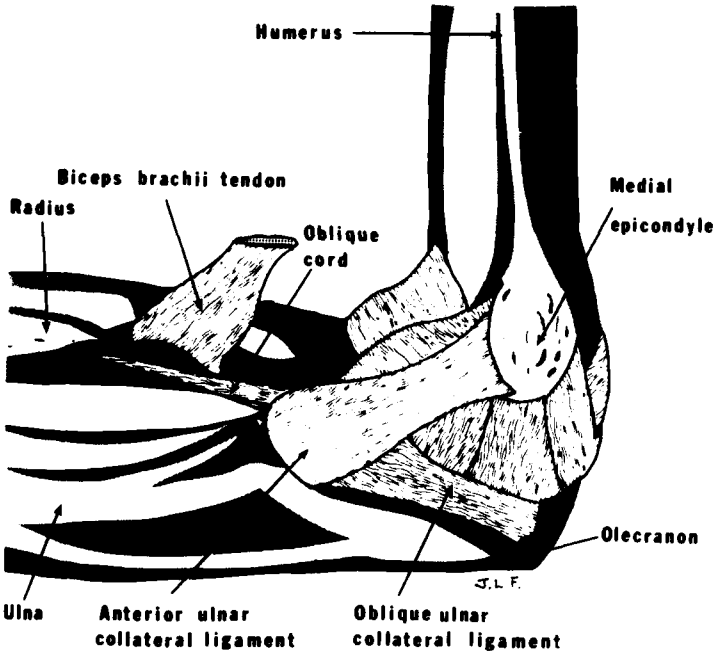

Figure 2. Medial aspect of the right elbow joint.

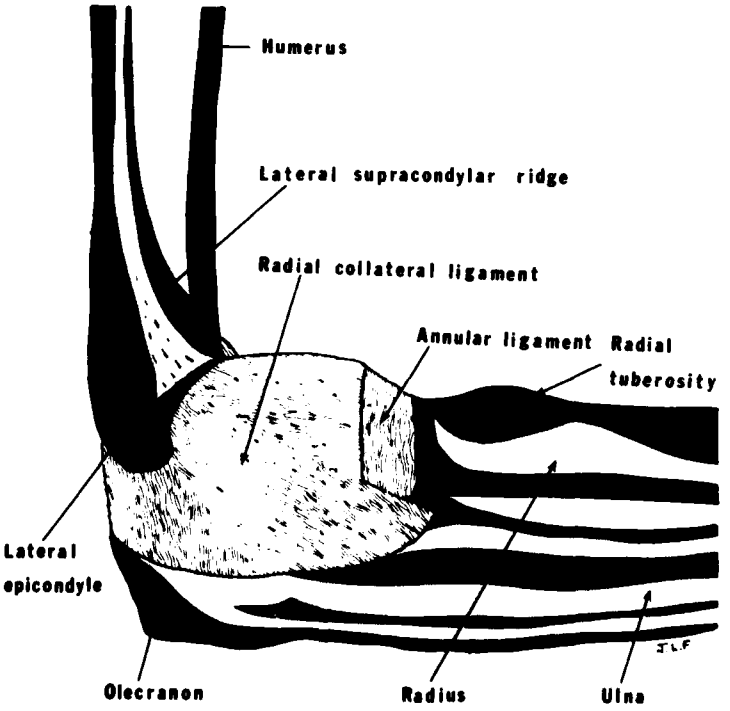

Figure 3. Lateral aspect of the right elbow joint.

Annular Ligament

This strong band encircles the head and neck of the radius, attaching to the anterior and posterior margins of the radial notch of the ulna. The radial collateral ligament blends into the proximal margin of the annular ligament (Figure 3). With the oblique cord, which extends medially and upwards from the radial tuberosity to the coronoid process of the ulna (Figure 3), the annular ligament maintains the radius head close to the radial notch of the ulna.

SHOULDER COMPLEX

The shoulder complex is composed of four independent articulations among the bones of the complex: the clavicle, scapula, humerus and the thorax (Figure 4). The shoulder girdle is composed of the clavicle and scapula. There are two clavicular articulations: the sternoclavicular joint, where the clavicle articulates with the manubrium of the sternum, and the acromioclavicular joint, where the clavicle articulates with the acromion process of the scapula. The glenohumeral joint is a ball and socket joint composed of the humerus and the glenoid cavity of the scapula. The final articulation is not, per se, a joint but is the scapulothoracic articulation of the scapula over the thorax.

Sternoclavicular Joint

This is a saddle-type joint with both concave and convex curvatures. The proximal end of the clavicle is separated from the manubrium of the sternum by a constant thickness, intra-articular meniscus. The fibrous joint capsule is strengthened by the anterior and posterior sternoclavicular ligaments. Further, both left and right clavicles are joined by the interclavicular ligament running over the sternal notch (Figure 4). The inferior portion of the clavicle connects to the first costal cartilage at the costal tuberosity by means of the costoclavicular ligament. The sternoclavicular

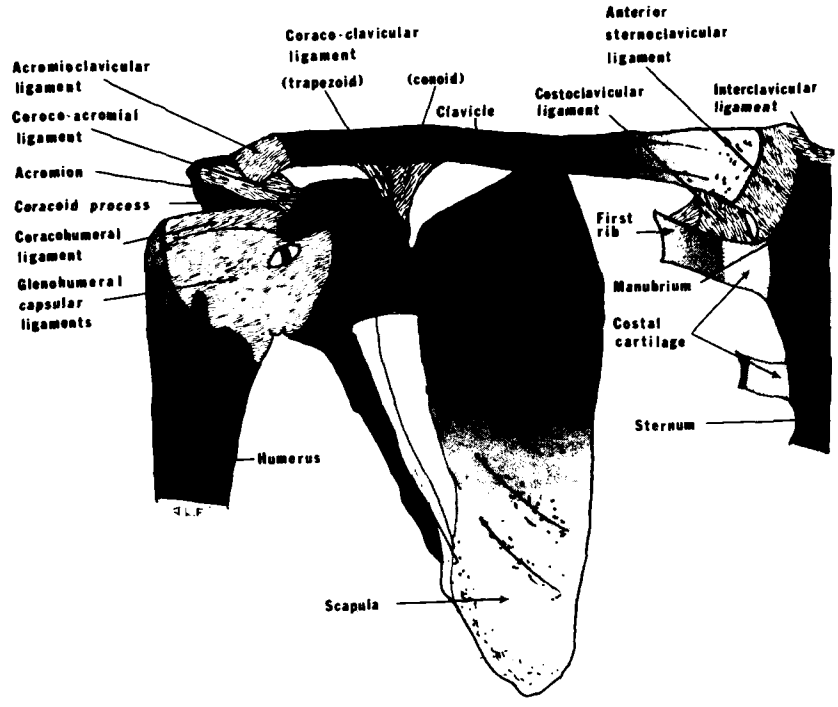

Figure 4. Anterior view of the right shoulder complex.

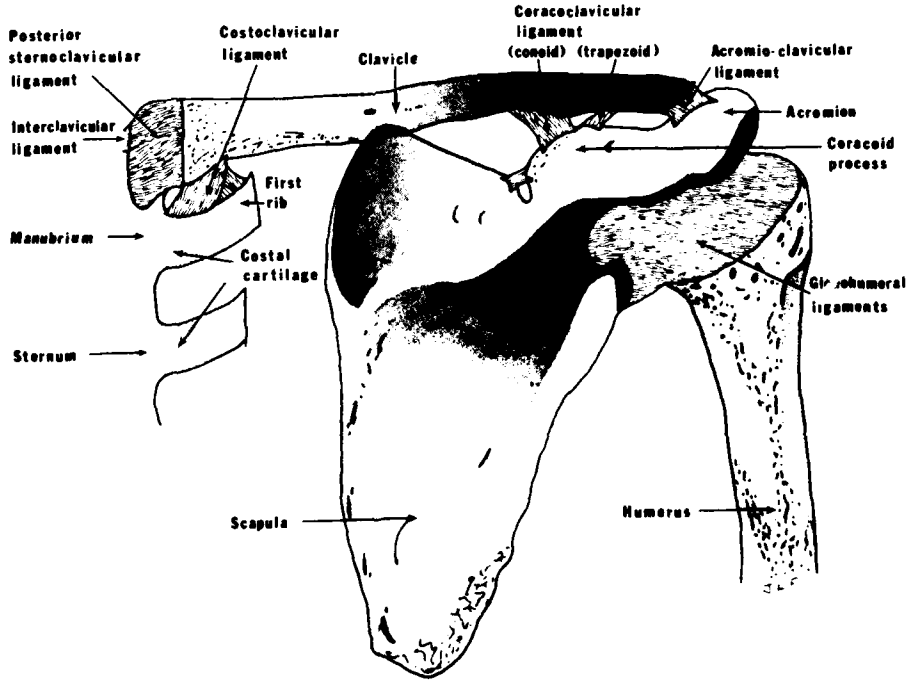

Figure 5. Posterior aspect of the right shoulder complex.

joint possesses three degrees of freedom with axes in the sagittal and frontal planes and the bone-axes of the clavicle. Elevation of the clavicle is limited by the lower portion of the joint capsule and the costoclavicular ligament. Depression is limited by the upper portion of the joint capsule and the interclavicular ligament.

Acromioclavicular Joint

This articulation between the distal end of the clavicle and the acromion of the scapula is surrounded by a fibrous capsule. The articulation provides little stability so that the ligamentous structures are the primary stabilizers. Reinforcing the capsule are the superior and inferior acromioclavicular ligaments (Figure 4). Additionally, the clavicle connects to the scapula by the conoid and trapezoid portions of the coracoclavicular ligament and by the coracoacromial ligament (Figure 5). The proximity of the coracoid process of the scapula to the clavicle (and the possible cartilagenous formation between them), sometimes is referred to as the coracoclavicular joint with the entire region being called the claviscapular joint.

Glenohumeral Joint

This ball and socket joint between the head of the humerus and the glenoid fossa of the scapula is surrounded by a loose sleeve composed of the joint capsule and its capsular ligaments. The contact surface is remarkably small with the head of the humerus possessing a much greater articulating surface than the glenoid fossa of the scapula. In addition to the gelnohumeral capsular ligaments, the coracohumeral ligament over the superior aspect of the joint provides reinforcement as the humerus is suspended along side of the torso as well as checks outward rotation of the humerus (Figure 6).

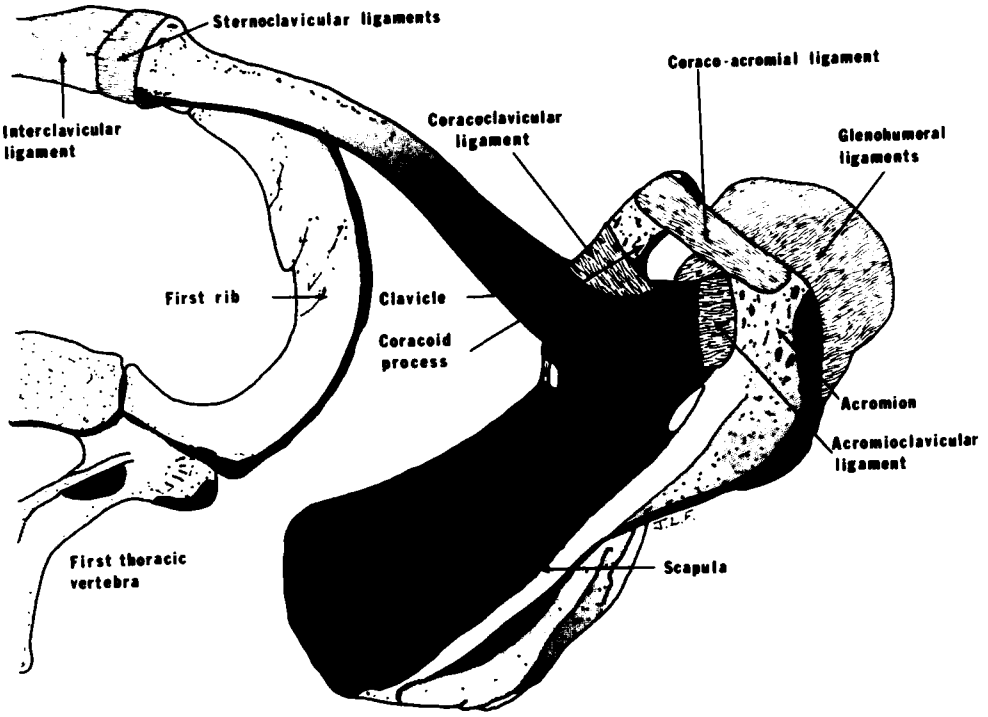

Figure 6. Superior aspect of the right shoulder complex.

HIP JOINT

The hip joint is a multi-axial, ball and socket joint, and therefore possesses three degrees of freedom. For convenience, movements can be considered to be about three mutually perpendicular axes: transverse, anteroposterior and longitudinal. Flexion and extension occur about the transverse axis; flexion being forward movement and extension being backward. Flexion is limited by tension on the hamstrings and soft tissues; extension is limited by the iliofemoral and pubofemoral ligaments. Abduction, movement of the thigh away from the midline of the body, and adduction, movement toward the midline, occurs about the anteroposterior axis. Abduction is limited by tension of the adductor muscles and by contact of the greater trochanter with the acetabulum (Figure 7).

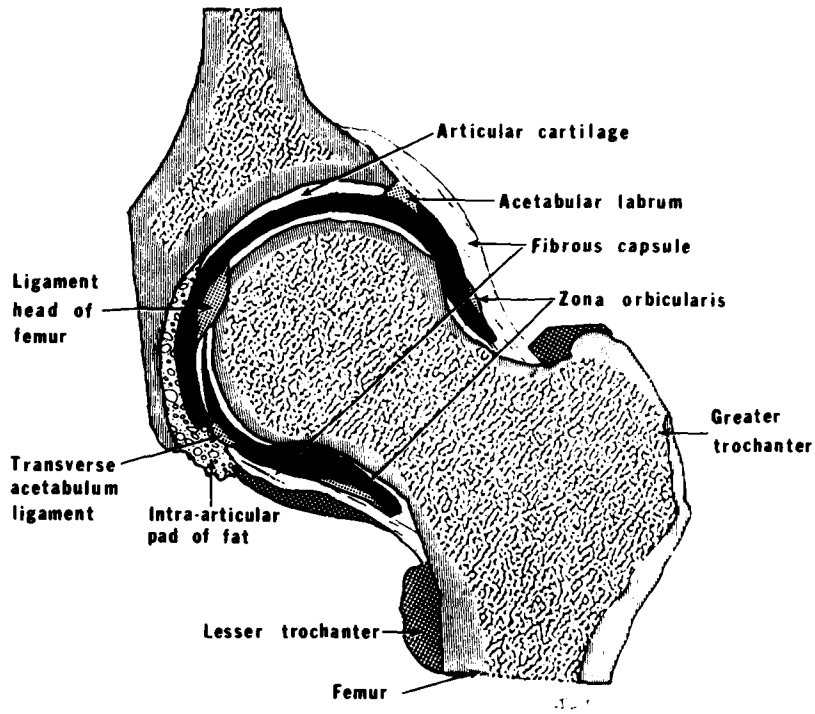

Figure 7. Posterior aspect of the medial-lateral section of the right hip joint.

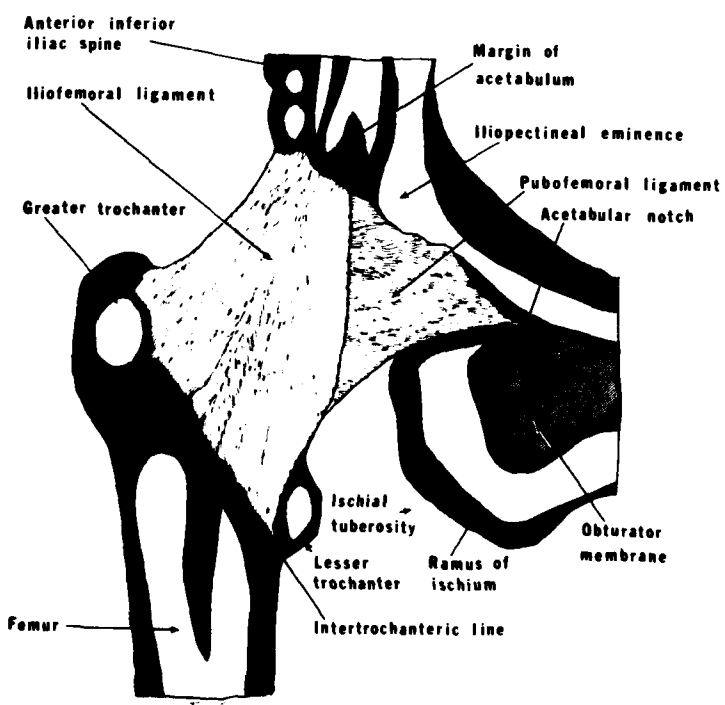

Figure 8. Anterior aspect of the right hip joint.

Adduction is limited by the opposing leg and by the iliofemoral and ischiofemoral ligaments. Lateral and medial rotation, movement of the anterior surface of the thigh laterally and medially, respectively, occurs about the longitudinal axis. Lateral rotation is limited by the iliofemoral and pubofemoral ligaments (Figure 8); medial rotation, by the ischiofemoral and iliofemoral ligaments (Figure 10).

Analysis of these movements must take into account the length and angulation of the neck of the femur in relation to the long axis of the femoral shaft. In flexion or extension, the femoral head rotates about a transverse axis within the acetabulum. Medial and lateral rotations occur about a longitudinal axis through the head of the femur and the lateral condyle, when the foot is weight-bearing. Thus, the medial condyle moves posteriorly and the greater trochanter moves anteriorly in relation to this axis during medial rotation However, when the foot is free or not weight-bearing, rotation may occur about variable axes through the femoral head. Abduction and adduction are produced about an anteroposterior axis through the approximate center of the femoral head.

Because of shifting axes, it is sometimes convenient to view movements as occurring about mechanical axes through the femoral neck and the approximate center of the femoral head. Thus, extension and flexion can be viewed as spins, producing respectively, tauting (spiralizing) and relaxing (straightening) of the ligaments and the capsule.

The joint itself is composed of the head of the femur and the acetabulum of the hip. The femoral head is approximately two-thirds of a sphere. The acetabulum is shaped like a horseshoe, closed by a non-articulating pad of fat. The socket is deepened by the acetabular labrum, a fibrocartilaginous rim, and the transverse ligament, which completes the encapsulation of the head of the femur. The femoral head aligns obliquely upwards, medially and slightly forwards.

The capsule attaches slightly beyond the acetabular labrum, blending with the labrum and the transverse ligament anteriorly and inferiorly. Femoral attachments are along the intertrochanteric line, anteriorly, and to the neck, medially to the obturator externus. Three ligaments strengthen the capsule:

1. iliofemoral ligament;
2. pubofemoral ligament; and
3. ischiofemoral ligament.

Iliofemoral Ligament

Triangular in shape and of great strength, the iliofemoral ligament covers the anterior portion of the joint. It attaches to the ilium above the acetabular rim and to the lower portion of the anterior inferior iliac spine (Figure 9). The ligament broadens and diverges, inferiorly, to form two bands. The superior or lateral band attaches to the upper part of the intertrochanteric line and is sometimes referred to as the iliotrochanteric ligament. The inferior or medial band attaches to the lower portion of the intertrochanteric line. The iliofemoral ligament is referred to as the "Y" ligament due to its inverted "Y"-shape. This ligament checks extension of the joint, as well as both lateral and medial rotation.

Pubofemoral Ligament

The pubofemoral ligament attaches medially to the anterior acetabular rim and the superior pubic ramus, and crosses to the inferior of the neck of the femur, attaching to the top of the lesser trochanter (Figure 8). Somewhat triangular in shape, this ligament checks abduction, extension and medial rotation.

Ischiofemoral Ligament

This ligament is less differentiated than the preceding. It attaches to the ischium posteriorly and inferiorly to the acetabulum, passing over the superior and posterior of the

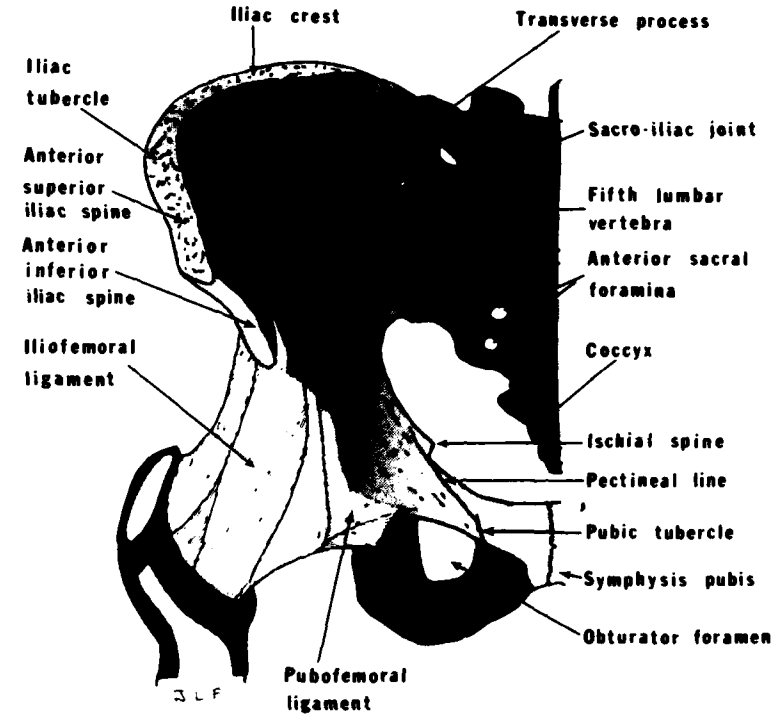

Figure 9. Anterior aspect of the right hip joint and pelvis.

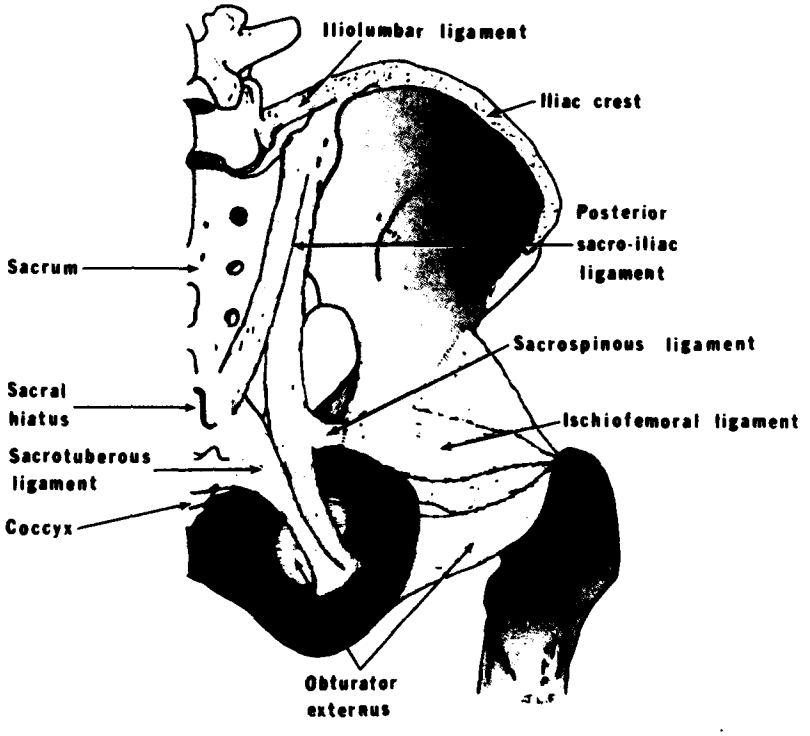

Figure 10. Posterior aspect of the right hip and joint pelvis.

neck of the femur (Figure 10). The superior portion is generally horizontal and the posterior or lower portion spirals. The ischiofemoral ligament limits medial rotation and adduction.

Teres Femoris (Head of Femur) Ligament

Structurally, this ligament is of little importance. Passing from the deep aspect of the transverse ligament to a depression in the head of the femur; it functions primarily as a conduit for blood vessels (Figure 7). In extreme abduction, this ligament becomes taut, but not before the iliofemoral ligament has become taut and possibly not until the iliofemoral ligament fails.

KNEE JOINT

A condyloid, synovial joint, the knee is the articulation of the distal condylar surfaces of the femur, the proximal condylar surfaces of the tibia and the posterior surface of the patella. While the primary movement is hinge-like, some rotation does occur. Flexion, backward movement of the thigh or leg, and extension, the opposite movement, occur about a moving transverse axis. This axis moves backward during flexion due to the curvatures of the femoral condyles.

At complete flexion, the posterior femoral condylar surfaces articulate with the posterior tibial condylar surfaces and with the posterior portions of the menisci. During extension with the tibia fixed, the femoral condyles roll forward while simultaneously sliding backward on the tibial condylar surfaces. The contact areas between these surfaces increases as the curvature of the femoral condyles decreases. Movement on the lateral condyle ends before extension is complete, while movement on the medial condyle continues since the lateral articular surface of the lateral condyle is shorter than the medial. This continued movement of the medial condyle causes the femur to rotate medially about a

longitudinal axis through the lateral condyle, causing the collateral and popliteus oblique ligaments to become taut. Thus, lateral rotation becomes a precursor to flexion.

During extension, there is a lateral rotation of the tibia with respect to the femur. Conversely, medial rotation of the tibia occurs in the beginning of flexion. When approaching complete extension, the anterior portions of the menisci are pushed forward by the femur and become less curved. The opposite occurs in flexion. As the tibial collateral ligament becomes taut during extension, it pulls the medial meniscus outward. The lateral meniscus is drawn outward, away from the femoral and tibial condyles, by the popliteus which is attached to the posterior of the lateral meniscus.

The cruciate ligaments are taut in most positions of the knee and prevent anteroposterior displacement of the tibia in relation to the femur. During rotational movements, the cruciates twist and untwist around each other. In full flexion, the anterior cruciate ligament is relaxed and in full extension the posterior cruciate is relaxed. The collateral ligaments are relaxed when the knee is flexed to a ninety-degree angle, thus allowing rotation about a vertical axis.

The articular surfaces of the femoral condyles are convex anteroposteriorly and from side-to-side, being more marked in the posterior portion of the anteroposterior curvature. The tibial surfaces are comparatively flat, being deepened by the wedge-shaped menisci. The patellar surface of the femur is also convex from side-to-side, with the lateral condyle extending further forward and upward.

The medial and lateral menisci are two crescent-shaped fibrocartilaginous structures attached to the upper surface of the tibia by the coronary ligaments. The inferior surface is flattened while the superior surface is concave, thus deepening the sockets for the femoral condyles. The outside

edges are firmly attached to the tibia through the capsule to the tibial condyles. The inner edges are thin and free. The anterior ends are attached by the transverse ligament. The posterior portion of the lateral meniscus (Figure 11) is continuous with the posterior cruciate ligament and attaches to the popliteous tendon. The medial meniscus attaches to the tibial collateral ligament (Figure 14). The lateral is broader and its ends closer than the medial meniscus. The lateral is more nearly circular while the medial meniscus is more elliptical.

Four major ligaments lend stability to the knee joint.

1. tibial collateral (medial) ligament;
2. fibular collateral (lateral) ligament;
3. anterior cruciate ligament; and
4. posterior cruciate ligament.

Tibial Collateral (Medial) Ligament

This is a broad, flat band in the medial portion of the capsule. It is attached proximately to the medial epicondyle of the femur below the adductor tubercle, and it broadens to an attachment at the medial condyle and upper body of the tibia (Figure 11). Its deep fibers attach to the medial meniscus periphery.

Fibular Collateral (Lateral) Ligament

Unlike the tibial collateral ligament, the fibular collateral ligament is distinctly separate from the fibrous capsule (Figure 11). It is a strong, rounded cord, attached to the lateral epicondyle above the groove for the popliteous tendon and passes to the lateral side of the head of the fibula. The popliteous tendon lies below it, separating it from the lateral meniscus.

Anterior Cruciate Ligament

The anterior cruciate ligament attaches to the tibia anterior to the intercondylar eminence, between the menisci,

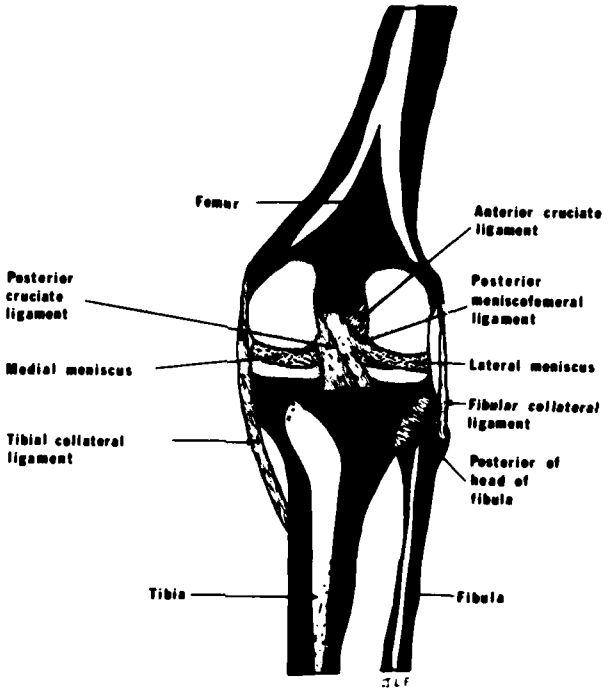

Figure 11. Dissected posterior aspect of the right knee joint.

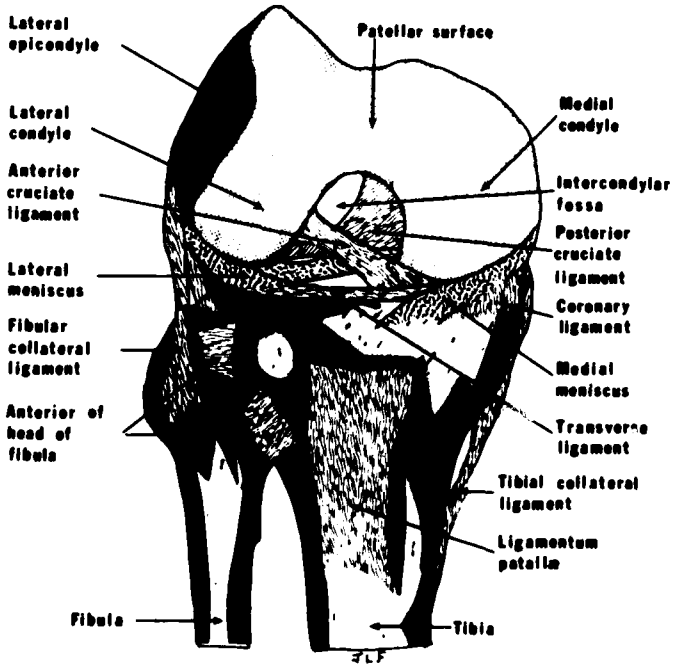

Figure 12. Anterior aspect of the right knee joint.

partly blending with the anterior end of the lateral meniscus (Figure 12). It crosses upward, backward and laterally, twisting on itself, fanning out to attach to the medial aspect of the femoral lateral condyle. It is anterolateral to the posterior cruciate ligament. It holds the femur from sliding backward, prevents hyperextension of the knee and checks medial rotation of the femur when the leg is weight-bearing.

Posterior Cruciate Ligament

The posterior cruciate ligament attaches to the posterior intercondylar area of the tibia and the lateral meniscus, crossing upward, forward and medially to attach to the lateral portion of the femoral medial condyle (Figure 13). It is stronger, shorter and less oblique in direction than the

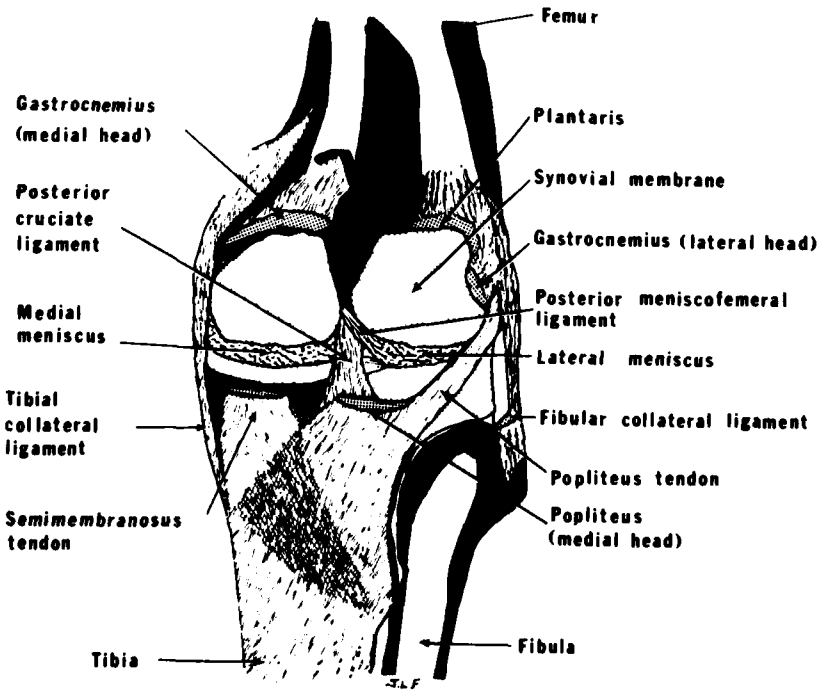

Figure 13. Posterior aspect of the right knee joint.

anterior cruciate ligament. It holds the femur from sliding forward. The two cruciates are slightly twisted around each other except when the knee is fully extended. At this position, the tibia is laterally rotated in relation to the femur.

ANKLE JOINT

The ankle or talocrural joint is a uni-axial hinge joint formed by the articulation of the talus with a three-sided socket composed of the distal surface of the tibia and the articular surfaces of the tibial and fibular malleoli with the inferior transverse tibiofibular ligament, posteriorly. The tibia and fibula are firmly united at the inferior tibio-fibular joint.

The hinge-like movement of the ankle occur about an axis through the body of the talus (Figure 14), which is slightly oblique, passing forward, medial to lateral. Dorsiflexion (extension) is raising the forepart of the foot while plantar flexion (flexion) is the lowering of the foot. There is maximal congruence of the joint surfaces and maximal ligamentous tension in dorsiflexion.

The joint capsule is thin anteriorly and posteriorly with lateral ligaments. There are deep fatty pads in the anterior and posterior portions of the joint. The joint cavity extends upward between the tibia fibula for a few millimeters. The anterior portion of the capsule is attached to the tibia near the articular surface and to the neck of the talus near its head.

The integrity of the ankle is determined in part by the bony structure and in part by two ligaments:

1. medial ligament and
2. lateral ligament.

<u>Medial Ligament</u>

The medial ligament (deltoid ligament) is a strong, thick triangular band connecting the medial malleolus of the tibia

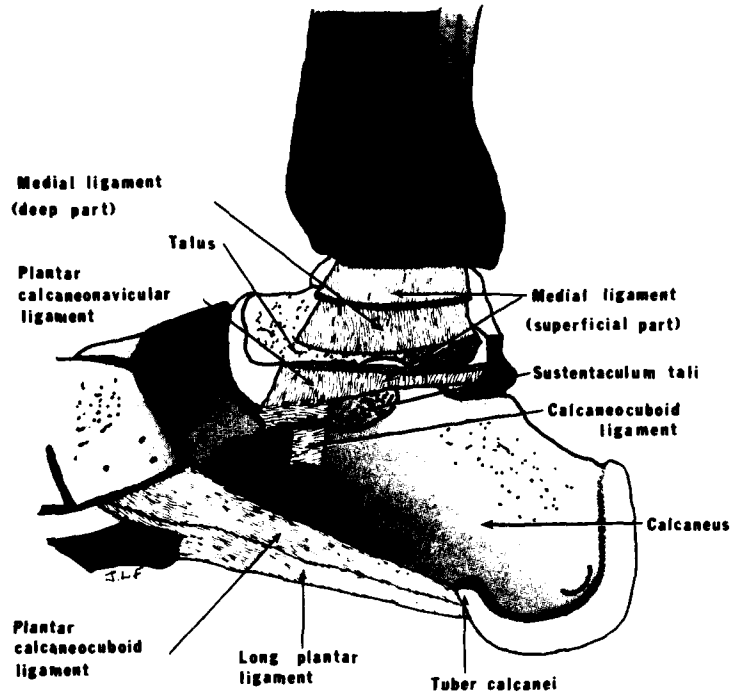

Figure 14. Medial aspect of the right ankle joint.

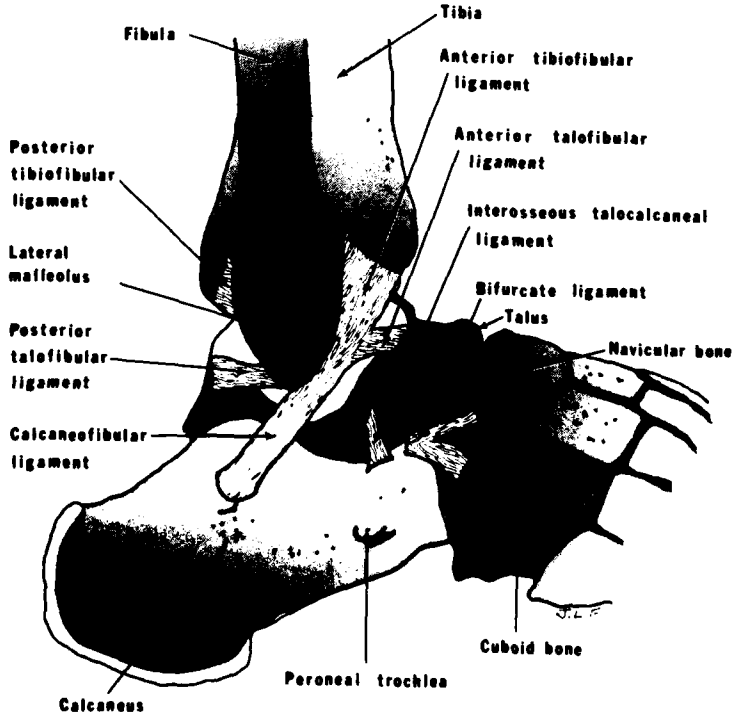

Figure 15. Lateral aspect of the right ankle joint.

to several tarsal bones (Figure 14). The deep portion passes from the malleolus to the medial surface of the talus. It is also known as the anterior tibiotalar ligament. The superficial portion consists of three parts: (1) the anterior or tibionavicular portion passes to the tuberosity of the navicular bone, blending with the medial margin of the plantar calcaneonavicular ligament; (2) the middle or tibiocalcanean portion crosses to the sustentaculum cali of the calcaneous; and (3) the posterior or posterior tibiotalar portion attaches to the medial tubercle of the talus.

Lateral Ligament

The lateral ligament consists of three parts. (1) The anterior talofibular ligament attaches to the anterior margin of the lateral malleolus of the fibula, and to the anterior of the talus between its neck and articular surface (fibular articulation) (Figure 15). (2) The calcaneofibular ligament passes down and back from the tip of the lateral malleolus to the lateral aspect of the calcaneous, posterior to the peroneal tubercle. (3) The posterior talofibular ligament passes from the malleolar fossa to the lateral tubercle of the talus.

GEOMETRY OF THE ARTICULATING SURFACES

Articulating surfaces play a major role in the physical motion of a joint. It is assumed that the deformations in the articular surfaces do not affect relative motions and forces in the joint. This assumption is based on the consideration that the deformations of the cartilage layer caused by the contact between the articulating bones is relatively slight compared to the range of motions in the joint (Wismans [1980]). Therefore, the articular surfaces are represented by rigid surfaces and the contact areas between the articulating surfaces are reduced to contact points.

No accurate quantitative data for the geometry of the articulating surfaces of the human joints are available in the literature. The knee joint is relatively the most studied joint and some techniques have been developed for measurements of its articular surfaces. Seedham, et al., [1972a] studied the femoral and tibial condyles by making a plastic mold of the condyles. These mouldings were cut in the sagittal planes, resulting in a number of contours of the articular surface. In the work of Wismans, et al., [1980], using dial gages, three-dimensional coordinates of 50-200 points on each condyle of the knee were determined and the surfaces were approximated by mathematical functions representing the collected data points. Most other studies in this field are restricted to the determination of a number of rough dimensions from roetgen photographs (Erkman and Walker [1974], Seedham, et al. [1972b]). Several other measuring techniques are also given in a survey by Wismans and Struben [1977] and in Devens [1979], where special attention is paid to optical methods.

In this study, coordinates of a large number of points on each of the articular surfaces of the elbow, hip, knee and ankle joints are determined using a sonic digitizing technique. This technique, its measuring apparatus and procedures will be presented below. A procedure for approximating the articular surfaces by mathematical functions will then be discussed and a brief description of the articulating surfaces, the location and orientation of coordinate systems and the mathematical functions representing the elbow, hip, knee and ankle joint surfaces will be presented.

MEASURING TECHNIQUE

Coordinates of a large number of points on the articulating surfaces are determined using a Graf/Pen Sonic Digitizer. Sonic digitizing is the process of converting information on location or position in one, two or three

dimensions, to digital values suitable for data processing, storage or transmission. The system used to accomplish this conversion consists of a stylus, two or three microphone/sensor assemblies (for two- and three-dimensional data conversion, respectively), an electronic control unit and a generator/multiplexer unit which is used to select and power sonic impulse emitters. As an example of the digitizer's operation, let us first consider the two-dimensional mode of operation.

The two-dimensional sensor assembly consists of two perpendicular, linear microphones as shown in Figure 16. These sensors define a planar effective working area of approximately 35 cm x 35 cm. The Graf/Pen uses impulses generated at the tip of the emitter to calculate its position in

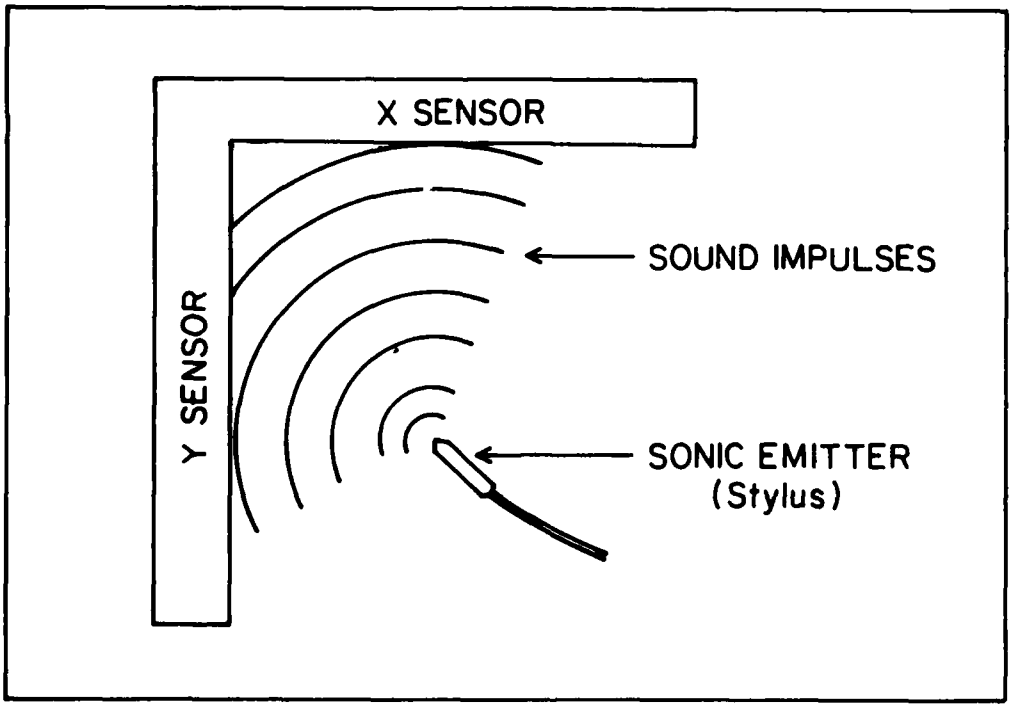

Figure 16. The two-dimensional microphone/sensor assembly of the Graf/Pen sonic digitizer.

the working area. The times required for the sound waves to reach the two microphone/sensors are converted into distance measurements (the x and y coordinates). The measurements are then transmitted to the computer in binary coded decimal (BCD) Cartesian form. The two-dimensional mode is primarily used to digitize joint surface curves which are obtained from x-ray projections (see Figure 32) or physical cross-sections of the joint. Additionally, the two-dimensional microphone/sensor assembly provides a menu capability of alphanumeric data entry to the computer.

An obvious advantage of using sound as a ranging device is that digitization need not be confined to a plane. The three-dimensional microphone/sensor unit utilized for the digitization of the articulating surfaces consists of four linear microphones arranged in a planar, rectangular manner. These microphones define a three-dimensional effective working volume of approximately 150 cm x 75 cm x 180 cm, along the x, y and z directions, respectively. The three-dimensional mode of operation is similar to that of the two-dimensional mode. In the three-dimensional set-up, however, the distances measured are slant ranges to each of the coplanar sensors. Thus, the information generated by each sensor represents the radius of a circular arc which includes the impulse source (the tip of the sonic emitter) and is in a plane perpendicular to the sensor. Four sensors are used merely for the purposes of accuracy. The digitizer examines the signals from all four sensors, selects the three smallest signals and disregards the fourth. The location of the sonic emitter is then calculated as being at the intersection of the three smallest arcs. The three slant ranges are easily converted into Cartesian x, y and z coordinates by a microprocessor in the control unit and converted for transmission.

Using the joints of a full-size human skeleton, each articulating joint segment was placed on the apparatus shown

in Figure 17, with its articular surface facing the microphone/sensor unit. Digitizing each surface, the coordinates of a large number of points (50-200) on the surfaces were measured with respect to the microphone/sensor unit's coordinate system. The output was recorded on an LA120 terminal, manufactured by Digital Equipment Corporation. Applying simple mathematics, these coordinates were then transformed into the local coordinate system of the particular joint segment under study.

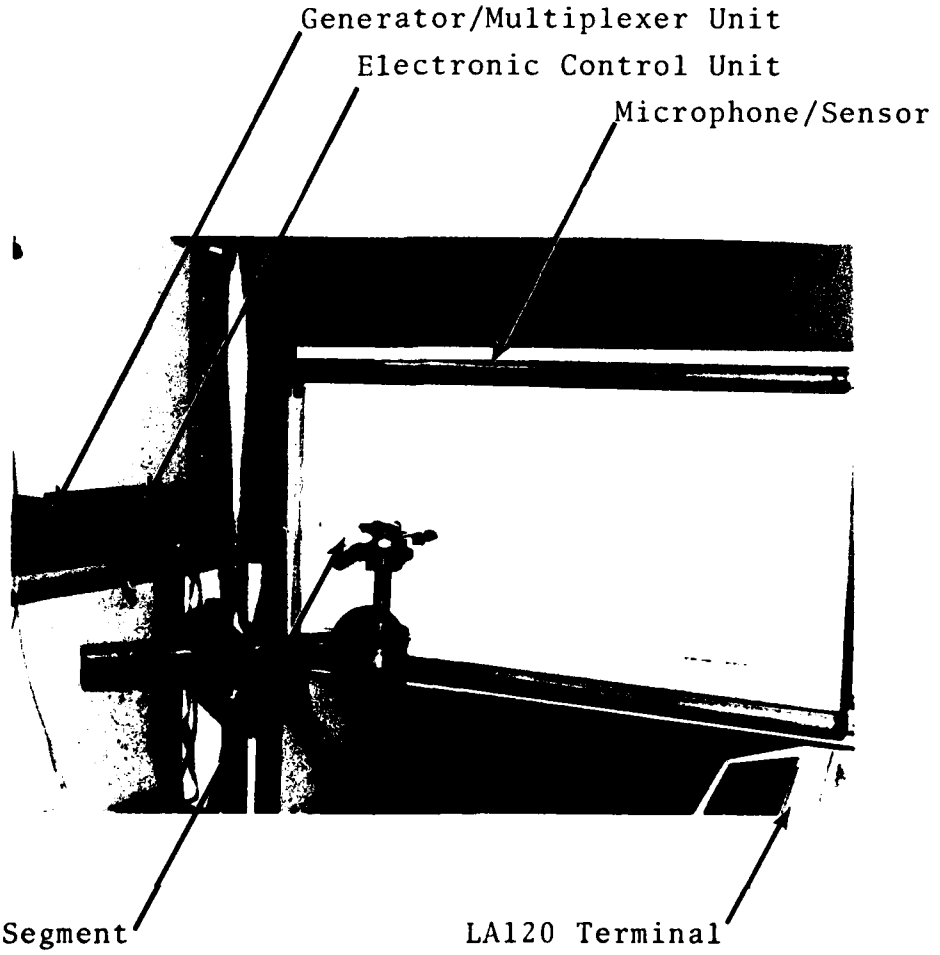

Figure 17. Experimental set-up for measuring the three-dimensional geometry of the articulating surfaces.

MATHEMATICAL DESCRIPTION OF THE ARTICULATING SURFACES

Based on the above procedure, coordinates (x_Q, y_Q, z_Q) of a sufficient number of points on each of the articulating surfaces are determined in their respective, local coordinate systems. The aim is to find a realistic and simple representation in the form of a mathematical approximation for the geometry of these surfaces. In this study, a polynomial of degree n (n>1) is used and expressed as:

$$y = f(x,z) = \sum_{p=0}^{n} \sum_{q=0}^{n-p} a_{pq} x^p z^q \qquad (1)$$

The coefficients a_{pq} of equation (1) have to be determined in such a way that for each point Q, the coordinate $\bar{y}_Q$ is approximated as accurately as possible by $y(\bar{x}_Q, \bar{z}_Q)$. In the present work, the coefficients a_{pq} are obtained by means of statistical operations using the 79.3A version of the GLM procedure of the Statistical Analysis System (SAS) subroutines (SAS [1979]). The GLM procedure uses the principle of least squares (Goodnight and Harvey [1978], Draper and Smith [1966], Graybill [1961]) to fit linear models and provides an output data set containing (a) predicted and residual values from the analysis, (b) standard deviation and (c) percentage accuracy of the fit. Summarized values for the degree of the polynomial, n, the standard deviation, σ, and the percentage accuracy, R, of the models obtained for the articulating surfaces of the elbow, hip, knee and ankle joints are presented in Table 1.

ARTICULATING SURFACES OF THE ELBOW JOINT

Anatomical Description

The two main articulating surfaces of the elbow joint are the trochlea and the trochlear notch. The trochlea (Figure 18a) is a grooved surface much like the circumference of a pully, which covers the anterior, inferior and posterior

Table 1

DEGREE OF POLYNOMIAL (n), STANDARD DEVIATION (σ) AND PERCENTAGE ACCURACY (%R) OF THE FIT FOR THE ARTICULATING SURFACES OF ELBOW, HIP, KNEE AND ANKLE JOINTS.

JOINT	ARTICULATING SURFACE	n	σ (cm)	%R
ELBOW	Trochlea	4	0.09	94.4
	Trochlear notch	4	0.07	94.5
HIP	Head of femur	4	0.08	98.2
	Acetabulum	4	0.15	99.1
KNEE	Tibia lateral	4	0.03	93.8
	Tibia medial	4	0.05	94.6
	Femur lateral	4	0.04	99.3
	Femur medial	4	0.07	98.7
ANKLE	Talus (trochlear)	4	0.03	98.5
	Medial malleolus	4	0.04	95.7

surfaces of the condyle of the humerus. It is separated from the capitulum on its lateral side by a faint groove, but its medial margin is salient and projects downward beyond the rest of the bone. The trochlea articulates with the trochlear notch of the ulna.

The trochlear notch (Figure 18b) is formed by the anterior surface of the olecranon and the superior surface of the coronoid process. The base is constricted at the junction between these two areas and they may be separated completely by a narrow, roughened strip. A smooth ridge which corresponds to the groove of the trochlea, divides the notch into a larger,

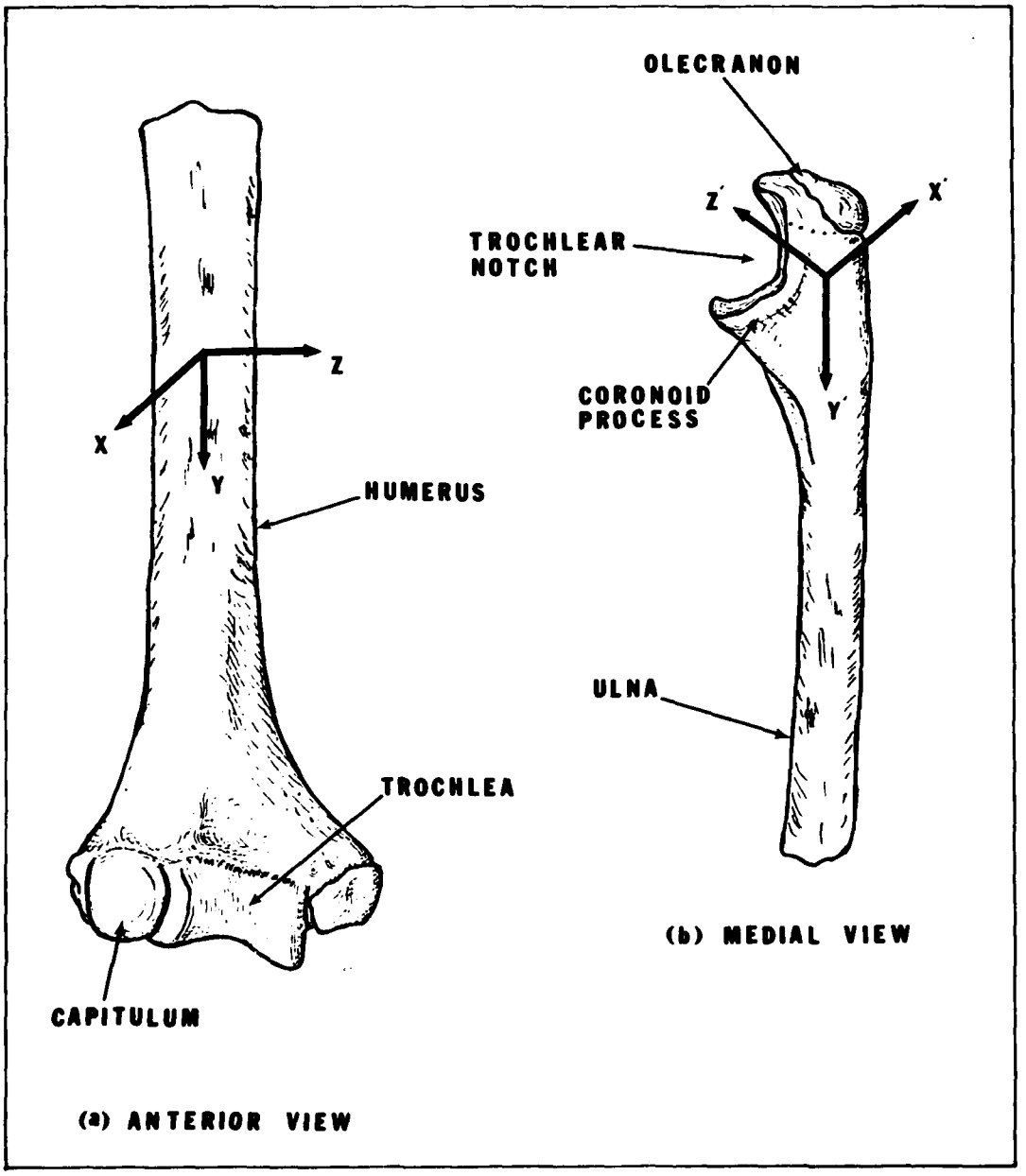

Figure 18. Anterior and medial aspects of the humerus and ulna.

medial portion and a smaller, lateral part. The medial part conforms to the large flange of the trochlea of the humerus.

Coordinate System

The origin of the (x,y,z) coordinate system is placed at the approximate geometric center of the humerus, with the x-axis directed along the posterior-anterior direction and the y-axis coinciding with the humerus longitudinal axis (Figure 18a). The origin of the coordinate system (x',y',z') coincides approximately with the geometric center of trochlear notch, with the x'-axis directed along the anterior-posterior direction and the y'-axis being directed along the longitudinal axis of the ulna (Figure 18b). The locations of the origins of these coordinate systems are 15.5 cm and -0.8 cm from the intersection points of the y and x' axes with the articular surfaces, respectively.

The articulating surfaces are digitized in their respective coordinate systems following the technique described above. The coefficients a_{pq} of equation (1) are summarized in Table 2. Note that to avoid multi-value function difficulties, the surface equation for the trochlear notch is presented as:

$$x' = f(y',z') = \sum_{p=0}^{n} \sum_{q=0}^{n-p} a_{pq} y'^{p} z'^{q} \qquad (2)$$

Proper consideration of this variable change must be made in future analysis and modeling of the elbow joint.

ARTICULATING SURFACES OF THE HIP JOINT

Anatomical Description

The two articulating surfaces of the hip joint are the head of the femur and the acetabulum of the pelvis. The head of the femur is rather more than half of a sphere (Figure 19a). It is directed upward, medially and slightly forward to articulate with the acetabulum. Its surface is smooth with a small fovea or roughened pit slightly below and behind its center.

Table 2

COEFFICIENTS OF THE EQUATIONS OF THE ELBOW JOINT ARTICULATING SURFACES.

COEFFICIENTS a_{pq} (cm)	ARTICULATING SURFACE	
	Trochlea	Trochlear Notch
a_{00}	15.5619	-0.8296
a_{01}*	0.5426	0.1613
a_{02}	0.9899	0.0410
a_{03}	-0.3204	-0.2188
a_{04}	-0.3807	0.1936
a_{10}*	0.5668	0.4230
a_{11}	-0.3387	-0.2996
a_{12}	0.1875	-0.1772
a_{13}	0.2360	0.3742
a_{20}	-0.4083	-0.5579
a_{21}	-0.0320	-0.0439
a_{22}	-0.2297	-0.7558
a_{30}	-0.0243	-0.2487
a_{31}	0.1307	-0.0776
a_{40}	-0.0891	0.1855

*unitless

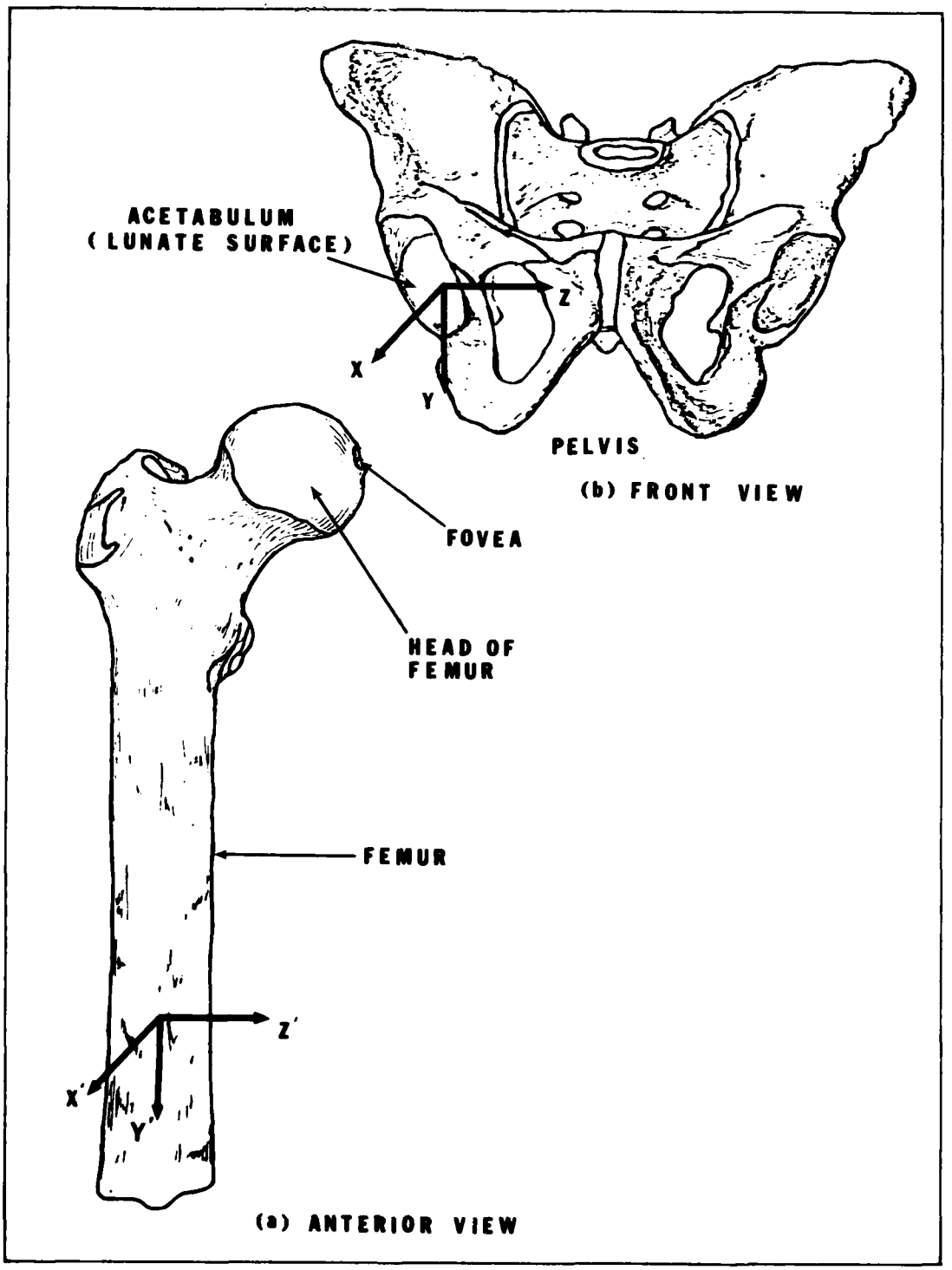

Figure 19. Anterior and front aspects of the femur and pelvis.

The acetabulum is an approximately hemispherical cavity on the lateral aspect of the inominate bone, about its center, and is directed laterally, downward and forward. It is surrounded by an irregular projecting margin which is defined inferiorly; this gap is the acetabular notch. The floor of the cavity is roughened and non-articular. The sides of the cup present an articular lunate surface which is widest superiorly. In this situation, the weight of the trunk is transmitted to the femur in the erect attitude. This horse-shoe shaped strip is covered with articular cartilage (Gray [1973]) and provides the surface on which the head of the femur rides within the hip joint.

Coordinate System

The origin of the (x,y,z) coordinate system is placed at the geometric center of the acetabulum floor (acetabular fossa), with the x-axis directed along the posterior-anterior direction and the y-axis directed along the superior-inferior direction (Figure 19b). The origin of the (x',y',z') coordinate system coincides with the approximate center of mass of the femur, with the x'-axis directed along the posterior-anterior direction and the y'-axis being directed along the longitudinal axis of the femur (Figure 19a). The location of the origins of these coordinate systems, as shown in Figure 19, are -1.5 cm and 19.5 cm from the intersection points of the y and y' axes with the articular surfaces, respectively.

The articulating surfaces of the hip joint are digitized in their respective coordinate systems as described previously and the results for the coefficients a_{pq} of equation (1) are summarized in Table 3.

ARTICULATING SURFACES OF THE KNEE JOINT

Anatomical Description

The tibial and femoral condyles are the major articulating surfaces of the knee joint (Figure 20). The upper end of the

Table 3

COEFFICIENTS OF THE EQUATIONS OF THE HIP JOINT ARTICULATING SURFACES.

COEFFICIENTS a_{pq} (cm)	ARTICULATING SURFACE	
	Head of Femur	Acetabulum
a_{00}	-19.5628	-1.5131
a_{01}*	-3.9686	-1.2324
a_{02}	1.7498	-0.0416
a_{03}	-0.3864	0.5052
a_{04}	0.0352	0.1025
a_{10}*	0.2045	4.5526
a_{11}	0.2260	10.5723
a_{12}	-0.1281	4.9788
a_{13}	0.0174	0.6813
a_{20}	0.9641	-0.0956
a_{21}	-0.4715	-0.4650
a_{22}	0.0800	0.0034
a_{30}	-0.0382	1.5829
a_{31}	0.0146	0.5512
a_{40}	0.0235	-0.1303

*unitless

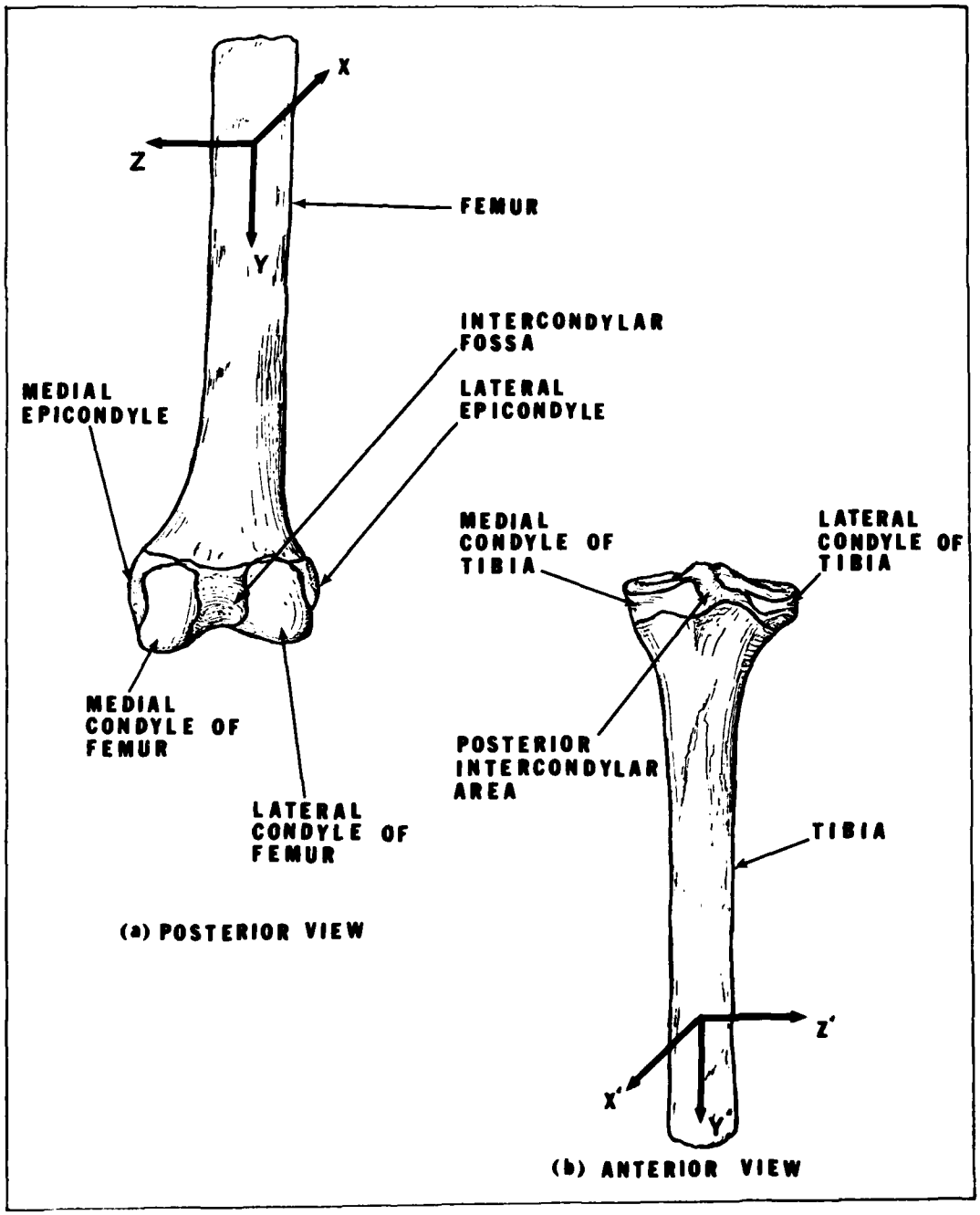

Figure 20. Posterior aspect of the femur and anterior view of the tibia.

tibia is expanded, especially in its transverse axis, providing an adequate bearing surface for the body weight transmitted through the lower end of the femur. It comprises of two prominent masses, the medial and lateral condyles, and a smaller projection, the tuberosity of the tibia. The condyles project backwards a little, so as to overhang the upper part of the posterior surface of the shaft. Superiorly, each is covered with an articular surface, the two being separated by an irregularly roughened intercondylar area. They form visible and palpable landmarks at the side of the ligamentum patella, the lateral condyle being the more prominent.

The medial condyle (Figure 20b) is the larger but does not overhang so much as the lateral condyle. Its upper articular surface, oval in outline, is concave in all diameters, and its lateral border projects upwards, deepening the concavity and covering an elevation, the medial intercondylar tubercle. The posterior surface of the condyle is marked, immediately below the articular margin, by a horizontal, roughened groove. Its medial and anterior surfaces form a rough strip, separated from the medial surface of the shaft by an inconspicuous ridge.

The lateral condyle (Figure 20b) overhangs the shaft, especially at its posterolateral part, which bears on its inferior surface a small circular facet for articulation with the upper end of the fibula. The upper surface is covered with an articular surface for the lateral condyle of the femur. Nearly circular in outline, it is slightly hollowed in its central part, and its medial border extends upwards to cover an elevation, termed the lateral intercondylar tubercle. The posterior, lateral and anterior surfaces of the condyle are rough.

The lower end of the femur is widely expanded and thus provides a good bearing surface for the transmission of the weight of the body to the top of the tibia. It consists of

two prominent masses of bone, the condyles (Figure 20a), which are partially covered by a large articular surface. Anteriorly, the two condyles are united and are continuous with the front of the shaft; posteriorly, they are separated by a deep gap, the intercondylar fossa (intercondylar notch), and they project backwards considerably beyond the plane of the popliteal surface.

The lateral condyle is flattened on its lateral surface and is not so prominent as the medial condyle, but it is stouter and stronger, for it is placed more directly in line with the shaft and probably takes a greater share in the transmission of the weight to the tibia. The most prominent point on its lateral aspect is termed the lateral epicondyle (Figure 20a), and the whole of this surface can be felt through the skin.

The medial condyle possesses a bulging, convex medial aspect, which can be palpated without difficulty. Its uppermost part is marked by a small projection, termed adductor tubercle because it gives insertion to the tendon of the adductor magnus. The most prominent point on the medial surface of the condyle is below and a little in front of the adductor tubercle and is termed the medial epicondyle (Figure 20a). The lateral surface of the condyle is the roughened medial wall of the intercondylar fossa.

Coordinate Systems

The origin of the (x,y,z) coordinate system is placed at the approximate geometric center of the femur with the x-axis directed along the posterior-anterior direction and the y-axis coinciding with the femural longitudinal axis (Figure 20a). The origin of the coordinate system (x',y',z') coincides with the approximate center of mass of the tibia, with the x'-axis directed along the anterior-posterior direction and the y'-axis being directed along the longitudinal axis of the tibia (Figure 20b). The location of the origins of these

coordinate systems, shown in Figure 20, are 19.5 and -20.6 cm from the intersection points of y and y' axes with the lateral articular surfaces.

The articulating surfaces of the knee joint are digitized in their respective coordinate systems according to the technique described previously and the coefficients, a_{pq}, of equation (1) for the tibial and femoral articulating surfaces of the knee joint are summarized in Tables 4 and 5, respectively.

ARTICULATING SURFACES OF THE ANKLE JOINT

Anatomical Description

The major articulating surfaces of the ankle joint are the trochlear surface of the talus and the medial malleolus (Figure 21).

The body of the talus is cuboidal in shape. Its dorsal surface is covered by the trochlear articular surface, which articulates with the lower end of the tibia at the ankle joint. It is convex from back to front and gently concave from side to side, and it is widest anteriorly (Figure 21a). The medial surface of the talus is covered in its upper part by a comma-shaped articular facet which is deeper in front than behind and articulates with the medial malleolus.

The medial malleolus is a short but stout process. Its lateral surface is smooth and occupied by a comma-shaped articular facet, which articulates with the medial side of the talus (Figure 21b). Its anterior surface is rough, and its posterior surface bears the lower end of the groove that marks the posterior surface of the lower end of the bone. The lower border of the malleolus is pointed anteriorly and depressed posteriorly.

Coordinate Systems

The origin of (x,y,z) coordinate system is placed at the approximate geometric center of the tibia, with the x-axis

Table 4

COEFFICIENTS OF THE EQUATIONS OF THE TIBIAL ARTICULATING SURFACES OF THE KNEE JOINT.

COEFFICIENTS a_{pq} (cm)	ARTICULATING SURFACE	
	Tibia Lateral	Tibia Medial
a_{00}	-20.6964	-18.7135
a_{01}*	-1.6128	-1.6587
a_{02}	-0.3786	1.9298
a_{03}	0.0215	-0.7677
a_{04}	0.0117	0.1001
a_{10}*	0.7539	-0.7837
a_{11}	1.0017	0.9363
a_{12}	0.3751	-0.4480
a_{13}	0.0421	0.0677
a_{20}	0.2212	-0.3921
a_{21}	0.1889	0.1772
a_{22}	0.0335	-0.0123
a_{30}	0.0885	-0.2331
a_{31}	0.0367	0.0670
a_{40}	0.0373	-0.0369

*unitless

Table 5

COEFFICIENTS OF THE EQUATIONS OF THE FEMORAL ARTICULATING SURFACES OF THE KNEE JOINT.

COEFFICIENTS a_{pq} (cm)	ARTICULATING SURFACE	
	Femur Lateral	Femur Medial
a_{00}	19.5520	18.5270
a_{01}*	-1.9895	8.9256
a_{02}	0.6298	-7.2093
a_{03}	0.8031	2.4873
a_{04}	-0.0055	-0.3193
a_{10}*	-1.4614	0.1211
a_{11}	-2.5323	-0.5608
a_{12}	-1.3528	0.1310
a_{13}	0.2354	-0.0500
a_{20}	-0.1912	-0.5928
a_{21}	0.0620	-0.0411
a_{22}	-0.4573	-0.0557
a_{30}	-0.1305	-0.2447
a_{31}	0.2058	-0.0332
a_{40}	-0.0544	-0.0376

*unitless

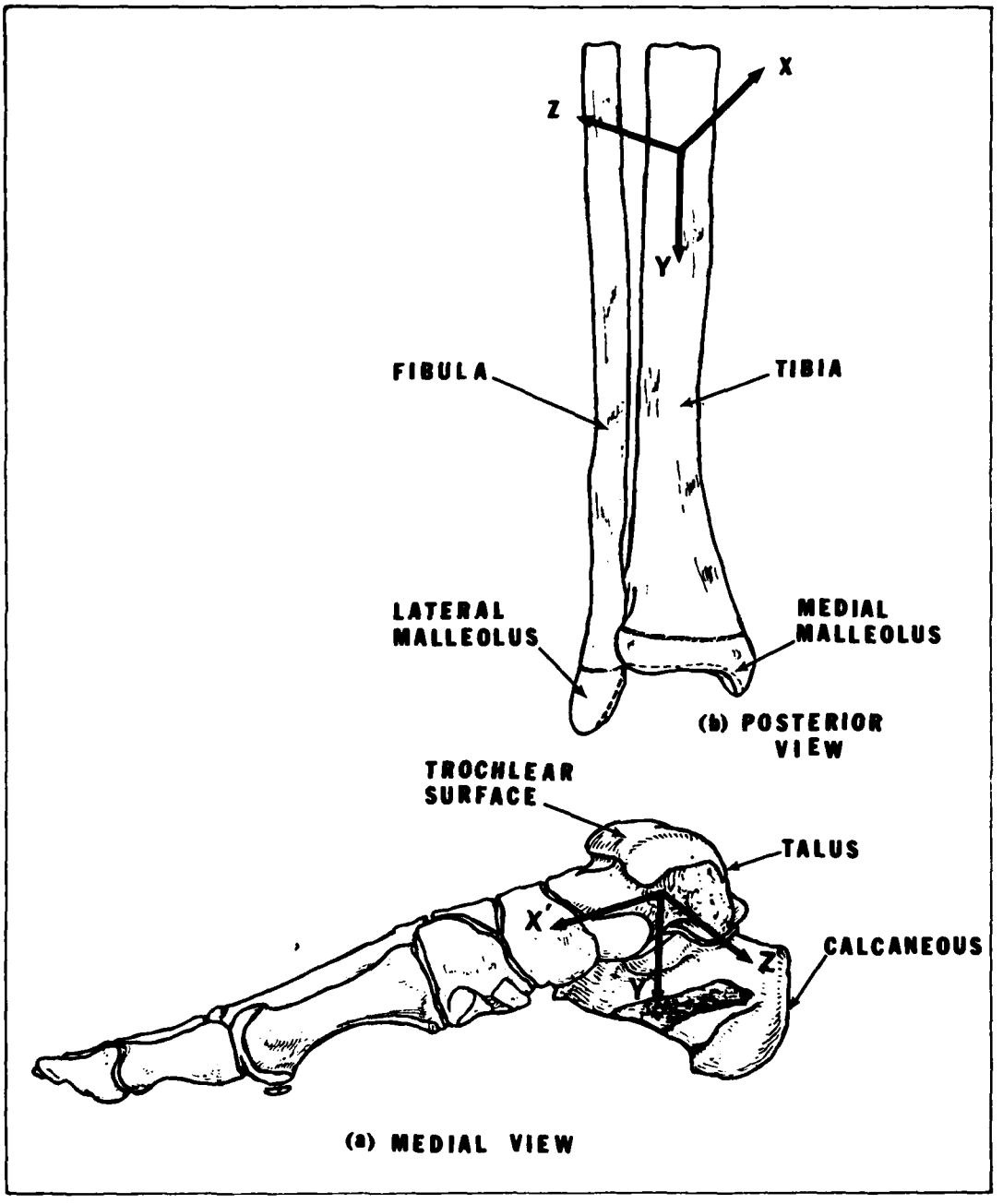

Figure 21. Medial and posterior aspects of the talus and malleolus.

directed along the posterior-anterior direction and the y-axis coinciding with the longitudinal axis of tibia (Figure 21b). The origin of the coordinate system (x',y',z') coincides with the approximate center of mass of the talus, with the x'-axis directed along the posterior-anterior direction and the y'-axis being directed along the inferior-superior direction of the talus (Figure 21a). The location of the origins of these coordinate systems, shown in Figure 21, are 20.2 cm and 1.3 cm from the intersection points of the y and y' axes with the articular surfaces, respectively.

The articulating surfaces of the ankle joint are digitized in their respective coordinate systems according to the technique described previously and the coefficients, a_{pq}, of equation (1) are summarized in Table 6.

MATHEMATICAL REPRESENTATION OF LIGAMENTS

Structural integrity of the articulating joints is maintained by capsular ligaments and both extra- and intra-articular ligaments. Capsular ligaments are formed by thickening of the capsule walls where functional demands are greatest. As the names imply, extra- and intra-articular ligaments at the joints reside external to and internal to the joint capsule, respectively. Extra-articular ligaments have several shapes, e.g. cord-like or flat depending on their locations and functions. These types of ligaments appear abundantly at the articulating joints. However, only the shoulder, hip and knee joints contain intra-articular ligaments. For example, the cruciate ligaments at the knee joint are probably the most well known intra-articular ligaments. Further information about the structure and mechanics of the joint can be found in Barnett, Davies, and Mac Conaill [1949].

Ligament configurations are largely dependent on arrangement of the joint and its articulation, the direction

Table 6

COEFFICIENTS OF THE EQUATIONS OF THE ARTICULATING SURFACES OF THE ANKLE JOINT.

COEFFICIENTS a_{pq} (cm)	ARTICULATING SURFACE	
	Talus (Trochlear)	Medial Malleolus
a_{00}	-1.4684	20.2305
a_{01}*	0.3722	-0.0445
a_{02}	-0.1347	-0.1872
a_{03}	-0.0227	0.0010
a_{04}	0.0549	0.0601
a_{10}*	0.1428	-0.0689
a_{11}	0.0018	0.1748
a_{12}	-0.1114	-0.0195
a_{13}	-0.0454	-0.0725
a_{20}	0.3446	0.1118
a_{21}	-0.0123	0.0319
a_{22}	-0.0115	0.0757
a_{30}	0.0516	0.0369
a_{31}	0.0154	-0.0232
a_{40}	-0.0072	0.0316

*unitless

of tendons, and the location of the organs. Thus, in different joints, according to their structure, ligaments may be more or less lax, or tight, or capable of more or less movement. Because of the difference in the direction of the tendons or the placement of the membranes and their site and magnitude, ligaments vary in their configurations, circumvolution and extension. On account of all these factors, some ligaments are twisted like cords, some are united in fibrous bonds and others flattened into membranous forms. This variation in form is indicated in their corresponding names according to size: major, minor, maximus; according to external form: large, thick, thin; according to configuration: long, wide, round, triangular, quadrate, circular; according to their positions: straight, transverse, oblique, horizontal, perpendicular, superficial, sublime, deep, lateral, right, left, anterior, posterior, superior and inferior; according to their insertion: interclavicular, brachioradial, etc. (Gray [1973]).

In this section, general aspects and material characteristics of soft tissues, in general, and ligaments in particular, are studied. Ligaments are modeled as non-linear elastic springs and their constitutive equation and stiffness values are presented. Attachment sites of the elbow, hip, knee and ankle joint ligaments are determined and summarized.

GENERAL CHARACTERISTICS

Ligaments, capsule and other connective tissues such as tendons, skin and blood vessels, consist mainly of collagen and elastin fibers embedded in a mucopolysaccharide intercellular ground substance (Wismans [1980]). Geometrical arrangements and the relative amount of each of the components of the fibers vary from tissue to tissue. Usually, in ligaments and tendons, collagen fibers are oriented in the direction of the transmitted force while the elastin fibers form a disordered network. Crisp [1972] reported that under no external

loading of the tissue, the collagen bundles are coiled. Due to the difficulties involved in the dissection of the components of biological structures, the mechanical properties of the collagen and elastin fibers are usually determined for a tissue in which one of the components is predominent. Material properties of collagen are often determined by the use of tendons. Elliot [1965] reported that in tendons of the human body, about 75% of the dry weight is collagen and just 2% is elastin.

Physical behavior and the stress in a biological tissue not only depends on strain but also on strain history. This behavior is evident in phenomena such as stress relaxation, creep, hysteresis and dependence of the elastic moduli on the strain rate and temperature. A number of mathematical descriptions characterizing this behavior are proposed in the literature. These descriptions may be divided into two groups.

In the first group, the measured microscopic response of the tissue is characterized by a continuous, nonlinear equation, as in the quasi-linear visco-elastic law of Fung [1972]. The most noticeable feature of the mechanical behavior of biological tissues is that measurable stresses develop only after the specimen has been stretched considerably from its original or relaxed length. In such an extension, the stress-strain law becomes highly nonlinear and classical theory of elasticity, which is restricted to linear stress-strain relations and small strains, is not applicable. The nonlinear stress-strain relations developed in the analysis of finite homogeneous deformations of elastomers have been studied by Mooney [1940], Rivlin [1948] and on the basis of strain energy function by Green and Adkins [1960]. Fung [1967] has shown that the elastic properties of mesentery are completely different from those of vulcanized rubber. He has concluded that the stress-strain relation in the one-dimensional case should be exponential in the stretch mode.

A generalization of Fung's result to three-dimensional problems was given by Gou [1970], who introduced a strain energy density which is an exponential function of the strain invariant. Various potential functions describing the large deformation of biological tissue and its response to various forces are presented in the literature. These include the works by Blatz, Chu and Wayland [1969], Lee, Frasher and Fung [1967], Hildebrandt, Fukaya and Martin [1969], Veronda and Westman [1970], Simon, et al., [1970], and Demiray [1972]. In general, however, these functions have been developed for a specific loading pattern and assumed material isotropy. A more general function permitting the study of a number of types of loads and interaction between combined loads is given by Snyder [1972].

In this first group, there are also represented models in which the tissue response is described by a mechanical analogy, consisting of a number of spring, dashpot and dry frictional elements. For example, nonlinear visco-elastic behavior of collagenous tissue has been simulated by Frisen, et al., [1969], using a Kelvin model and a number of nonlinear springs.

In the second group the mathematical description is based on an idealization of the microstructures and on the mechanical properties of the constituent materials. Based on the knowledge that the connective tissues are composed of fibrous and amorphous materials they may be treated as fiber-reinforced materials. The initial part of the loading phase is a geometrical rearrangement of the microstructural network due to uncoiling of the coiled fibers of collagen. Linear constitutive equations are assumed for the second part of the loading in which the collagen fibers are elongated. The models by Comninou and Yannas [1976], and Drouin [1980] on the one-dimensional stress field studies of elastic behavior of

collagenous tissues and two material composite prosthesis, respectively, fall in this group.

In this study simulation of joint ligaments is accomplished by a mathematical description based on an approximation of experimental data reported in the literature. Ligaments will be represented by nonlinear elastic springs as the experiments were limited to a one-dimensional stress field and information is available only on the elastic behavior. Due to the microstructure and the orientation of the collagen fibers, representation of ligaments by springs would seem to be a realistic approach. The general form of the constitutive equation and the values of the parameters characterizing the constitutive equations of the different springs are discussed below.

CONSTITUTIVE EQUATION

A constitutive equation representing ligamentous behavior is based on available data in the literature. Data concerned with the knee joint ligaments is considered since the general theoretical analysis developed later in this report will be applied to the knee joint.

Brantigan and Voshell [1941] presented a review of the conflicting theories on the function of knee ligaments prior to 1940 and reported the results of study on approximately 100 knees. Since that time many investigators have discussed the function of various ligamentous structures (Hallen and Lindhal [1965] and [1966]; Hughston and Eilers [1973]; Kennedy and Grainger [1967]; Kennedy and Fowler [1971]; Kennedy, Weinberg and Wilson [1974]; Robinson and Romero [1968]; Slocum and Larson [1968]; Warren, Marshall and Girgis [1974]; Girgis, et al., [1975]; Trent and Walker, [1975]; Piziali, Rastegar and Nagel [1977]; Piziali, et al., [1980]; and Seering, et al., [1980]), and the length of primary structures as a function of knee flexion (Edwards, Lafferty and Lange [1969]; Wang,

Walker and Wolf [1973]; and Crowninshield, Pope and Johnson [1976]. In addition, pure torsional rotation with and without contact pressure has been measured by Wang and Walker [1974].

Force-deflexion characteristics of several types of ligaments under uniaxial tension has been reported by Trent, Walker and Wolf [1976], Kennedy, et al., [1976], Noyes and Grood [1976] and Dorlot, et al., [1980]. Usually four characteristic regions of the force-deflexion curve of collagenous tissue are identified. The location of these regions (Figure 22) can be explained in terms of microarchitecture (Crisp [1972]; Wismans [1980]). The stiffness of the tissue, defined by the slope of the load-deflexion curve, is rather slight in region 1. This initial region is considered mainly to correspond to the geometrical rearrangement of the microstructural network (uncoiling of the coiled collagen fibers). Therefore, the stiffness is determined mainly by the stiffness of the elastin network. The stiffness increases in region 2 as some of the fibers become aligned. All collagenous fibers are assumed to be fully uncoiled at the end of this region. As the force on the tissue steadily increases, the collagen fibers themselves elongate. In region 3, the stiffness is reported to correspond mainly to the stiffness of the collagen fibers and is found to be almost constant. Finally in region 4, disruption of some collagen fibers is observed, followed by a complete failure of the tissue itself.

The force-elongation curve of Figure 22 can be represented by a quadratic equation. Haut and Little [1972] carried out a number of tension tests on rat-tail collagen bundles and reported that at low strains, the elastic behavior of this tissue could be described by a quadratic stress-strain equation. Crowninshield, Pope and Johnson [1976] tested human medial collateral ligaments and indicated that a quadratic stress-strain function is a good approximation for the elastic

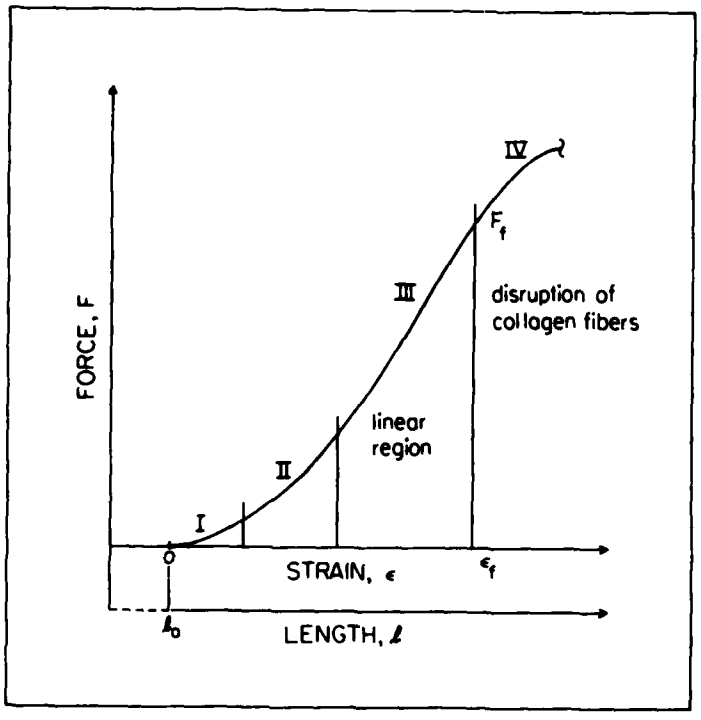

Figure 22. Force-elongation curve for collagenous tissues.

behavior of such tissue. In this study the following force-elongation relationship is assumed for each ligament:

$$|\bar{F}_j| = k_j(L_j - \ell_j)^2 \quad \text{for} \quad L_j > \ell_j \tag{3}$$

in which k_j is the spring constant, L_j and ℓ_j are, respectively the current and initial lengths of the ligament, j. It is assumed that the ligaments cannot carry any compressive force; accordingly:

$$|\bar{F}_j| = 0 \quad \text{for} \quad L_j < \ell_j \tag{4}$$

The direction of the force, F_j, exerted by a spring on the articulating body segment coincides with the direction of the line segment through the origin and insertion points of that spring. The length, ℓ_j, of spring j is equal to the distance between its insertion and origin points.

LIGAMENT STIFFNESS

Several studies concerned with the tension tests of human knee joint ligaments have been reported in the literature. Among these studies, the work of Noyes and Grood [1976], Trent, Walker and Wolf [1976], and Kennedy, et al., [1976] will be considered in this section.

Twenty-one anterior cruciate ligaments have been tested by Noyes and Grood [1976]. The intact knee joints were kept in a frozen condition for about four weeks. They were thawed at room temperature a day before testing. The specimens were then mounted in the testing machine at 45° of flexion and, at an elongation rate of 25 mm/sec., they were tested to failure. The stiffness, k, the strain ε_f, and the corresponding force, F_f, were determined. The mean values of these quantities are summarized in Table 7. Large deviations between the specimens are evident and the younger ligaments are much stiffer than older ones.

The cruciates and the collateral ligaments of six fresh specimens together with a piece of their bony attachments were tested by Trent, Walker and Wolf [1976]. The specimens were loaded to failure in a normal saline solution at 37°C and at an elongation rate of 0.8 mm/sec. Table 7 shows the mean-values for the stiffness, k. The values for the anterior cruciate is close to the mean values reported by Noyes and Grood [1976] for the older specimens.

Kennedy, et al., [1976] tested twenty anterior, posterior and collateral ligaments at two different strain rates of 2 and 8 mm/second. The specimens were tested some fourteen hours after death and were kept in isotonic saline. The ligaments were tested without their bony attachments. Each ligament was fixed in an upper clamp initially and allowed to hang freely, seeking its own orientation. A lower clamp was then applied. Special care was made to avoid twisting the ligaments. The mean values of the strain, ε_f, and

Table 7

COMPARISON OF SOME AVERAGE LIGAMENT CHARACTERISTICS REPORTED BY TRENT, WALKER AND WOLF [1976], KENNEDY, ET AL. [1976], AND NOYES AND GROOD [1976]. (REPRODUCED FROM WISMANS [1980]).

LIGAMENT	REFERENCE	NUMBER OF SPECIMENS	AGE (YEARS)	ELONGATION RATE (mm/sec)	F_f (N)	ε_f (%)	K (N/ε)
ANTERIOR CRUCIATE	Trent	6	29-55	0.8	--	--	3000
	Kennedy	10	--	2.0	394	23	--
	Kennedy	10	--	8.0	502	28	--
	Noyes	20	48-86	25.0	622	22	3500
	Noyes	6	16-26	25.0	1170	26	4900
POSTERIOR CRUCIATE	Trent	6	29-55	0.8	--	--	4500
	Kennedy	10	--	2.0	798	21	--
	Kennedy	10	--	8.0	868	19	--
LATERAL COLLATERAL	Trent	5	29-55	0.8	--	--	3000
MEDIAL COLLATERAL	Trent	4	29-55	0.8	--	--	5100
	Kennedy	10	--	2.0	454	20	--
	Kennedy	10	--	8.0	534	17	--

corresponding force, F_f, are given in Table 7. No stiffness data or age of specimens were reported in this study. The variation in the results reported by Kennedy, et al., [1976] and those of Noyes and Grood [1976] may be explained partly by possible slipping of the specimens between the clamps and differences in elongation rates.

In this study, the values of the stiffness, k_j, for different springs is based on the mean data reported by Trent, Walker and Wolf [1976]. For the stiffness of the medial collateral ligament a correction reported by Wisman [1980] is used in order to account for the oblique and the deep medial collateral ligament, since these parts were not included in the specimens tested by Trent, Walker and Wolf [1976]. This correction is based on data presented by crowninshield, Pope and Johnson [1976]. Stiffness values used in this study for the lateral collateral (LC), the medial collateral (MC), the anterior cruciate (AC), and the posterior cruciate (PC) ligaments are summarized in Table 8.

Table 8

LIGAMENT STIFFNESS FOR THE LATERAL COLLATERAL (LC), MEDIAL COLLATERAL (MC), ANTERIOR CRUCIATE (AC) AND POSTERIOR CRUCIATE (PC) LIGAMENTS.

Ligament	$K_m (N/mm^2)$
LC	15
MC	15
AC	30
PC	35

INSERTIONS AND ORIGINS

Accurate determination of attachment sites or the so-called insertions and origins, of ligaments are of considerable importance in the mathematical modeling of the articulating joint. Very little quantitative information is available on this subject. Attachment sites and the lengths of the knee joint ligaments have been measured in vivo and in vitro and reported by Crowninshield, Pope, and Johnson [1976].

In this study, by close physical and anatomical study of the elbow, hip, knee, and ankle joints (Grant [1962]; Gray [1973]), the attachment sites of their respective ligaments have been measured and summarized in Table 9. For each joint, insertion points are measured with respect to its (x',y',z') coordinate system and origins with respect to its (x,y,z) coordinate system. Note that attachment sites of only those ligaments which significantly contribute to the integrity and functional aspects of the joints have been measured, and due to the expanded shape of some of the ligaments, slight variation may be inherent in these measurements.

TWO-DIMENSIONAL DYNAMIC FORMULATION OF A TWO-BODY SEGMENTED JOINT

The mathematical descriptions of the articular surfaces, ligaments and capsule thus far presented can now be integrated into a two-dimensional mathematical formulation of a general two-body, segmented articulating joint.

For the purpose of studying the joint motion, one segment is assumed to be fixed while the other segment is executing a relative motion. The coordinate systems (x,y) and (x',y') are attached to the fixed and the moving body segments, respectively, and their relative position and angular orientation will be discussed. Next the contact conditions between the two articulating surfaces are presented, and the description of ligaments, contact and applied external forces and

Table 9

INSERTIONS AND ORIGINS FOR THE LIGAMENTS OF THE ELBOW, HIP, KNEE AND ANKLE JOINTS

JOINT	LIGAMENT	ORIGIN (cm)			INSERTION (cm)		
		x_j	y_j	z_j	x'_j	y'_j	z'_j
ELBOW	Ulnar Collateral	0.10	14.10	2.70	-0.10	1.20	-2.40
	Radial Collateral	0.30	14.60	-3.10	0.10	2.10	1.70
HIP	Iliofemoral	3.10	-1.60	-2.90	1.10	-17.80	-0.30
	Pubofemoral	2.30	1.20	-2.20	1.10	-17.40	0.20
	Ischiofemoral	-1.80	-2.30	-3.10	-0.70	-19.80	-0.90
	Teres Femoris	0.50	2.50	-1.60	-0.80	-21.30	4.10
KNEE	Tibial Collateral	-2.00	20.30	4.00	0.50	-10.50	1.20
	Fibular Collateral	-1.80	19.70	-3.50	-1.30	16.30	-5.00
	Anterior Cruciate	-2.50	20.40	-0.80	1.50	-19.50	0.50
	Posterior Cruciate	-2.00	21.30	1.00	-2.00	-18.50	-0.30
ANKLE	Tibionavicular	0.20	20.70	2.40	2.80	-0.80	1.70
	Tibiocalcanean	-0.90	20.90	2.10	-0.80	0.10	1.40
	Posterior Tibiotalar	-1.60	20.90	2.00	-1.90	3.10	1.10
	Anterior Talofibular	1.10	21.10	-2.60	1.80	1.70	-1.20
	Posterior Talofibular	-0.90	22.00	-2.80	-0.50	0.10	-0.90
	Calcaneo Fibular	0.60	22.20	-3.30	-1.70	2.90	-3.40

moments, along with the governing dynamic equations of motion are presented. A numerical procedure employing the Newmark method of differential approximation and Newton-Raphson iteration process is suggested for the solution of these coupled, nonlinear algebraic and differential equations.

CHARACTERIZATION OF THE RELATIVE POSITIONS

A joint connects two segments of a body which are designated as segments 1 and 2 and, for illustrative purposes, will be represented as shown in Figure 23. The position of moving body segment 1 relative to the fixed body segment 2 is described by two independent coordinate systems shown in Figure 23. An inertial coordinate system (x,y) with unit

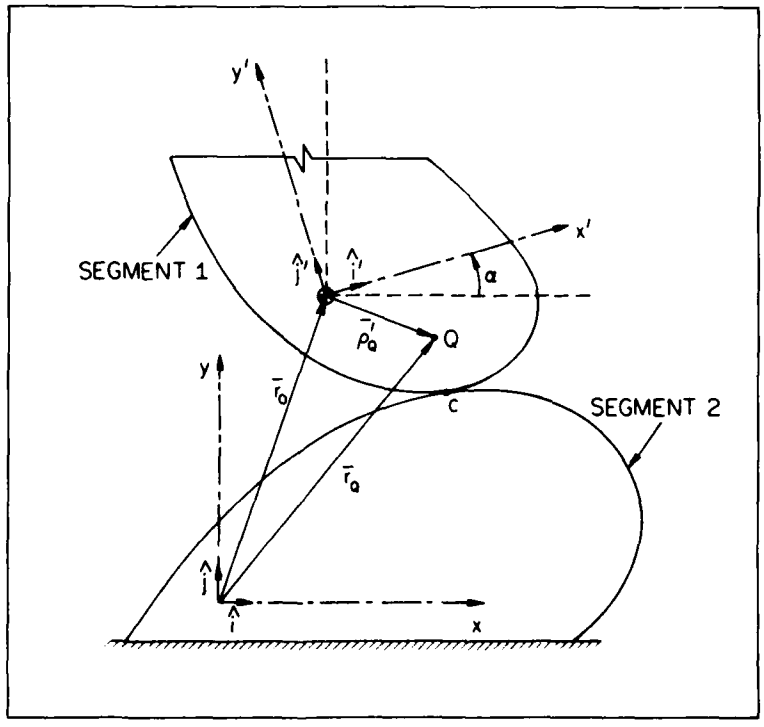

Figure 23. A two-body segmented joint is illustrated showing the position of a point, Q, attached to the moving coordinate system (x',y').

vectors $\hat{i}$ and $\hat{j}$ is connected to the fixed body segment, while the coordinate system (x',y') with unit vectors $\hat{i}'$ and $\hat{j}'$ is attached to the center of mass of the moving body segment 1.

The motion of the moving (x',y') system relative to the fixed (x,y) system may be characterized by three quantities: the translational movement of the origin of the (x',y') system in the x and y-directions, and its rotation, α, with respect to the x and y-axis.

Let the position vector of the origin of the (x',y') system, in terms of the fixed system, be given by:

$$\bar{r}_o = \hat{x}_o i + y_o \hat{j} \tag{5}$$

Let the vector $\bar{\rho}'_Q$ be the position vector of an arbitrary point, Q, on the moving body segment in the base $(\hat{i}',\hat{j}')$. Let $\bar{r}_Q$ be the position vector of the same point in the base $(\hat{i},\hat{j})$. That is,

$$\bar{\rho}'_Q = x'_Q i' + y'_Q j' \tag{6}$$

$$\bar{r}_Q = x_Q \hat{i} + y_Q \hat{j} \tag{7}$$

Referring to Figure 23, for vectors $\bar{\rho}'$ and $\bar{r}$, the following relationship can be written:

$$[r_Q] = [r_o] + [T][\rho'_Q] \tag{8}$$

where [T] is a 2x2 orthogonal transformation matrix. The angular orientation of the (x',y') system with respect to the (x,y) system is specified by the four components of [T] matrix. Assuming α to be the angle between the positive direction of x-axis and the positive direction of x'-axis (Figure 23), then the transformation matrix [T] is written as:

$$[T] = \begin{bmatrix} \cos\alpha & -\sin\alpha \\ \sin\alpha & \cos\alpha \end{bmatrix} \tag{9}$$

Therefore, the position in the (x,y) system of any given point in (x',y') system can be determined knowing [T] and $\bar{r}_o$.

CONTACT CONDITIONS

Assuming rigid body contact between the two body segments at point C as shown in Figure 24, let us represent the contact surfaces by smooth mathematical functions of the following form:

$$y = f_1(x) \tag{10}$$

$$y' = f_2(x') \tag{11}$$

As implied, equations (10) and (11) represent the fixed and moving surfaces, respectively.

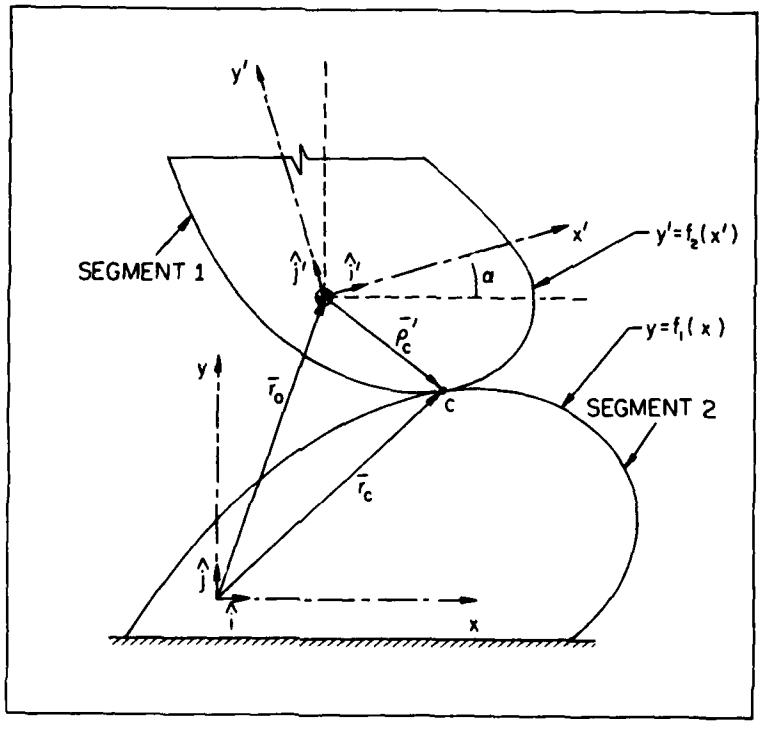

Figure 24. A two-body segmented joint is illustrated showing contact point, C, location and relevant vectors.

The position vectors of the contact point, C, in the base $(\hat{i},\hat{j})$, is denoted by:

$$\bar{r}_c = x_c\hat{i} + f_1(x_c)\hat{j} \tag{12}$$

and the corresponding one in the base $(\hat{i}',\hat{j}')$, is given by

$$\bar{\rho}_c' = x_c'\hat{i}' + f_2(x_c')\hat{j}' \tag{13}$$

Then at the contact point, C, the following relationship must hold:

$$[r_c] = [r_o] + [T][\rho_c'] \tag{14}$$

This is a part of the geometric compatibility condition for the two contacting surfaces. In addition, the unit normals to the surfaces of the moving and fixed body segments must be colinear.

Let $\hat{n}_1$ and $\hat{t}_1$ be, respectively, the unit normal and unit tangential vectors to the fixed surface, $y = f_1(x)$, at the contact point, C, (Figure 25) and represented by:

$$\hat{n}_1 = n_{1x}\hat{i} + n_{1y}\hat{j} \tag{15}$$

$$\hat{t}_1 = t_{1x}\hat{i} + t_{1y}\hat{j} \tag{16}$$

or for $\hat{t}_1$:

$$\hat{t}_1 = \frac{d\bar{r}_c}{ds} \tag{17}$$

By definition, a unit normal vector directed toward the center of curvature is given by:

$$\hat{n}_1 = R\,\frac{d\hat{t}_1}{ds} \tag{18}$$

where R is the radius of curvature and is defined as

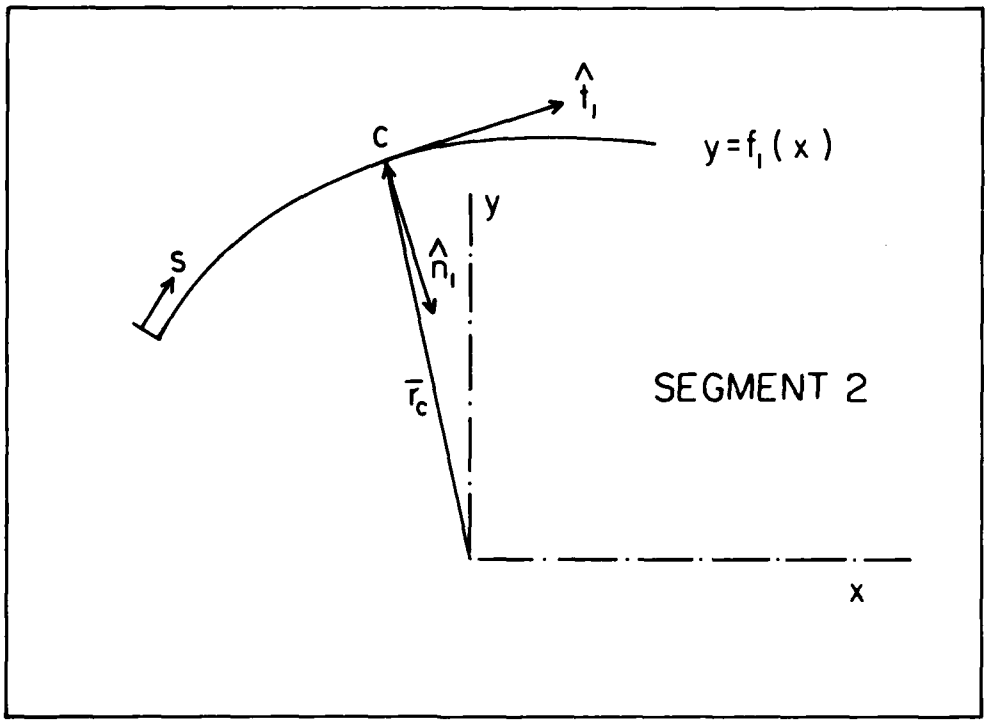

Figure 25. Unit normal, $\hat{n}_1$, and tangential, $\hat{t}_1$, vectors at the contact point, C.

$$R = \frac{[1 + (df_1/dx)^2]^{3/2}}{|d^2f_1/dx^2|} \tag{19}$$

The distance, ds, along the surface, $y = f_1(x)$, is defined as:

$$ds = \sqrt{(dx)^2 + (dy)^2}$$

or

$$ds = \sqrt{1 + \left(\frac{df_1}{dx}\right)^2}\ dx \tag{20}$$

Substituting equation (20) in equation (17) gives:

$$\hat{t}_1 = \frac{1}{\sqrt{1 + (df_1/dx)^2}} \frac{d\bar{r}_c}{dx} \tag{21}$$

Consequently, equation (18) can be written as:

$$\hat{n}_1 = \frac{R}{\sqrt{1 + (df_1/dx)^2}} \frac{d\hat{t}_1}{dx} \tag{22}$$

But from equation (21):

$$\frac{d\bar{t}_1}{dx} = \frac{1}{\sqrt{1 + (df_1/dx)^2}} \frac{d^2\bar{r}_c}{dx^2} - \frac{(df_1/dx)(d^2f_1/dx^2)}{[1 + (df_1/dx)^2]^{3/2}} \frac{d\bar{r}_c}{dx}$$

or:

$$\frac{d\bar{t}_1}{dx} = \frac{1}{[1 + (df_1/dx)]^{1/2}} \left[\frac{d^2\bar{r}_c}{dx^2} - \frac{(df_1/dx)(d^2f_1/dx^2)}{[1 + (df_1/dx)^2]} \frac{d\bar{r}_c}{dx} \right] \tag{23}$$

Combining equations (22) and (23):

$$\hat{n}_1 = \frac{[1 + (df_1/dx)^2]^{1/2}}{|d^2f_1/dx^2|} \left[\frac{d^2\bar{r}_c}{dx^2} - \frac{(df_1/dx)(d^2f_1/dx^2)}{[1 + (df_1/dx)^2]} \frac{d\bar{r}_c}{dx} \right] \tag{24}$$

But:

$$\frac{d\bar{r}_c}{dx} = \hat{i} + \left(\frac{df_1}{dx} \right) \hat{j} \tag{25}$$

and

$$\frac{d^2\bar{r}_c}{dx^2} = \left(\frac{d^2f_1}{dx^2} \right) \hat{j} \tag{26}$$

Substituting equations (25) and (26) into equation (24):

$$\hat{n}_1 = \frac{[1 + (df_1/dx)^2]^{1/2}}{|d^2f_1/dx^2|} \frac{d^2f_1}{dx^2} \left\{ \hat{j} - \frac{df_1/dx}{[1 + (df_1/dx)^2]} \left(\hat{i} + \frac{df_1}{dx} \hat{j} \right) \right\}$$

or:

$$\hat{n}_1 = \frac{(d^2f_1/dx^2)}{|d^2f_1/dx^2|}\left[1 + (df_1/dx)^2\right]^{1/2}\left\{ - \frac{df_1/dx}{[1 + (df_1/dx)^2]}\,\hat{i} + \left[1 - \frac{(df_1/dx)^2}{[1 + (df_1/dx)^2]}\right]\hat{j}\right\}$$

Simplifying the above equation yields:

$$\hat{n}_1 = \frac{(d^2f_1/dx^2)}{|d^2f_1/dx^2|}\left[1 + \left(\frac{df_1}{dx}\right)^2\right]^{-1/2}\left[- \left(\frac{df_1}{dx}\right)\hat{i} + \hat{j}\right]_{x=x_c} \tag{27}$$

where x_c is the x-coordinate of the contact point, C, in the base $(\hat{i},\hat{j})$. From equations (15) and (27) it can be shown that

$$n_{1x}^2 + n_{1y}^2 = 1 \tag{28}$$

which is an expected result since n_{1x} and n_{1y} are respectively the x and y components of unit vector $\hat{n}$. Similarly, following the same procedure as was outlined for $\hat{n}_1$, at the point of contact, C, the unit normal vector, $\hat{n}_2'$, to the surface, $y' = f_2(x')$, directed toward its center of curvature, can be written as:

$$\hat{n}_2' = \frac{\left(\frac{d^2f_2}{dx'^2}\right) \Big/ \left|\frac{d^2f_2}{dx'^2}\right|}{\left[1 + \left(\frac{df_2}{dx'}\right)^2\right]^{1/2}}\left[- \left(\frac{df_2}{dx'}\right)\hat{i}' + \hat{j}'\right]_{x'=x'_c} \tag{29}$$

where x_c' is the x'-coordinate of the contact point, C, in the base $(\hat{i}',\hat{j}')$. From the transformation matrix [T], given in equation (9), the coordinate base $(\hat{i}',\hat{j}')$ is related to coordinate base $(\hat{i},\hat{j})$ by:

$$\hat{i}' = \cos\alpha\,\hat{i} + \sin\alpha\,\hat{j} \tag{30}$$

$$\hat{j}' = -\sin\alpha\ \hat{i} + \cos\alpha\ \hat{j} \tag{31}$$

Substituting equations (30) and (31) into equation (29), yields:

$$\hat{n}_2 = \frac{(d^2f_2/dx'^2)}{|d^2f_2/dx'^2|}\left[1 + \left(\frac{df_2}{dx'}\right)^2\right]^{-1/2}\left[-\left(\cos\alpha\,\frac{df_2}{dx'} + \sin\alpha\right)\hat{i} + \left(\cos\alpha - \sin\alpha\,\frac{df_2}{dx'}\right)\hat{j}\right] \tag{32}$$

The colinearity of the normals at the point of contact, C, requires that:

$$\hat{n}_1 \times \hat{n}_2 = 0 \quad \text{at} \quad x=x_c\ ,\ x'=x'_c \tag{33}$$

that is:

$$\left\{\frac{\left(\frac{d^2f_1}{dx^2}\right)\Big/\left|\frac{d^2f_1}{dx^2}\right|}{\left[1 + \left(\frac{df_1}{dx}\right)^2\right]^{1/2}}\left(-\frac{df_1}{dx}\,\hat{i} + \hat{j}\right)\right\} \times \left\{\frac{\left(\frac{d^2f_2}{dx'^2}\right)\Big/\left|\frac{d^2f_2}{dx'^2}\right|}{\left[1 + \left(\frac{df_2}{dx'}\right)^2\right]^{1/2}}\left[-\left(\cos\alpha\,\frac{df_2}{dx'} + \sin\alpha\right)\hat{i} + \left(\cos\alpha - \sin\alpha\,\frac{df_2}{dx'}\right)\hat{j}\right]\right\} = 0 \tag{34}$$

or:

$$\sin\alpha\,\frac{df_1}{dx}\,\frac{df_2}{dx'} - \cos\alpha\,\frac{df_1}{dx} + \cos\alpha\,\frac{df_2}{dx'} + \sin\alpha = 0 \tag{35}$$

Finally, the contact condition takes the following form:

$$\sin\alpha\left[1 + \left(\frac{df_1}{dx}\right)_{x=x_c}\left(\frac{df_2}{dx'}\right)_{x'=x'_c}\right] - \cos\alpha\left[\left(\frac{df_1}{dx}\right)_{x=x_c} - \left(\frac{df_2}{dx'}\right)_{x'=x'_c}\right] = 0 \tag{36}$$

DYNAMIC EQUATIONS OF THE MOVING BODY SEGMENT

The total load acting on the moving body segment is divided into forces exerted by nonlinear springs which are simulating the ligament and capsule forces, contact forces between the moving and fixed body segments and applied external forces and moments (Figure 26). In the following sections, each of these forces will be mathematically formulated and final equations of motion for the moving body segment will be presented.

Ligament Forces

Representation of ligaments and capsules as nonlinear elastic springs along with their governing constitutive equations were discussed previously. The force, F_j, in nonlinear spring, j, is a function of its length, ℓ_j, that is:

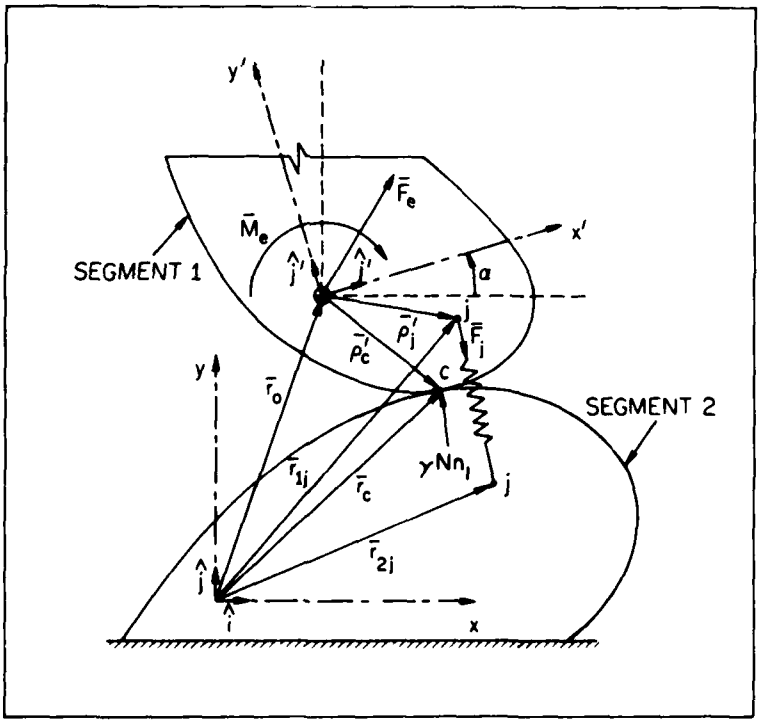

Figure 26. Forces acting on the moving body segment of a two-body segmented joint.

$$F_j = \dot{f}(\ell_j) \tag{37}$$

Let $(\bar{\rho}'_j)_m$ be the position vector in the base $(\hat{i}',\hat{j}')$ of the insertion point of the ligament, j, in the moving body segment. The position vector of the origin point of the same ligament, j, in the fixed body segment is denoted by $(\bar{r}_{2j})_f$ in the base $(\hat{i},\hat{j})$. Here the subscripts m and f outside the parenthesis imply "moving" and "fixed", respectively. The current length of the ligament is given by:

$$L_j = \sqrt{[(\bar{r}_{2j})_f - \bar{r}_o - T(\bar{\rho}'_j)_m] \cdot [(\bar{r}_{2j})_f - \bar{r}_o - T(\bar{\rho}'_j)_m]} \tag{38}$$

The unit vector, $\hat{\lambda}_j$, along the ligament, j, directed from the moving to the fixed body segment is:

$$\hat{\lambda}_j = \frac{1}{L_j} [(\bar{r}_{2j})_f - \bar{r}_o - T(\bar{\rho}'_j)_m] \tag{39}$$

Thus, the axial force in the ligament, j, in its vectorial form, becomes:

$$\bar{F}_j = F_j \hat{\lambda}_j \tag{40}$$

where F_j is given by equation (3).

Contact Forces

Since the friction force between the moving and fixed body segment is neglected, the contact force will be in the direction of the normal to the surface at the point of contact. The contact force, $\bar{N}$, acting on the moving body segment is given by:

$$\bar{N} = \gamma N \hat{n}_1 \quad \text{at} \quad x=x_c \tag{41}$$

where N is the magnitude of the contact force and

$$\gamma = \frac{(d^2f_1/dx^2)}{|d^2f_1/dx^2|} \quad \text{at} \quad x=x_c \tag{42}$$

γ is either +1 or -1 and it ensures the correct direction of the contact force acting on the moving body segment.

Applied External Forces and Moments

In order to achieve the desired joint motion, an external force, $\bar{F}_e$, and a moment, $\bar{M}_e$, of known magnitude and direction are applied to the center of mass of the moving body segment. The force, $\bar{F}_e$, and moment, $\bar{M}_e$, are applied in the base $(\hat{i},\hat{j})$ and their resultants are given as:

$$\bar{F}_e = (F_e)_x \hat{i} + (F_e)_y \hat{j} \tag{43}$$

$$\bar{M}_e = M_e \hat{k} \tag{44}$$

where M_e is the magnitude of the applied moment vector, $\bar{M}_e$.

Equations of Motion

The dynamic equations of motion of the moving body relative to the fixed body segment are as follows:

$$(F_e)_x + \gamma N(n_1)_x + \sum_{j=1}^{p} F_j(\lambda_j)_x = M\ddot{x}_o \tag{45}$$

$$(F_e)_y + \gamma N(n_1)_y + \sum_{j=1}^{p} F_j(\lambda_j)_y = M\ddot{y}_o \tag{46}$$

$$M_e + (T\bar{\rho}'_c) \times (\gamma N\bar{n}_1) + \sum_{j=1}^{p} (T\bar{\rho}'_j) \times (F_j\bar{\lambda}_j) = I_z\ddot{\alpha} \tag{47}$$

where p is the number of ligaments and the subscripts, x and y, denote the components of the related quantities in the x and y-directions. The mass of the moving body segment is denoted by M and the dots denote derivatives with respect to time, t. The mass moment of inertia of the moving body segment

about the z-axis is I_z and $\ddot{\alpha}$ designates its angular acceleration. The problem description is completed by assigning the initial conditions, which are:

$$\dot{x}_o = \dot{y}_o = \dot{\alpha} = 0 \tag{48}$$

along with the specified values for x_o, y_o and α at $t = 0$.

Three nonlinear second order differential equations, (45), (46) and (47), along with the geometric compatibility and contact conditions of equations (14) and (36), provide the necessary relationships in order to determine the following unknowns:

a) x_o and y_o: the components of vector $\bar{r}_o$;
b) x_c and x'_c: the x and x'-coordinates of the contact point, C, in the base $(\hat{i},\hat{j})$ and $(\hat{i}',\hat{j}')$, respectively;
c) α: the orientation angle of the moving (x',y') system relative to the fixed (x,y) system; and
d) N: the magnitude of the contact force.

The numerical procedure employed in the solution of the governing equations is described in the following section.

NUMERICAL METHOD OF SOLUTION

Newmark Method of Differential Approximation

The first step in arriving at a numerical solution of these equations is the replacement of the time derivatives with a temporal operator; in the present work, the Newmark operators (Bathe and Wilson [1976]) are chosen for this purpose. For instance, $\ddot{x}_o$ is expressed in the following form:

$$\ddot{x}_o^t = \frac{4}{(\Delta t)^2}\left(x_o^t - x_o^{t-\Delta t}\right) - \frac{4}{\Delta t}\dot{x}^{t-\Delta t} - \ddot{x}_o^{t-\Delta t} \quad , \tag{49}$$

$$\dot{x}_o^t = \dot{x}_o^{t-\Delta t} + \frac{\Delta t}{2}\ddot{x}_o^{t-\Delta t} + \frac{\Delta t}{2}\ddot{x}_o^t \quad , \tag{50}$$

in which Δt is the time increment and the superscripts refer to the time stations. Similar expressions are used for $\ddot{y}_o$ and

$\ddot{\alpha}$. In the application of equations (49) and (50), the conditions at the previous time station (t-Δt) are, of course, assumed to be known.

Numerical Procedure

After the time derivatives in equations (45), (46) and (47) are replaced with the temporal operators defined in the previous section, the governing equations take the form of a set of nonlinear algebraic equations. The solution of these equations is accomplished by an iteration method. In this work, the Newton-Raphson (Kao [1974]) iteration process is used for the solution. To linearize the resulting set of simultaneous algebraic equations, we assume:

$$ {}^{k}x_{o}^{t} = {}^{k-1}x_{o}^{t} + \Delta x_{o} \qquad (51) $$

and similar expressions for the other variables are written. Here, the right subscripts denote the time station under consideration and the left subscripts denote the iteration number. At each iteration, k, the values of the variables at the previous (k-1) iteration are assumed to be known. The delta quantities denote incremental values. Equation (51) and the corresponding ones for the other variables are substituted into the governing nonlinear algebraic equations and the higher order terms in the delta quantities are dropped. The set of n simultaneous algebraic (now linearized) equations can be put into matrix form:

$$ [K]\ \{\Delta\} = \{D\} \qquad (52) $$

where [K] is an nxn coefficient matrix, $\{\Delta\}$ is a vector of incremental quantities and {D} is a vector of known values.

The iteration process at a fixed time station continues until the delta quantities of all the variables become negligibly small. A solution is accepted and the iteration process is terminated when the delta quantities become less than or equal to a prescribed percentage of the previous

values of the corresponding variables. The converged solutions of each variable is then used as the initial value for the next time step and the process is repeated for consecutive time steps.

The only problem that the Newton-Raphson process may present in the solution of dynamic problems is due to the fact that the period of the forced motion of the system may turn out to be quite short. In this case it becomes necessary to use very small time steps; otherwise a significantly large number of iterations is required for convergence. This matter will be further discussed in later sections.

Any joint can be modeled with this general formulation. The knee joint will be modeled accordingly and results will be presented in the remaining sections of this report.

MATHEMATICAL DESCRIPTION OF A THREE-DIMENSIONAL DYNAMIC MODEL

In the previous section, a mathematical description for the dynamic motion of a two-dimensional articulating joint was presented. Using the knowledge and the insight from the discussion along with the mathematical descriptions of the articular surfaces, ligaments and capsule discussed in prior sections, a general formulation for a three-dimensional mathematical model of an articulating joint will be presented in this section.

Once again for the purpose of studying the joint section, one segment is assumed to be fixed while the other segment is executing a relative motion. Coordinate systems (x,y,z) and (x',y',z') are attached to the fixed and moving body segments, respectively, and their relative position is discussed below. This relative position is determined by six variables: three components of a vector specifying the origin of the (x',y',z') system, and three rotations which determine the orientation of the (x',y',z') system. Contact conditions and dynamic equations of motion are then presented.

CHARACTERIZATION OF RELATIVE POSITIONS

A joint connects two body members which are here designated as segment 1 and segment 2. The position of the moving body segment 1 relative to fixed body segment 2 is described by two coordinate systems as shown in Figure 27. Inertial coordinate system (x,y,z) with unit vectors $\hat{i}$,$\hat{j}$ and $\hat{k}$ is connected to the fixed body segment and coordinate system (x',y',z') with unit vectors $\hat{i}'$,$\hat{j}'$ and $\hat{k}'$ is attached to the center of mass of the moving body segment. The (x',y',z') coordinate system is also taken to be the principal axis system of the moving body segment.

The motion of the moving (x',y',z') system relative to the fixed (x,y,z) system may be characterized by six quantities: the translational movement of the origin of the

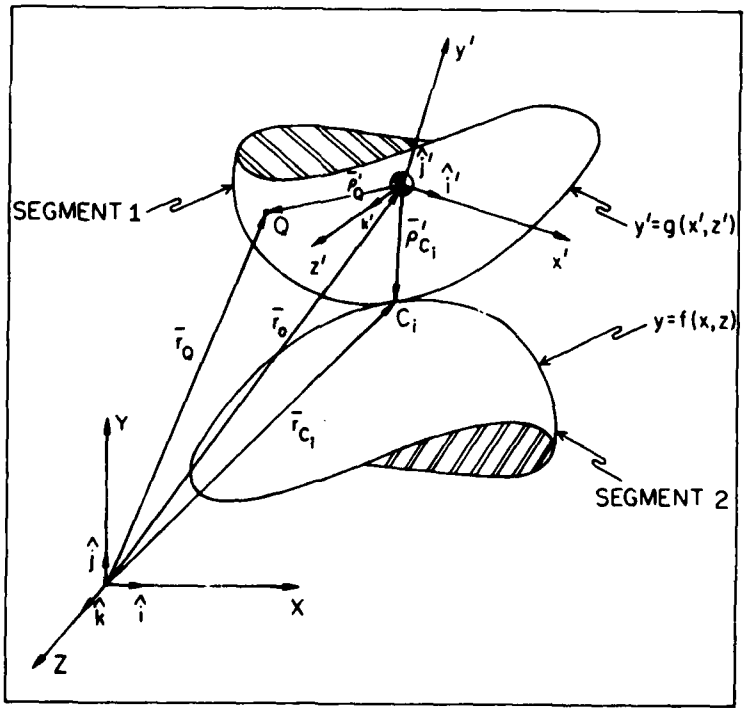

Figure 27. A two-body segmented joint is illustrated in three dimensions, showing the position of a point, Q, attached to the moving coordinate system (x',y',z').

(x',y',z') system in the x, y and z-directions, and θ, ϕ and ψ rotations with respect to the x, y, and z-axes.

Let the position vector of the origin of the (x',y',z') system in the fixed system be given by (Figure 27):

$$\bar{r}_o = x_o\hat{i} + y_o\hat{j} + z_o\hat{k} \tag{53}$$

Let the vector, $\bar{\rho}'_Q$, be the position vector of an arbitrary point, Q, on the moving body segment in the base $(\hat{i}',\hat{j}',\hat{k}')$. Let $\bar{r}_Q$ be the position vector of the same point in the base $(\hat{i},\hat{j},\hat{k})$. That is,

$$\bar{\rho}'_Q = x'_Q\hat{i}' + y'_Q\hat{j}' + z'_Q\hat{k}' \tag{54}$$

$$\bar{r}_Q = x_Q\hat{i} + y_Q\hat{j} + z_Q\hat{k} \tag{55}$$

Referring to Figure 27, vectors $\bar{\rho}'_Q$ and $\bar{r}_Q$ have the relationship:

$$\{r_Q\} = \{r_o\} + [T]^T\{\rho'_Q\} \tag{56}$$

where [T] is a 3x3 orthogonal transformation matrix. The angular orientation of the (x',y',z') system with respect to the (x,y,z) system is specified by the nine components of the [T] matrix and can be written as a function of the three variables, θ, ϕ and ψ:

$$T = T(\theta,\phi,\psi) \tag{57}$$

There are several systems of variables such as θ, ϕ and ψ which can be used to specify T. In this study the Euler angles will be utilized.

The orientation of the moving coordinate system $(\hat{i}',\hat{j}',\hat{k}')$ is obtained from the fixed coordinate system $(\hat{i},\hat{j},\hat{k})$ by applying successive rotation angles, ϕ, θ and ψ (Figure 28). First the $(\hat{i},\hat{j},\hat{k})$ system is rotated through an angle ϕ about the z-axis (Figure 28a), which results in the intermediary system $(\hat{i}_1,\hat{j}_1,\hat{k}_1)$, where:

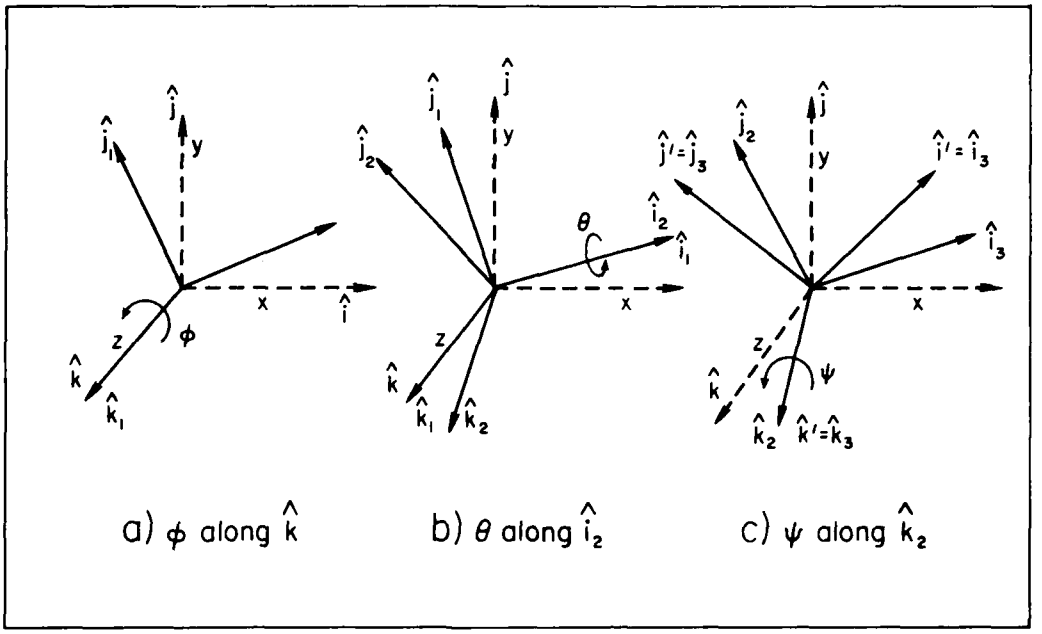

Figure 28. Successive rotations of ϕ, θ and ψ, of the (x,y,z) coordinate system.

$$\hat{i}_1 = \cos\phi\ \hat{i} + \sin\phi\ \hat{j} \tag{58a}$$

$$\hat{j}_1 = -\sin\phi\ \hat{i} + \cos\phi\ \hat{j} \tag{58b}$$

$$\hat{k}_1 = \hat{k} \tag{58c}$$

The second rotation through an angle θ about the $\hat{i}_1$-axis (Figure 28b), produces the intermediary system $(\hat{i}_2,\hat{j}_2,\hat{k}_2)$, where:

$$\hat{i}_2 = \hat{i}_1 \tag{59a}$$

$$\hat{j}_2 = \cos\theta\ \hat{j}_1 + \sin\theta\ \hat{k}_1 \tag{59b}$$

$$\hat{k}_2 = -\sin\theta\ \hat{j}_1 + \cos\theta\ \hat{k}_1 \tag{59c}$$

The third rotation through an angle ψ about the $\hat{k}_2$-axis (Figure 28c), gives the final orientation of the moving $(\hat{i}',\hat{j}',\hat{k}')$ system relative to the fixed $(\hat{i},\hat{j},\hat{k})$ system, where:

$$\hat{i}' = \hat{i}_3 = \cos\psi\ \hat{i}_2 + \sin\psi\ \hat{j}_2 \tag{60a}$$

$$\hat{j}' = \hat{j}_3 = -\sin\psi\ \hat{i}_2 + \cos\psi\ \hat{j}_2 \tag{60b}$$

$$\hat{k}' = \hat{k}_3 = \hat{k}_2 \tag{60c}$$

Substituting equations (58) and (59) into equation (60), the final orientation of the $(\hat{i}',\hat{j}',\hat{k}')$ system relative to the $(\hat{i},\hat{j},\hat{k})$ system may be written as:

$$\hat{i}' = [(\cos\psi\cos\phi - \sin\psi\cos\theta\sin\phi)\hat{i} + (\cos\psi\sin\phi + \sin\psi\cos\theta\cos\phi)\hat{j} + (\sin\psi\sin\theta)\hat{k}] \tag{61a}$$

$$\hat{j}' = [(-\sin\psi\cos\phi - \cos\psi\cos\theta\sin\phi)\hat{i} + (-\sin\psi\sin\phi + \cos\psi\cos\phi\cos\theta)\hat{j} + (\cos\psi\sin\theta)\hat{k}] \tag{61b}$$

$$\hat{k}' = [(\sin\theta\sin\phi)\hat{i} - (\sin\theta\cos\phi)\hat{j} + \cos\theta\ \hat{k}] \tag{61c}$$

or, in matrix notation:

$$\begin{Bmatrix} \hat{i}' \\ \hat{j}' \\ \hat{k}' \end{Bmatrix} = [T] \begin{Bmatrix} \hat{i} \\ \hat{j} \\ \hat{k} \end{Bmatrix} \tag{62}$$

where:

$$[T] = \begin{bmatrix} \cos\phi\cos\psi & \cos\psi\sin\phi & \sin\theta\sin\psi \\ -\sin\psi\cos\theta\sin\phi & +\sin\psi\cos\theta\cos\phi & \\ -\sin\psi\cos\phi & -\sin\psi\sin\phi & \cos\psi\sin\theta \\ -\cos\psi\cos\theta\sin\phi & +\cos\psi\cos\theta\cos\phi & \\ \sin\phi\sin\theta & -\sin\theta\cos\phi & \cos\theta \end{bmatrix} \tag{63}$$

CONTACT CONDITIONS

Assuming rigid body contacts between the two body segments at points C_i (i=1,2) as shown in Figure 27, let us represent the contact surfaces by smooth mathematical functions of the form:

$$y = f(x,z) \tag{64}$$

$$y' = g(x',z') \tag{65}$$

As implied, equations (64) and (65) represent the fixed and the moving surfaces, respectively.

The position vectors of the contact points C_i (i=1,2) in the base $(\hat{i},\hat{j},\hat{k})$ is denoted by

$$\bar{r}_{c_i} = x_{c_i}\hat{i} + f(x_{c_i},z_{c_i})\hat{j} + z_{c_i}\hat{k} \tag{66}$$

and the corresponding ones in the base $(\hat{i}',\hat{j}',\hat{k}')$ are given by:

$$\bar{\rho}'_{c_i} = x'_{c_i}\hat{i}' + g(x'_{c_i},z'_{c_i})\hat{j}' + z'_{c_i}\hat{k}' \tag{67}$$

Then, at each contact point C_i the following relationship must hold:

$$\{r_{c_i}\} = \{r_o\} + [T]^T\{\rho'_{c_i}\} \tag{68}$$

This is a part of the geometric compatibility condition for the two contacting surfaces. Furthermore, the unit normals to the surfaces of the moving and fixed body segments at the points of contacts must be colinear.

Let $\bar{n}_{c_i}$ (i=1,2) be the unit normals to the fixed surface, $y = f(x,z)$, at the contact points, C_i (i=1,2), then:

$$\bar{n}_{c_i} = \frac{1}{\sqrt{DET[G]}}\left(\frac{\partial \bar{r}_{c_i}}{\partial x_{c_i}}\right) x \left(\frac{\partial \bar{r}_{c_i}}{\partial z_{c_i}}\right) \qquad i=1,2 \tag{69}$$

where $\bar{r}_{c_i}$ is given in equation (66) and the components of the matrix [G] are determined by:

$$G_{k\ell} = \left(\frac{\partial \bar{r}_{c_i}}{\partial x^k} \cdot \frac{\partial \bar{r}_{c_i}}{\partial x^\ell} \right) \qquad i=1,2 \tag{70}$$

with

$$x^1 = x_{c_i} \quad , \quad x^2 = z_{c_i} \quad , \quad x^3 = F(x_{c_i}, z_{c_i})$$

Therefore the components of matrix $[G_{k\ell}]$ may be written as:

$$G_{xx} = \left[\left(\frac{\partial x_{c_i}}{\partial x_{c_i}} \right)^2 + \left(\frac{\partial y_{c_i}}{\partial x_{c_i}} \right)^2 + \left(\frac{\partial z_{c_i}}{\partial x_{c_i}} \right)^2 \right] \tag{71a}$$

$$G_{zz} = \left[\left(\frac{\partial x_{c_i}}{\partial z_{c_i}} \right)^2 + \left(\frac{\partial y_{c_i}}{\partial z_{c_i}} \right)^2 + \left(\frac{\partial z_{c_i}}{\partial z_{c_i}} \right)^2 \right] \tag{71b}$$

$$G_{xz} = G_{zx} = \left[\left(\frac{\partial x_{c_i}}{\partial x_{c_i}} \right) \left(\frac{\partial x_{c_i}}{\partial z_{c_i}} \right) + \left(\frac{\partial y_{c_i}}{\partial x_{c_i}} \right) \left(\frac{\partial y_{c_i}}{\partial z_{c_i}} \right) + \left(\frac{\partial z_{c_i}}{\partial x_{c_i}} \right) \left(\frac{\partial z_{c_i}}{\partial z_{c_i}} \right) \right] \tag{71c}$$

Since $(\partial z_{c_i}/\partial x_{c_i}) = 0$ and $(\partial x_{c_i}/\partial z_{c_i}) = 0$, then the components of matrix $[G_{k\ell}]$ reduce to:

$$G_{xx} = 1 + \left(\frac{\partial f}{\partial x_{c_i}} \right)^2 \tag{72a}$$

$$G_{zz} = 1 + \left(\frac{\partial f}{\partial z_{c_i}} \right)^2 \tag{72b}$$

$$G_{xz} = G_{zx} = \left(\frac{\partial f}{\partial x_{c_i}} \right) \left(\frac{\partial f}{\partial z_{c_i}} \right) \tag{72c}$$

From equations (72), the DET[G] can be written as:

$$\text{DET}[G] = 1 + \left(\frac{\partial f}{\partial x_{c_i}}\right)^2 + \left(\frac{\partial f}{\partial z_{c_i}}\right)^2 \tag{73}$$

and therefore, the unit outward normals expressed in equation (69) will have the following form:

$$\hat{n}_{c_i} = \frac{\gamma}{\sqrt{1 + \left(\frac{\partial f}{\partial x_{c_i}}\right)^2 + \left(\frac{\partial f}{\partial z_{c_i}}\right)^2}} \left[\left(\frac{\partial f}{\partial x_{c_i}}\right)\hat{i} - \hat{j} + \left(\frac{\partial f}{\partial z_{c_i}}\right)\hat{k}\right] \tag{74}$$

where the parameter, γ, is chosen such that $\hat{n}_{c_i}$ represents the outward normal.

Similarly, following the same procedure as outlined above $\hat{n}'_{c_i}$ (i=1,2), the unit outward normal to the moving surface, $y' = g(x',z')$, at contact points, C_i (i=1,2), and expressed in $(\hat{i}',\hat{j}',\hat{k}')$ system, can be written as:

$$\hat{n}'_{c_i} = \frac{\beta}{\sqrt{1 + \left(\frac{\partial g}{\partial x'_{c_i}}\right)^2 + \left(\frac{\partial g}{\partial z'_{c_i}}\right)^2}} \left[\left(\frac{\partial g}{\partial x'_{c_i}}\right)\hat{i}' - \hat{j}' + \left(\frac{\partial g}{\partial z'_{c_i}}\right)\hat{k}'\right] \tag{75}$$

where parameter, β, is chosen such that $\hat{n}'_{c_i}$ represents the outward normal.

Colinarity of unit normals at each contact point C_i (i=1,2), requires that:

$$\{n_{c_i}\} = -[T]^T\{n'_{c_i}\} \tag{76}$$

Note that colinearity condition can also be satisfied by requiring that the cross product $(n_{c_i} \times T^T n'_{c_i})$ be zero.

DYNAMIC EQUATIONS OF THE MOVING BODY SEGMENT

The total load acting on the moving body segment is divided into forces exerted by nonlinear springs which simulate the ligaments and capsule forces, contact forces

between the moving and the fixed body segments and applied external forces and moments (Figure 29). Ligament and capsule forces were discussed and formulated previously. The coefficient of friction between the articulating surfaces, owing to the presence of the synovial fluid in the joints, is known to be very low (Radin and Paul [1972]). Accordingly, the friction force between the two body segments will be neglected. Therefore, the contact forces, $\bar{N}_i$, acting on the moving body segment are given by:

$$\bar{N}_i = |N_i|[(n_{c_i})_x\hat{i} + (n_{c_i})_y\hat{j} + (n_{c_i})_z\hat{k}] \qquad (77)$$

where $|N_i|$'s are the unknown magnitudes of the contact forces and $(n_{c_i})_x$, $(n_{c_i})_y$ and $(n_{c_i})_z$ are the components of the unit normal, n_{c_i}, in the x, y and z-directions, respectively.

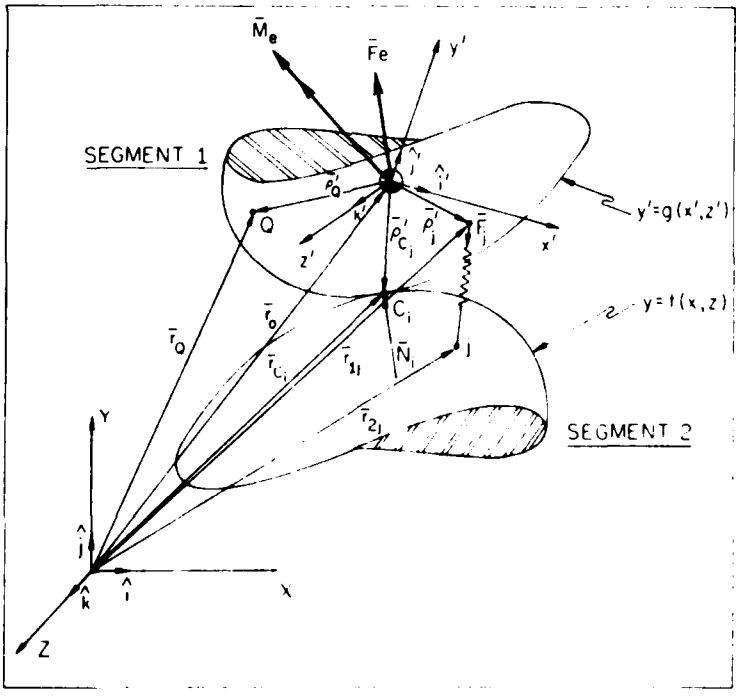

Figure 29. Forces acting on the moving body segment of a two-body segmented joint in three dimensions.

The desired dynamic motion is achieved by applying an external force and moment to the center of mass of the moving body segment whose resultants are given as:

$$\bar{F}_e = (F_e)_x\hat{i} + (F_e)_y\hat{j} + (F_e)_z\hat{k} \tag{78}$$

$$\bar{M}_e = (M_e)_x\hat{i} + (M_e)_y\hat{j} + (M_e)_z\hat{k} \tag{79}$$

Equations of motion will be presented next.

Equations of Motion

The equations governing the forced motion of the moving body segment are:

$$(F_e)_x + \sum_{i=1}^{q} |N_i|(n_{c_i})_x + \sum_{j=1}^{p} F_j(\lambda_j)_x = M\ddot{x}_o \tag{80a}$$

$$(F_e)_y + \sum_{i=1}^{q} |N_i|(n_{c_i})_y + \sum_{j=1}^{p} F_j(\lambda_j)_y = M\ddot{y}_o \tag{80b}$$

$$(F_e)_z + \sum_{i=1}^{q} |N_i|(n_{c_i})_z + \sum_{j=1}^{p} F_j(\lambda_j)_z = M\ddot{z}_o \tag{80c}$$

$$\sum M_{x'x'} = I_{x'x'}\dot{\omega}_{x'} + (I_{z'z'} - I_{y'y'})\omega_{y'}\omega_{z'} \tag{81a}$$

$$\sum M_{y'y'} = I_{y'y'}\dot{\omega}_{y'} + (I_{x'x'} - I_{z'z'})\omega_{z'}\omega_{x'} \tag{81b}$$

$$\sum M_{z'z'} = I_{z'z'}\dot{\omega}_{z'} + (I_{y'y'} - I_{x'x'})\omega_{x'}\omega_{y'} \tag{81c}$$

where p and q represent the number of ligaments and the contact point, respectively. $I_{x'x'}$, $I_{y'y'}$ and $I_{z'z'}$ are the principal moments of inertia of the moving body segment about its centroidal principal axis system (x',y',z'), and $\omega_{x'}$, $\omega_{y'}$ and $\omega_{z'}$, are the components of the angular velocity vector which are given below in terms of the Euler angles:

$$\omega_{x'} = \dot{\theta}\cos\psi + \dot{\phi}\sin\theta\sin\psi \tag{82a}$$

$$\omega_{y'} = -\dot{\theta}\sin\psi + \dot{\phi}\sin\theta\cos\psi \tag{82b}$$

$$\omega_{z'} = \dot{\phi}\cos\theta + \dot{\psi} \tag{82c}$$

The angular acceleration components, $\dot{\omega}_x$, $\dot{\omega}_y$, and $\dot{\omega}_z$ are directly obtained from equation (82):

$$\dot{\omega}_{x'} = \ddot{\theta}\cos\psi - \dot{\psi}(\dot{\theta}\sin\psi - \dot{\phi}\cos\psi\sin\theta) + \ddot{\phi}\sin\theta\sin\psi + \dot{\phi}\dot{\theta}\cos\theta\sin\psi \tag{83a}$$

$$\dot{\omega}_{y'} = -\ddot{\theta}\sin\psi - \dot{\psi}(\dot{\theta}\cos\psi + \dot{\phi}\sin\psi\sin\theta) + \ddot{\phi}\sin\theta\cos\psi + \dot{\phi}\dot{\theta}\cos\theta\cos\psi \tag{83b}$$

$$\dot{\omega}_{z'} = \ddot{\phi}\cos\theta - \dot{\phi}\dot{\theta}\sin\theta + \ddot{\psi} \tag{83c}$$

Note that the moments components shown on the left-hand side of equation 81 are obtained from:

$$\bar{M} = \bar{M}_e + \sum_{i=1}^{q} [T]^T(\bar{\rho}'_{c_i}) \times (|N_i|\bar{n}_{c_i}) + \sum_{j=1}^{p} [T]^T(\bar{\rho}'_j) \times (F_j\bar{\lambda}_j) \tag{84}$$

where $\bar{M}_e$ is applied external moment, and p and q represent the number of ligaments and contact points, respectively.

The equations (80) and (81) form a set of six nonlinear second order differential equations which, together with the contact conditions (68) and (76), form a set of 16 nonlinear equations (assuming two contact points, i.e. i=1,2) with 16 unknowns:

a) θ, ϕ and ψ, which determine the components of transformation matrix [T];

b) x_o, y_o, and z_o: the components of position vector $\bar{r}_o$;

c) x_{c_i}, z_{c_i}, x'_{c_i} and z'_{c_i} (i=1,2): the coordinates of contact points;

d) $|N_i|$ (i=1,2): the magnitudes of the contact forces.

Numerical procedure outlined previously can be utilized for the solution of the three-dimensional joint model equations presented in this section. However, becuase of the extreme complexity of these equations, in this report we will present in some detail only the numerical solution of a two-dimensional joint model applied to the human knee joint.

TWO-DIMENSIONAL DYNAMIC MODEL OF THE KNEE JOINT

Thus far, mathematical descriptions of the articular surfaces, the ligaments and capsule have been developed as well as general formulations for two- and three-dimensional dynamic model of an articulating joint. These formulations can now be applied to a mathematical description for the dynamic motion of the knee joint. The most general and realistic model of the knee should be three-dimensional. However, a simpler two-dimensional model can be helpful and rewarding in understanding the essentials of the problem and serve as the groundwork for the sound development of a three-dimensional model. Before we present our two-dimensional dynamic model of the knee joint we will briefly discuss the previously developed models of the knee.

PREVIOUSLY DEVELOPED KNEE JOINT MODELS

The models of the knee joint can be subdivided into pure kinematical models and models describing the force action in the joint. Kinematical models try to describe the motions between femur and tibia without considering the forces and moments in the joint. A model of this type, developed by Strasser [1917] is a four-bar mechanism (Figure 30). Two bars represent the cruciates, while the other bars represent femur and tibia, respectively. Menschik [1974a,1974b] extended this planar model by two curves representing the tibial and femoral articular surfaces and also studied location of the insertion areas of the collateral ligaments

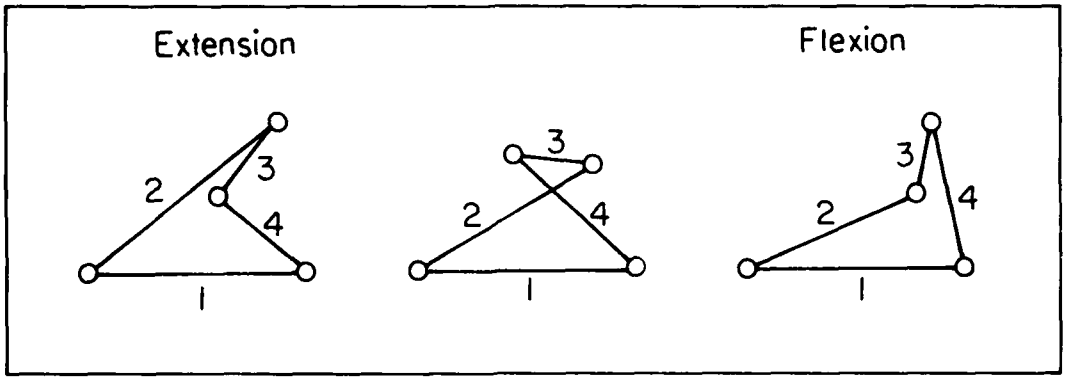

Figure 30. Four-bar mechanism according to Strasser [1917] is shown. Components are identified as 1 = tibia, 2 = anterior cruciate ligament, 3 = femur and 4 = posterior cruciate ligament.

in this model. Similarly, the model of Huson [1974,1976] is based on the idea of a four-bar mechanism, but it is also able to simulate internal-external free range of motion by means of a certain inclination of the plane representing the lateral tibial articular surface.

Several planar mechanisms simulating the motion of the human knee joint in the sagittal plane have been proposed by Freudenstein and Woo [1969]. The aim of this study was to serve as a guideline in the kinematical design of joint prostheses. Investigations aimed at accurate in-vivo measurements of three-dimensional relative motions in a human knee joint so far have not been fully described in the literature. A study by Levens, Inman and Blosser [1948] was limited to relative rotations in a transverse plane. In this study, stainless steel pins of 2.5 mm diameter were drilled firmly into the femur and the tibia, sterility precautions and local anesthesia being used. No further attempts using this method are described in the literature.

The mechanical analysis of the human knee joint has in the past been carried out mostly with human knee joint

specimens which can be considered as the best available representation of the living human joint. The shortcomings of the knee specimens are the lack of muscle forces and the difference in material properties from those of the living joint. Moreover, the availability of the knee specimens for research purposes is limited. Living and dead animals have often been used as surrogates for human material in the study of special problems. For example, the mechanical behavior of the menisci in canines and pigs have been studied by Krause et al. [1976] and Jaspers et al. [1978], respectively.

In general, kinematical models offer valuable possibilities of gaining a better insight into some aspects of joint behavior. However, their application is restricted to phenomena in which force actions are of no interest.

A number of knee models, described in literature, were not concerned with relative joint motions but were developed to determine the forces in ligaments, muscles or between articular surfaces. In these models the joint structures are simplified in such a way that a so-called statically determinant system is achieved. Consequently, the constitutive equations of the ligaments are not necessary and the conditions of equilibrium are sufficient to determine the relevant forces. Two-dimensional models of this type are reported by Kettelkamp and Chao [1972], Smidt [1973], Perry, Antonelli and Ford [1975], Seedhom and Terayama [1976], Rens and Huiskes [1976], while Morrison [1967,1970] presented a three-dimensional model.

Although the studies on the biomechanics of the knee joint have a long history, those studies which are essentially a mathematical modeling of this largest and, apparently, most complicated joint in the body are few. Crowninshield, Pope and Johnson [1976] felt justified in stating that there were, at that time, no analytical models of the knee available which permit the prediction of the response of the joint to

AD-A121 076 MODELING OF HUMAN JOINT STRUCTURES(U) OHIO STATE UNIV 2/2
COLUMBUS DEPT OF ENGINEERING MECHANICS
A E ENGIN ET AL. SEP 82 AFAMRL-TR-81-117
UNCLASSIFIED F33615-78-C-0510 F/G 6/19 NL

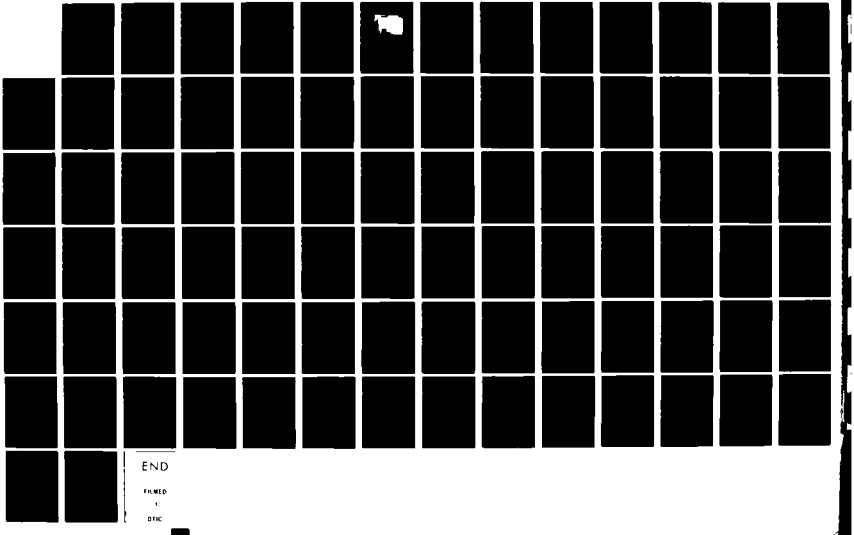

END

FILMED
DTIC

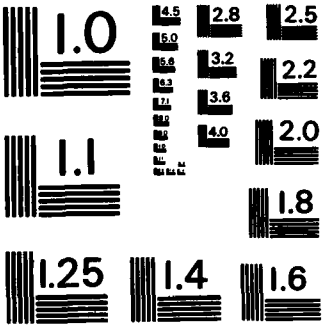

MICROCOPY RESOLUTION TEST CHART
NATIONAL BUREAU OF STANDARDS - 1963 - A

either external forces or displacements. In their analytical model, on the other hand, only the quasi-static response of the joint was studied and the overall joint stiffness was obtained as a function of the flexion angle. The method used by Crowninshield, Pope and Johnson [1976] is the so-called inverse method in which the ligament forces caused by a specified set of translations and rotations in specified directions are determined by comparing the geometries of the initial and displaced configurations of the knee joint. In this method the externally applied displacements do not need to be continuous; however, the discrete values used are to be realistic. In Crowninshield, Pope and Johnson [1976] these values were based on experimental data available in the literature. The purpose of the work was to obtain the stiffness of the joint which, in turn, required the calculation of the ligament lengths at various knee configurations. Thus, it was not necessary to consider the contribution of the curved joint surfaces to the overall mechanical behavior of the knee. Moreover, the external forces required for equilibrium were not determined either.

Improvements to the quasi-static model discussed above have been provided recently by Wismans et al. [1980], in which a three-dimensional analytical model of the femorotibial joint is presented. The study considers not only the geometry but also the static equilibrium of the system. The three-dimensional curved geometry of the joint surfaces are included in the model. Ligaments are modeled as non-linear elastic springs. The solution method employed by Wismans et al. [1980] is also a quasi-static, inverse method. The flexion-extension motion is simulated by prescribing several flexion-extension angles. The dependent variables of the problem, including the ligament forces, are determined from the equilibrium equations and the geometric compatibility conditions. However, for nonlinear problems of this kind it

is known that there can exist more than one equilibrium configuration for a given flexion-extension angle unless an external force is also specified. Accordingly, in the inverse method utilized by Wismans et al. [1980] it is necessary to specify the external force required for the preferred equilibrium configuration. Such an approach is applicable only in quasi-static analysis. In dynamic analysis, the equilibrium configuration preferred by the system is the unknown and the mathematical analysis itself is to provide that equilibrium configuration.

Biomechanics of the knee joint has also been investigated by Andriacchi et al. [1977,1978]. They reported a statically indeterminate model for the analysis of motion and forces in the knee joint. Like Crowninshield, Pope and Johnson [1976], they represent ligaments and capsule by a number of springs, while the articular surfaces and menisci are also represented in the model. Numerical predictions are consistent with experimental observations. The models of Andriacchi et al. [1977,1978] and Wismans et al. [1980], are essentially the same in the sense that both deal with the quasi-static response of the knee joint. Detailed discussions of various anatomical and functional aspects of the human knee joint can also be found in Gray [1973], Engin and Korde [1974], Blacharski, Somerset and Murray [1975], Jacobsen [1976], Pope, et al. [1976], and Engin [1978].

As seen from the preceding discussion, mathematical modeling of the knee joint has not yet reached a definitive stage of development. It is interesting to note that a biodynamic model of the knee joint is, to the best of the authors' knowledge, not yet available in the literature. It is more appropriate to study via a dynamic model the response of the joint to dynamically applied loads. The artificial restrictions of the quasi-static inverse method, such as the necessity to specify the preferred configuration, can be

eliminated if the dynamics of the problem are incorporated into the model.

TWO-DIMENSIONAL GEOMETRY OF THE KNEE JOINT

Coordinate Systems

Previous sections have discussed the relative positions and coordinate systems for a general, two-body segmented joint. Uniquely specifying the locations of these coordinate systems is virtually impossible because of the lack of well-defined anatomical landmarks in the human body. However, the relative motions in a joint are not affected by the choice of coordinate systems and only some parameters describing the relative displacements have different values for different coordinate systems.

The position of the tibia, defined as the moving segment, relative to the femur, defined as the fixed segment, is shown in Figure 31. The origin of the moving coordinate system (x',y') coincides with the center of mass of the tibia, with the y'-axis being directed along the longitudinal axis of the tibia. The inertial coordinate system (x,y) is attached to the fixed femur with the x-axis directed along the posterior-anterior direction and the y-axis coinciding with the femoral longitudinal axis. The locations of the origins of these coordinate systems, shown in Figure 31, are 4.01 cm and 21.34 cm from the intersection points of the y and y' axes with the articulating surfaces. The rotation of the moving (x',y') coordinate system with respect to the fixed (x,y) system is denoted by α.

Mathematical Descriptions of the Articulating Surfaces

The two dimensional profiles in the plane of motion of the femoral and tibial articulating surfaces are obtained from X-ray of a human knee joint. The coordinates (x_k,y_k) of a number of points on these profiles are measured using a

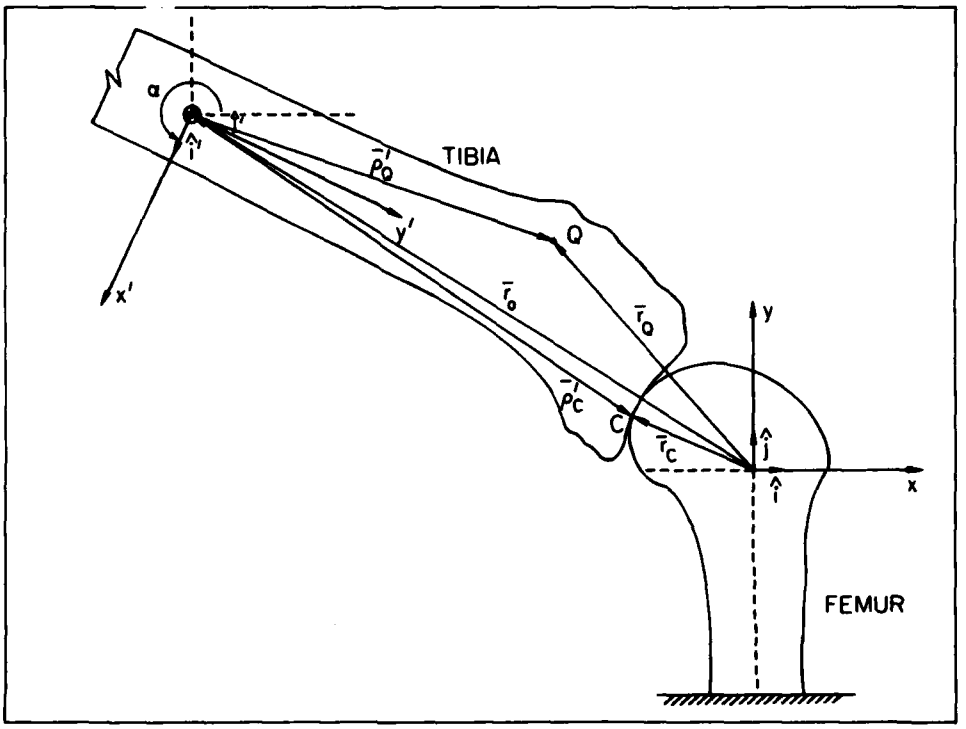

Figure 31. Coordinate systems locations and relative positions of the tibia and femur are shown for the two-dimensional dynamic model of the knee joint.

two-dimensional sonic digitizing technique described previously (Figure 32).

A polynomial equation of degree n(n>1) is used as an approximate mathematical representation of the profile under consideration. This polynomial has the form

$$y(x) = \sum_{i}^{n} A_i x^i \qquad (85)$$

where A_i's are the polynomial coefficients. These coefficients are determined by the use of the subroutine program CHEPLS (Appendix A). This subroutine is capable of determining, by means of statistical tests, where the set of given data points are linear or nonlinear. If the data are nonlinear at the

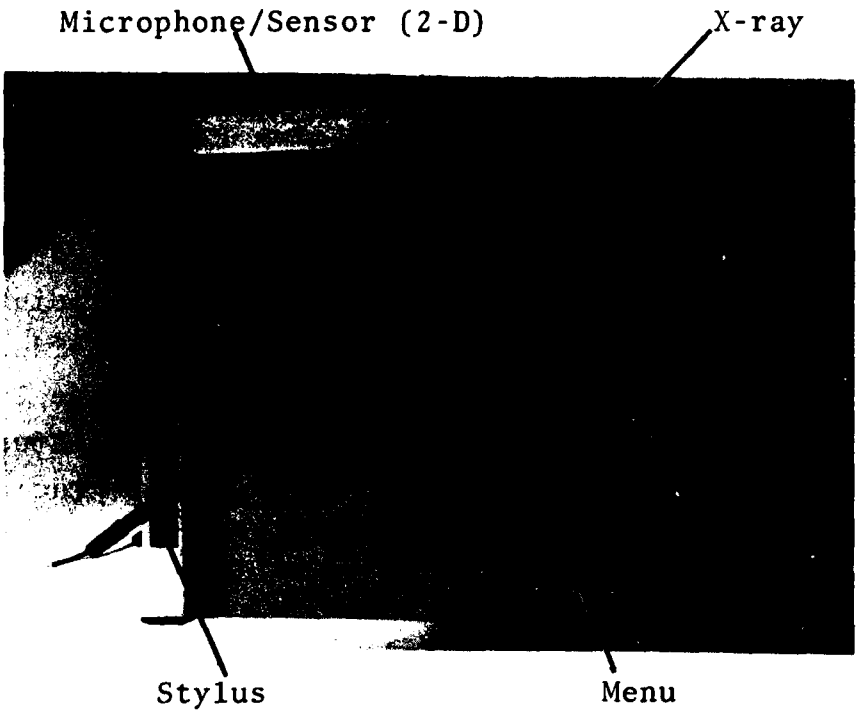

Figure 32. Two-dimensional microphone/sensor with menu capability, and sonic emitter/stylus for the Graf/Pen sonic digitizer is shown with x-ray of the knee joint in place for obtaining the profiles of the articulating surfaces.

95% confidence level, then the routine finds the lowest degree polynomial which adequately represents the data. The calculation procedure is to compare the standard deviation of the model of degree n with that of $(n+1)^{th}$ degree model. If there is no significant difference at the 95% confidence level, then the polynomial of degree n is accepted as the lowest degree polynomial which adequately represents the data. In the present study, this method yields the following equations for the femoral and tibial profiles, respectively:

$$f_1(x) = 0.04014 - 0.247621\,x - 6.889185\,x^2 - 270.4456\,x^3 - 8589.942\,x^4 \quad (86)$$

$$f_2(x') = 0.213373 - 0.0456051\ x' + 1.073446\ x'^2 \qquad (87)$$

with the aid of the Versatec plotter, the tibial and femoral articulating surfaces predicted by equations (86) and (87) are shown in Figure 33.

DESCRIPTION OF THE LIGAMENT MODEL

Selection of the Springs and Corresponding Parameters

Only four major ligaments of the knee joint will be considered in the present work although consideration of any other ligament presents no difficulty. These ligaments are the lateral collateral (LC), the medial collateral (MC), the anterior cruciate (AC), and the posterior cruciate (PC). The ligaments are modeled as nonlinear elastic springs having a

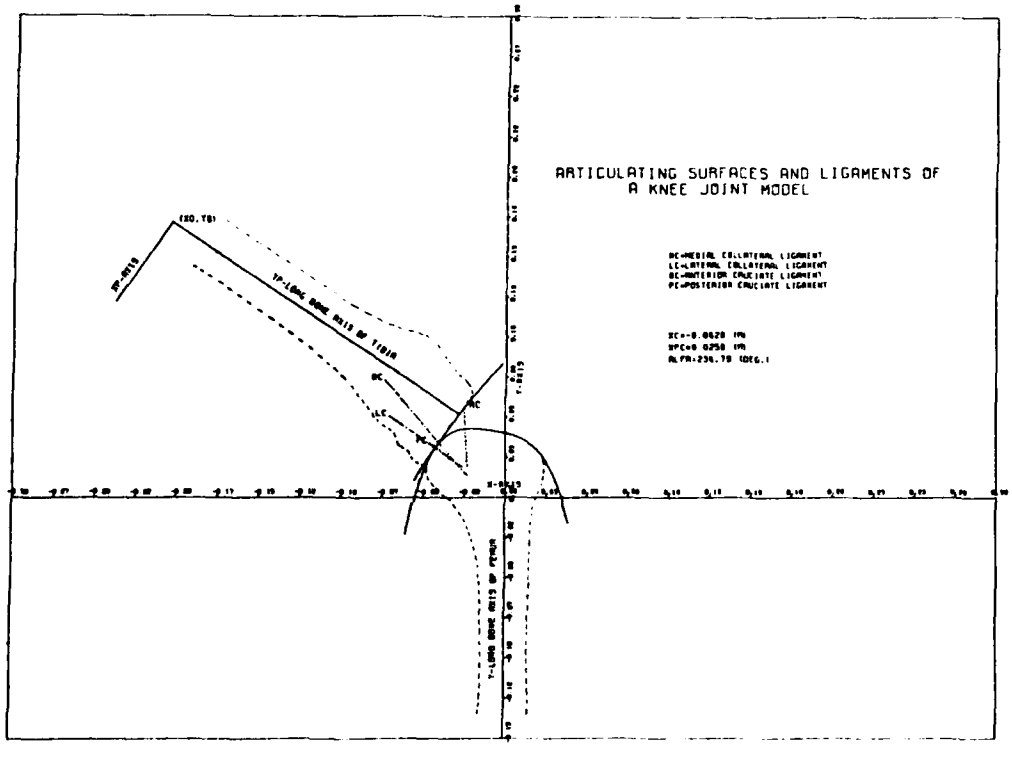

Figure 33. Versatec plot of the two-dimensional representations of the tibial and femoral articulating surfaces.

constitutive relation given by equation (3). The stiffness values for these ligaments are summarized in Table 8. Initial strains in the ligaments are taken as zero since, at present, there is no accurate data available on strains as a function or flexion angle. Zero strain condition for the ligaments can be partially justified if an appropriate starting flexion angle under no external load is chosen.

Insertions and Origins

The coordinates of the insertion points of the ligaments in both the tibia and the femur are determined from the available information in the literature (Wang, Walker and Wolf, [1973], Crowninshield, Pope and Johnson [1976]) and close anatomical study of the knee joint. These coordinates on the tibia are denoted by x_j' and y_j', and those on the femur are denoted by x_j and y_j. The values used in the present work are summarized in Table 10. Obviously, these values are determined with respect to coordinate systems shown in Figure 31, and for the specific specimen used in our study.

Table 10

COORDINATE VALUES FOR THE INSERTIONS AND ORIGINS OF THE KNEE JOINT LIGAMENTS, IN METERS.

LIGAMENT	TIBIA		FEMUR	
	x_j'	y_j'	x_j	y_j
Medial Collateral (MC)	0.008	0.163	-0.023	0.014
Lateral Collateral (LC)	0.025	0.178	-0.025	0.019
Anterior Cruciate (AC)	-0.005	0.213	-0.023	0.019
Posterior Cruciate (PC)	0.025	0.208	-0.032	0.024

MATHEMATICAL DESCRIPTION OF THE DYNAMIC MOTION OF THE KNEE JOINT

The total external forces acting on the tibia are shown in Figure 34. These forces are: ligament forces, $\bar{F}_j$ (j=1,--4); normal contact force $\bar{N}$; and the applied external force, $\bar{F}_e$, and moment, $\bar{M}_e$. Frictional forces between the femoral and tibial surfaces will be neglected since the coefficient of friction between the articulating surfaces, owing to the presence of the synovial fluid, is known to be very low (Radin and Paul [1972]; Dowson [1976]). Therefore, the contact force, $\bar{N}$, will be in the direction of the normal to the surface at the point of contact.

The equations governing the forced motion of the tibia are:

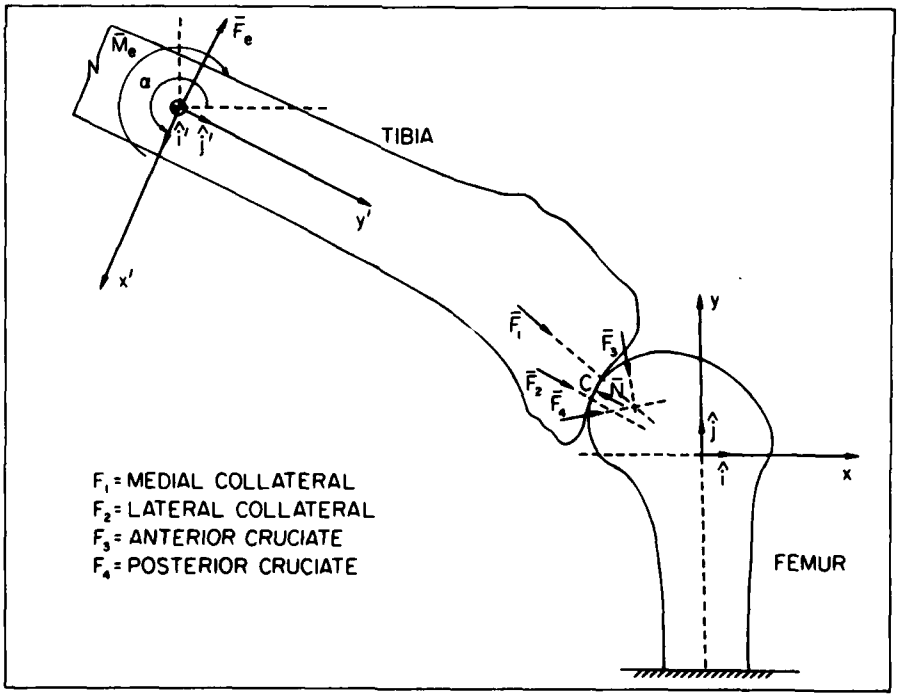

Figure 34. Forces acting on the moving tibia are shown for the two-dimensional model of the knee joint.

$$(F_e)_x + \gamma N(n_1)_x + \sum_{j=1}^{4} F_j(\lambda_j)_x = M\ddot{x}_o \tag{88}$$

$$(F_e)_y + \gamma N(n_1)_y + \sum_{j=1}^{4} F_j(\lambda_j)_y = M\ddot{y}_o \tag{89}$$

$$M_e + (T\bar{\rho}_c') \times (\gamma N\bar{n}_1) + \sum_{j=1}^{4} (T\bar{\rho}_j') \times (F_j\bar{\lambda}_j) = I_z\ddot{\alpha} \tag{90}$$

where all the parameters in the above governing equations have been defined in previous discussion on the two-dimensional general formulation for dynamic motion.

NUMERICAL ANALYSIS AND DERIVATIONS

The differential variables, $\ddot{x}_o$, $\ddot{y}_o$, and $\ddot{\alpha}$ are substituted by their corresponding Newmark approximations given in equations (49) and (50). Subsequently, these simultaneous nonlinear algebraic equations along with geometric compatibility and contact conditions of equations (8) and (36) are linearized by applying the Newton-Raphson iteration process. After considerable amount of mathematical operations and eliminations of the second order variational terms (see Appendix B for complete derivations), the following final form of the linearized governing equations of motion are obtained:

$$\begin{aligned}&(\gamma n_{1x}^k)\delta_N + (\gamma N^k)\delta_{n_{1x}} - \left(\frac{4M}{\Delta t^2}\right)\delta_{x_o} = -\sum_{j=1}^{4} F_{jx} - (F_e)_x \\ &-\gamma N^k n_{1x}^k + M\left\{\frac{4}{\Delta t^2}[x_o^k - x_o^{t-\Delta t}] - \frac{4}{\Delta t}\dot{x}_o^{t-\Delta t} - \ddot{x}_o^{t-\Delta t}\right\}\end{aligned} \tag{91}$$

$$\begin{aligned}&(\gamma n_{1y}^k)\delta_N + (\gamma N^k)\delta_{n1y} - \left(\frac{4M}{\Delta t^2}\right)\delta_{y_o} = -\sum_{j=1}^{4} F_{jy} - (F_e)_y \\ &-\gamma N^k n_{1y}^k + M\left\{\frac{4}{\Delta t^2}[y_o^k - y_o{}^{t-\Delta t}] - \frac{4}{\Delta t}\dot{y}_o{}^{t-\Delta t} - \ddot{y}_o{}^{t-\Delta t}\right\}\end{aligned} \tag{92}$$

$$\sum_{j=1}^{4} F_{jy}\delta_{x_j} - [\sum_{j=1}^{4} F_{jy} + \gamma N^k n_{1y}^k]\delta_{x_o} - \sum_{j=1}^{4} F_{jx}\delta_{yj}$$

$$+ [\sum_{j=1}^{4} F_{jx} + \gamma N^k n_{1x}^k]\delta_{y_o} + [(x_c^k - x_o^k)n_{1y}^k - (y_c^k - y_o^k)n_{1x}^k]\delta_N$$

$$- [\gamma N^k (y_c^k - y_o^k)]\delta_{n_{1x}} + [\gamma N^k (x_c^k - x_o^k)]\delta_{n1y} + [\gamma N^k n_{1y}^k]\delta_{x_c} \quad (93)$$

$$- (\gamma N^k n_{1x}^k)\delta_{y_c} - \frac{4I_z}{\Delta t^2}\delta_\alpha = - \sum_{j=1}^{4} (x_j^k - x_o^k)F_{jy} + \sum_{j=1}^{4} (y_j^k - y_o^k)F_{jx}$$

$$- \gamma N^k [(x_c^k - x_o^k)n_{1y}^k - (y_c^k - y_o^k)n_{1x}^k] + I_z \left\{ \frac{4}{\Delta t^2}(\alpha^k - \alpha^{t-\Delta t}) \right.$$

$$\left. - \frac{4}{\Delta t}\dot{\alpha}^{t-\Delta t} - \ddot{\alpha}^{t-\Delta t} \right\} - M_e$$

Similarly, the linearized geometric constraint equations are:

$$\delta_{x_c} - \delta_{x_o} + (x_c'^k \sin\alpha^k + y_c'^k \cos\alpha^k)\delta_\alpha - \cos\alpha^k \delta_{x_c'} \quad (94)$$

$$+ \sin\alpha^k \delta_{y_c'} = x_o^k - x_c^k + x_c'^k \cos\alpha^k - y_c'^k \sin\alpha^k$$

$$\delta_{y_c} - \delta_{y_o} - (x_c'^k \cos\alpha^k - y_c'^k \sin\alpha^k)\delta_\alpha - \sin\alpha^k \delta_{x_c'} \quad (95)$$

$$- \cos\alpha^k \delta_{y_c'} = y_o^k - y_c^k + x_c'^k \sin\alpha^k + y_c'^k \cos\alpha^k$$

$$[P^k \sin\alpha^k + \cos\alpha^k]\delta_Q + [Q^k \sin\alpha^k - \cos\alpha^k]\delta_p$$

$$+ [\cos\alpha^k (1 + P^k Q^k) + \sin\alpha^k (P^k - Q^k)]\delta_\alpha \quad (96)$$

$$= - [\sin\alpha^k (1 + P^k Q^k) - \cos\alpha^k (P^k - Q^k)]$$

Other variational relationships which must be solved simultaneously with equations (91) through (96) (See Appendix B) are:

(a) Variation of ligament insertion coordinates, (x_j, y_j):

$$\delta_{x_j} - \delta_{x_o} + (x'_j \sin\alpha^k + y'_j \cos\alpha^k)\delta_\alpha = - x_j^k + x_o^k + x'_j \cos\alpha^k - y'_j \sin\alpha^k \quad (j=1,..,4) \tag{97}$$

$$\delta_{y_j} - \delta_{y_o} - (x'_j \cos\alpha^k - y'_j \sin\alpha^k)\delta_\alpha = - y_j^k + y_o^k + x'_j \sin\alpha^k + y'_j \cos\alpha^k \quad (j=1,..,4) \tag{98}$$

(b) Variation of articulating surfaces, $y_c = f_1(x_c)$ and $y'_c = f_2(x'_c)$:

$$\delta_{y_c} - [A_2 + 2A_3 x_c^k + 3A_4 (x_c^k)^2 + 4A_5 (x_c^k)^3]\delta_{x_c} = A_1 + A_2 x_c^k + A_3 (x_c^k)^2 + A_4 (x_c^k)^3 + A_5 (x_c^k)^4 - y_c^k \tag{99}$$

$$\delta_{y'_c} - (A'_2 + 2A'_3 x_c'^k)\delta_{x'_c} = A'_1 + A'_2 x_c'^k + A'_3 x_c'^{k2} - y_c'^k \tag{100}$$

(c) Variation of first derivatives, P and Q of the articulating surfaces, $y = f_1(x)$ and $y' = f_2(x')$, respectively:

$$\delta_P - (2A_3 + 6A_4 x_c^k + 12A_5 x_c^{k2})\delta_{x_c} = A_2 + 2A_3 x_c^k + 3A_4 x_c^{k2} + 4A_5 x_c^{k3} - P^k \tag{101}$$

$$\delta_Q - 2A'_3 \delta_{x'_c} = A'_2 + 2A'_3 x_c'^k - Q^k \tag{102}$$

(d) Variation of the components of unit normals, $\hat{n}_1$ and $\hat{n}_2'$:

$$\delta n_{1x} + \left[\frac{\gamma}{(1 + P^{k^2})^{3/2}} \right] \delta_P = \frac{-\gamma P^k}{(1 + P^{k^2})^{1/2}} - n_{1x}^k \qquad (103)$$

$$\delta n_{1y} + \left[\frac{\gamma P^k}{(1 + P^{k^2})^{3/2}} \right] \delta_P = \frac{\gamma}{(1 + P^{k^2})^{1/2}} - n_{1y}^k \qquad (104)$$

$$\delta n_{2x'} + \left[\frac{\beta}{(1 + Q^{k^2})^{3/2}} \right] \delta_Q = \frac{-\beta Q^k}{(1 + Q^{k^2})^{1/2}} - n_{2x'}^k \qquad (105)$$

$$\delta n_{2y'} + \left[\frac{\beta Q^k}{(1 + Q^{k^2})^{3/2}} \right] \delta_Q = \frac{\beta}{(1 + Q^{k^2})^{1/2}} - n_{2y'}^k \qquad (106)$$

where $\beta = \dfrac{d^2 f_2}{dx'^2} \Big/ \left| \dfrac{d^2 f_2}{dx'^2} \right|$, and $\gamma = \dfrac{d^2 f_1}{dx'^2} \Big/ \left| \dfrac{d^2 f_1}{dx'^2} \right|$

Equations (91) through (106) form a set of 22 simultaneous algebraic equations defined by equation (52). The vector, Δ, of equation (52) has the following elements: δx_o, δy_o, $\delta\alpha$, δN, δx_c, $\delta x_c'$, δx_j (j=1,..,4), δy_j (j=1,..,4), δn_{1x}, δn_{1y}, $\delta n_{2x'}$, $\delta n_{2y'}$, δy_c, $\delta y_c'$, δP and δQ, where

δx_o = x-coordinate variation of the center of mass of the tibia.

δy_o = y-coordinate variation of the center of mass of the tibia.

$\delta\alpha$ = variation of the orientation angle, α, of the tibia with respect to the femur.

δN = variation of the normal force, N.

δx_c = x-coordinate variation of the contact point, C, in the (x,y) system.

$\delta x_c'$ = x-coordinate variation of the contact point, C, in the (x',y') system.

δ_{x_j} = x-coordinate variation of the ligament insertion points, (j=1,..4).

δ_{y_j} = y-coordinate variation of the ligament insertion points, (j=1,..4).

$\delta_{n_{1x}}$ = x-component variation of the unit normal vector to the articulating surface of the femur.

$\delta_{n_{1y}}$ = y-component variation of the unit normal vector to the articulating surface of the femur.

$\delta_{n_{2x'}}$ = x-component variation of the unit normal vector to the articulating surface of the tibia.

$\delta_{n_{2y'}}$ = y-component variation of the unit normal vector to the articulating surface of the tibia.

δ_{y_c} = y-coordinate variation of the contact point, C, in the fixed (x,y) system.

$\delta_{y'_c}$ = y-coordinate variation of the contact point, C, in the moving (x',y') system.

δ_P = variation of the first derivative of the femoral articulating surface equation.

δ_Q = variation of the first derivative of the tibial articulating surface equation.

After applying an external force and moment to the center of mass of the tibia, the above system of 22 equations are solved for the 22 variables by the computer program JNTMDL.

SOME ASPECTS OF THE COMPUTER PROGRAM, JNTMDL

Following the numerical procedure described previously, the system of 22x22 equations defined by equation (52) are solved using the JNTMDL program given in Appendix C. Prescribed constant parameters used in the program are:

(a) the coordinates (x_j,y_j) and (x'_j,y'_j) of, respectively, the insertions and origins of the ligaments.

(b) stiffness values of the ligaments, k_j.

(c) mass, M, and mass moment of inertia, I_z, of the moving tibia.

(d) initial linear ($\dot{x}_o$, $\dot{y}_o$, $\ddot{x}_o$, $\ddot{y}_o$) and angular ($\dot{\alpha}$, $\ddot{\alpha}$) velocities and accelerations of the center of mass of the moving tibia.

(e) coefficients, A_i and A'_i, of the articulating surface equations, $y = f_1(x)$ and $y' = f_2(x')$, respectively.

(f) applied external force, $\bar{F}_e$, and moment, $\bar{M}_e$.

(g) time increment, Δt.

(h) convergence criterion, omega.

By specifying the initial contact points, x_c and x'_c, the JNTMDL program first determines the starting configuration of the moving tibia relative to the fixed femur. This is done by satisfying the geometric compatibility equations (14) and contact conditions (36). After applying the prescribed external force and moment, by the use of iteration process, the JNTMDL program calculates the 22 delta variations at each iteration. The iteration process at a fixed time station continues until the delta quantities of all variables become negligibly small. In the present work, a solution is accepted and the iteration process is terminated when the delta quantities become less than or equal 0.01% of the previous values of the corresponding variables. The converged solution of each variable is then used as the initial value for the next time step and the process is repeated for consecutive time steps. In our application of the method, only 5-6 iterations were necessary for convergence most of the time. But there were also cases where more iterations were required for convergence. This was especially true at instants at which there was a sudden, sharp change in the response of the tibia. Such behavior manifested itself usually when the tibia started moving in the opposite direction due to the fact that the pulling force of a ligament(s) became the governing force of the problem. Shorter time steps required fewer iterations, as expected, even at the situation described. The time increment used in the present work is $\Delta t = 0.0001$ second.

At each converged solution, the following quantities are determined by JNTMDL program:

(a) The orientation angle, α (flexion angle), of the moving tibia relative to the fixed femur.

(b) The position (x_o, y_o) of the center of mass of tibia.

(c) The linear $(\ddot{x}_o, \ddot{y}_o)$ and angular accelerations of the center of mass of the moving tibia.

(d) The location of contact points, x_c and x_c', on the fixed femur and moving tibia, respectively.

(e) The magnitude of the contact force, N, exerted on the moving tibia.

(f) The magnitude of ligament forces, F_j.

(g) The external energy supplied to and internal energy generated by the moving tibia, for comparison purposes.

The final section of this report will present results from this program for several loading conditions applied through the center of mass of the tibia.

NUMERICAL RESULTS

The numerical results to be presented are only for an external force acting on the tibia without the presence of an external moment. It is assumed that the force is always perpendicular to the longitudinal axis of the tibia (y'-axis) and passes through its center of mass. Let this force be denoted by P(t). A parametric study of the effect of various combinations of moment and force acting simultaneously on the response of the knee joint may prove to be rewarding. However, for the present work we will only consider an external force and believe that this will be sufficient to illustrate the capabilities of the model. The effect of the shape of the forcing function on the knee joint response will be studied by considering the following two functions for P(t):

$$P(t) = A[H(t) - H(t-t_0)] \tag{107}$$

which is a rectangular pulse of duration t_0, and amplitude A; and

$$P(t) = Ae^{-4.73(t/t_0)^2} \sin\left(\frac{\pi t}{t_0}\right) \tag{108}$$

which is an exponentially decaying sinusoidal pulse of duration t_0, and amplitude A. A dynamic loading in the form of equation (107) is extremely difficult to simulate experimentally; however, the study of these two functions will hopefully be helpful in understanding the effect of rise time of the dynamic load on the joint response. Equation (108) is a more realistic forcing function and it has been previously used as a typical representation of the dynamic load in head impact analysis (Engin and Akkas, [1978]).

The following are obtained as a function of time from the computer program, JNTMDL; the coordinates x_o,y_o of the center of mass of tibia; the flexion angle α; the coordinates x_c and x_c' of the contact point in (x,y) and (x',y') coordinate systems respectively; the magnitude, N, of the contact force; the elongations of the ligaments and the ligament forces, F_j; and the internal and external energies of the system.

The initial values for x_o, y_o and α are obtained by specifying the location of the starting contact point. Here, the following values are used for the coordinates of the contact point at t = 0:

$$x_c = -4.2 \text{ cm} \quad , \quad x_c' = 2.5 \text{ cm}$$

which yields

$$x_o = -20.16 \text{ cm} \quad , \quad y_o = 17.49 \text{ cm} \quad , \quad \text{and } \alpha = 234.79°$$

This angle of rotation α, corresponds to a flexion angle of 54.79° for which the ligaments of the knee joint are in a

relatively relaxed condition. It was reported as early as 1907 by Pringle that the position of maximum relaxation of the knee joint ligaments was approximately halfway between full flexion and full extension of the knee joint.

The effect of pulse duration on the response of the knee joint motion is studied by taking t_o = 0.05S, 0.10S, and 0.15S for both rectangular and exponentially decaying sinusoidal pulses. The effect of pulse amplitude, is also examined by taking A = 20N, 60N, 100N, 140N and 180N for both types of pulses.

Ligament forces as functions of flexion angle of the knee joint for the two previously described forcing functions are presented in Figures 35 through 40. Results indicate that when the knee joint is extended, by a dynamic application of a pulse on the tibia, lateral collateral, medial collateral and anterior cruciate ligaments are elongated while the posterior cruciate ligament is shortened. The load carried by the anterior cruciate ligament is substantially higher than those of the lateral collateral and medial collateral ligaments.

The variation of the lengths of ligaments and the forces carried by them during normal knee motion has been the subject of various studies reported in the literature and in these studies several different opinions and conclusions have been expressed in regard to the biomechanical role and function of various ligaments of the knee joint. The function of the anterior cruciate as depicted in the dynamic knee-model developed in this research program is to resist anterior displacement of the tibia. This function is in general agreement with the experimental and clinical studies of Kennedy and Fowler [1971]; Girgis, Marshall and Monajem [1975]; Van Dijk, Huiskes and Selvik [1979]; and quasi-static model analyses of Crowninshield, Pope and Johnson [1976]; and Wismans [1980].

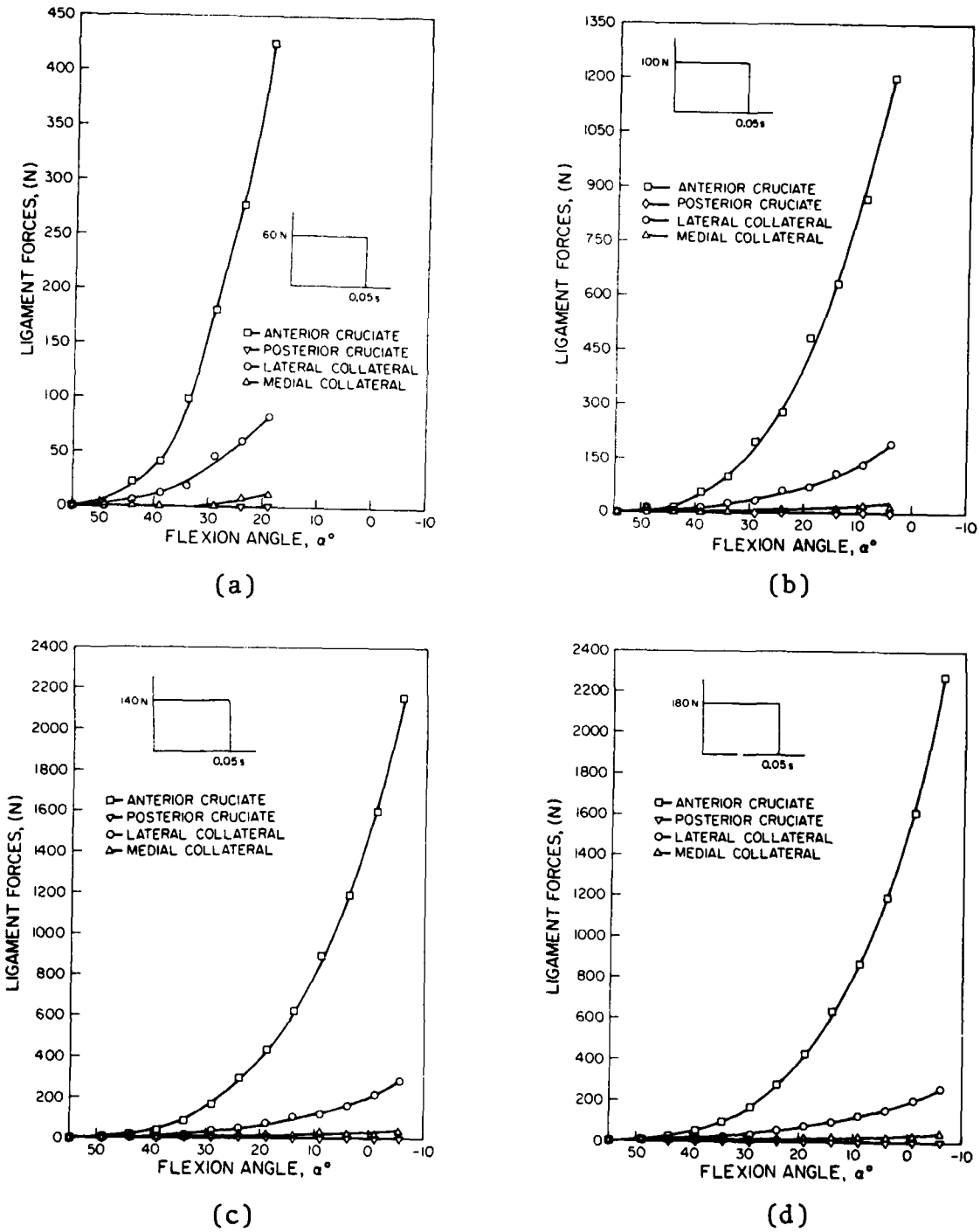

Figure 35. Ligament forces as functions of flexion angle, for an externally applied rectangular pulse of 0.05 second duration and amplitude of (a) 60 N, (b) 100 N, (c) 140 N and (d) 180 N.

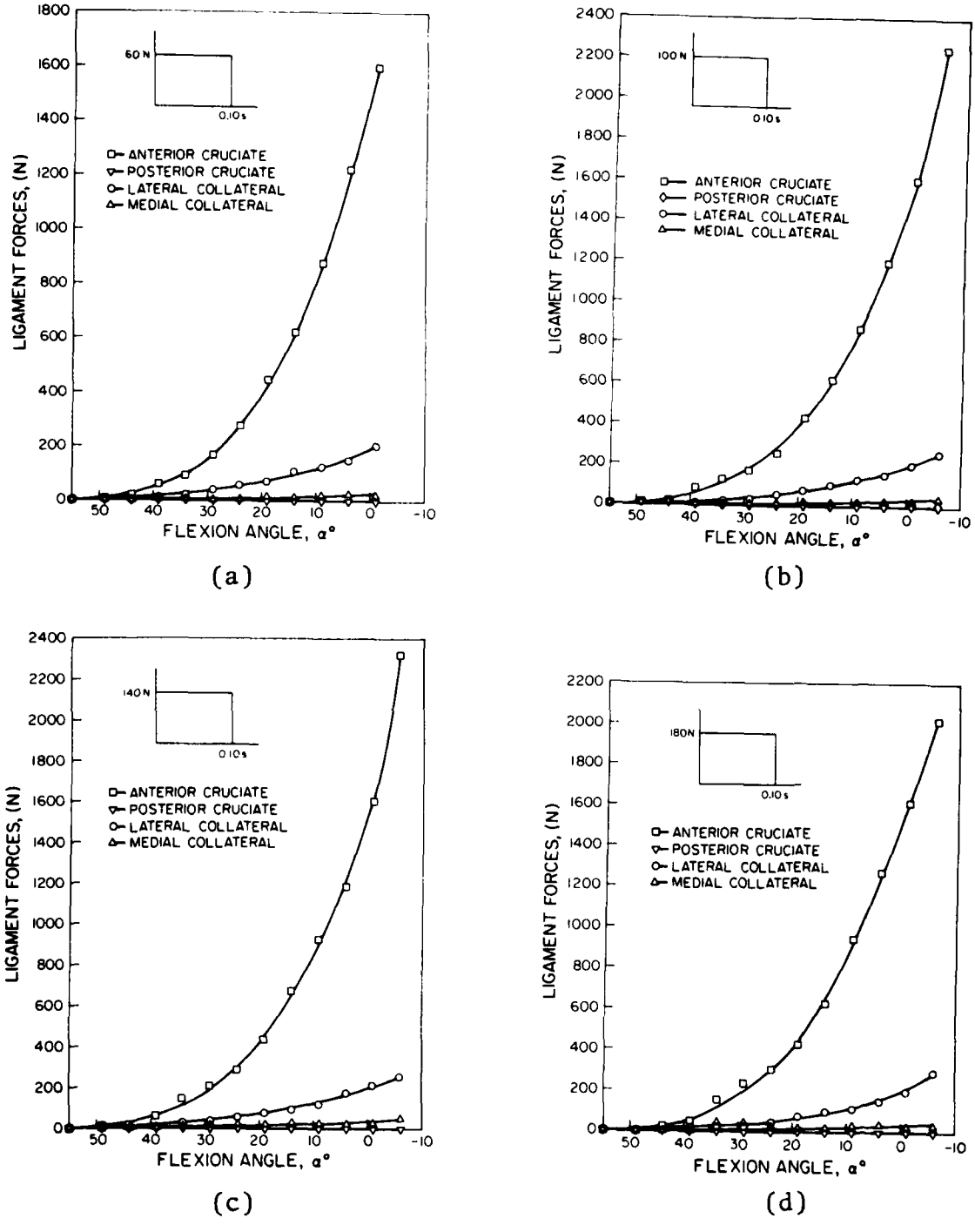

Figure 36. Ligament forces as functions of flexion angle, for an externally applied rectangular pulse of 0.10 second duration and amplitude of (a) 60 N, (b) 100 N, (c) 140 N and (d) 180 N.

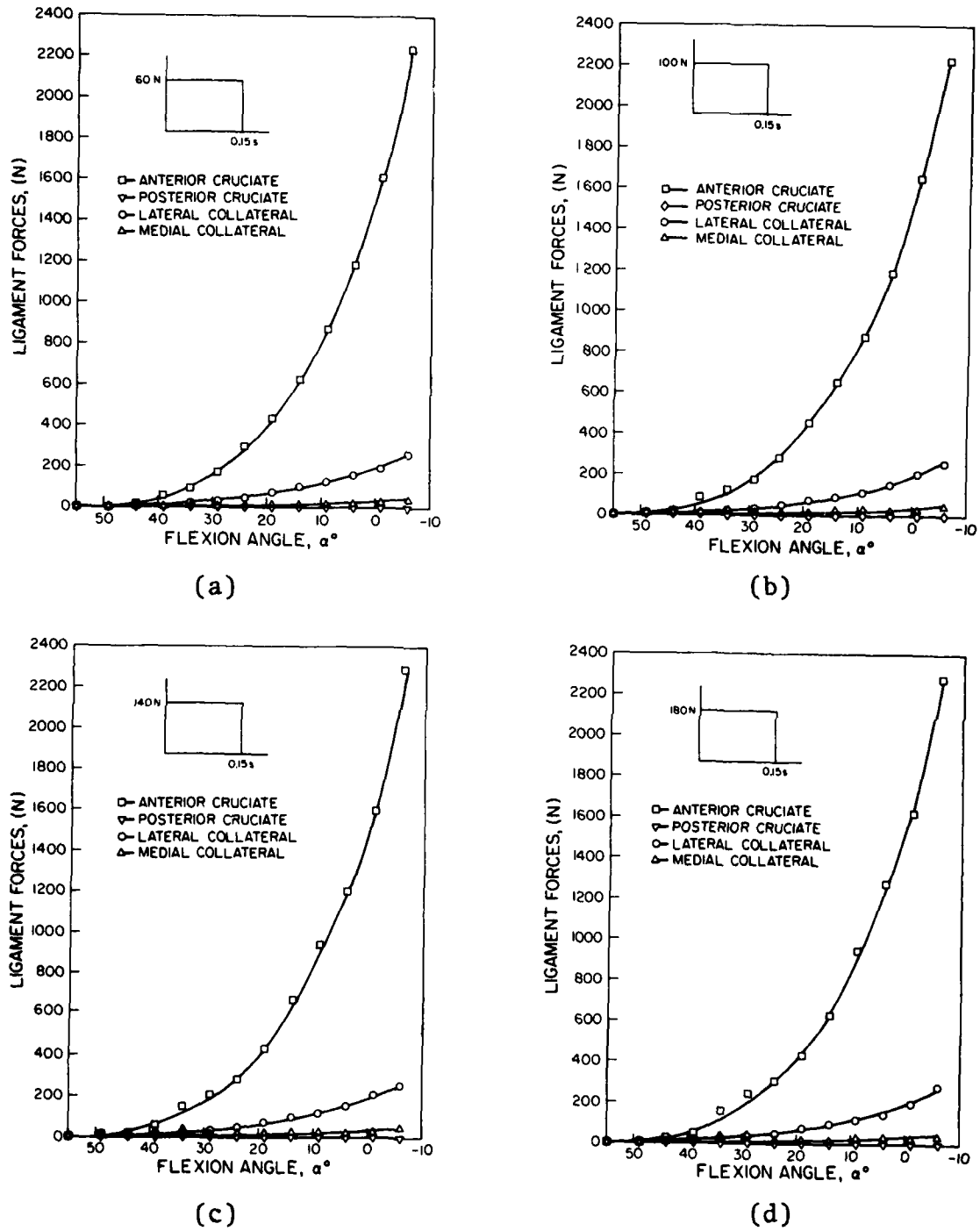

Figure 37. Ligament forces as functions of flexion angle, for an externally applied rectangular pulse of 0.15 second duration and amplitude of (a) 60 N, (b) 100 N, (c) 140 N and (d) 180 N.

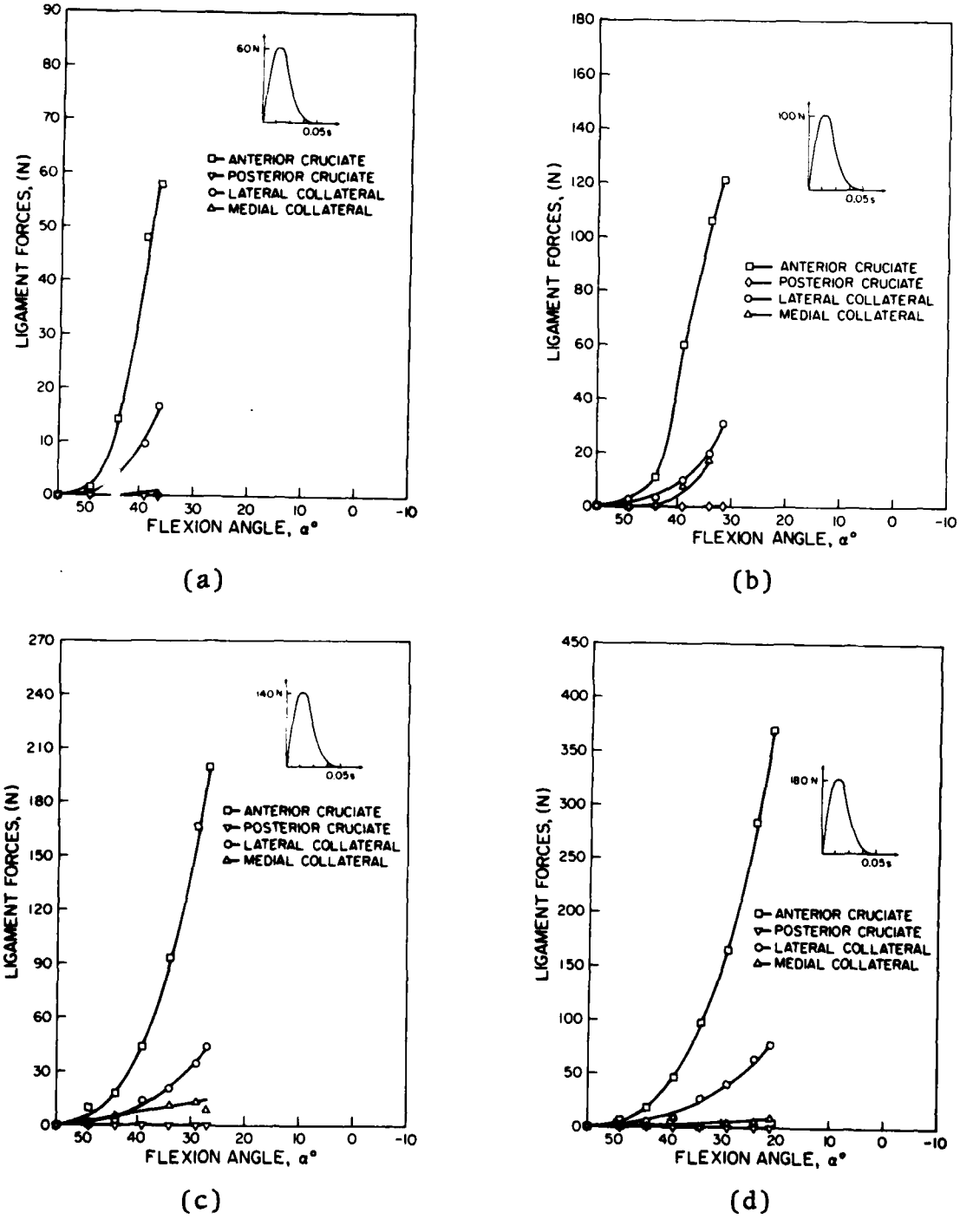

Figure 38. Ligament forces as functions of flexion angle, for an externally applied, exponentially decaying sinusoidal pulse of 0.05 second duration and amplitude of (a) 60 N, (b) 100 N, (c) 140 N and (d) 180 N.

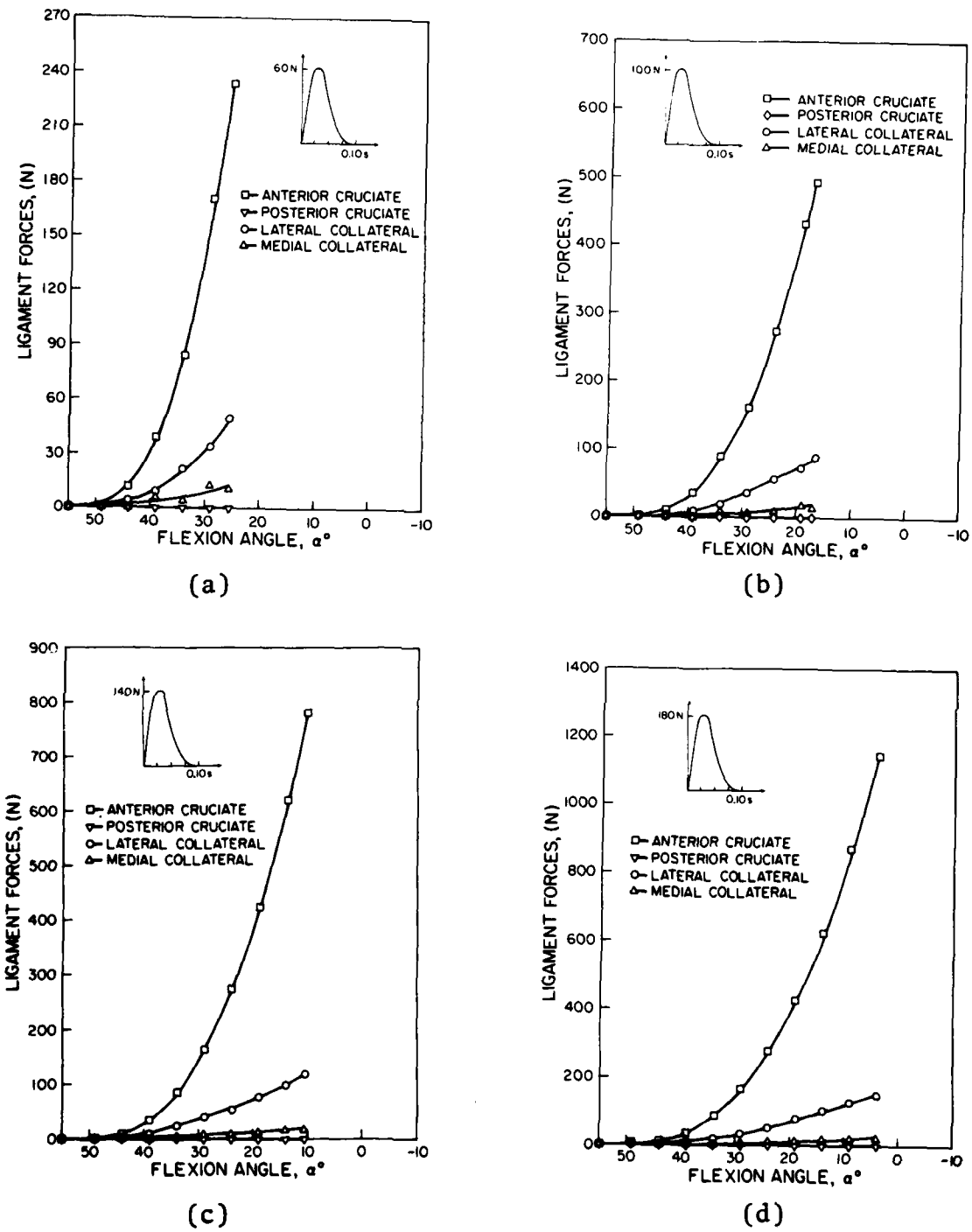

Figure 39. Ligament forces as functions of flexion angle, for an externally applied, exponentially decaying sinusoidal pulse of 0.10 second duration and amplitude of (a) 60 N, (b) 100 N, (c) 140 N and (d) 180 N.

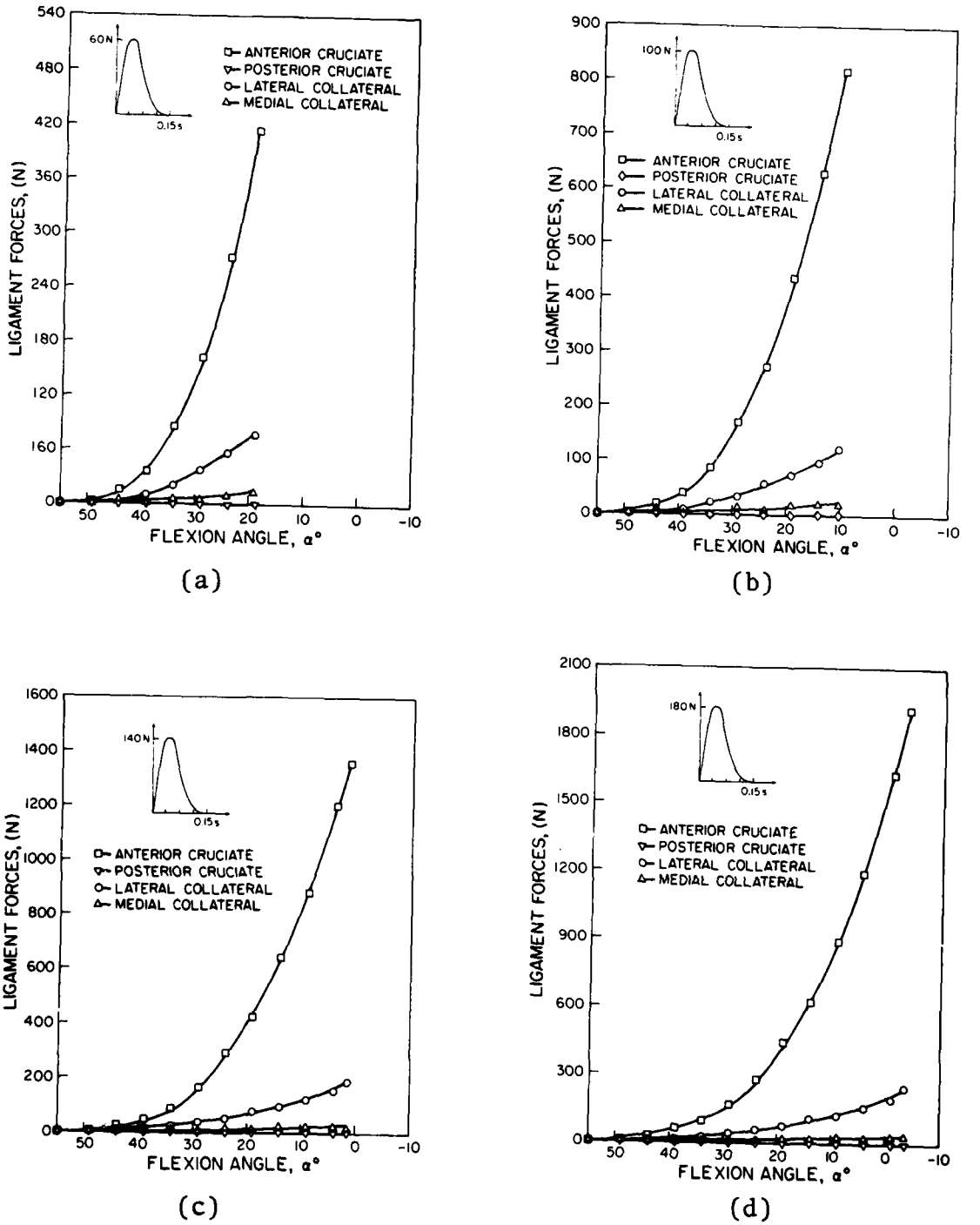

Figure 40. Ligament forces as functions of flexion angle, for an externally applied, exponentially decaying sinusoidal pulse of 0.15 second duration and amplitude of (a) 60 N, (b) 100 N, (c) 140 N and (d) 180 N.

The role of the posterior cruciate as predicted by the model is to resist posterior displacement of the tibia. This function of the posterior cruciate ligament is in agreement with the experimental studies of Kennedy and Grainger [1967]; Edwards, Lafferty and Lange [1970]; Girgis, Marshall and Monajem [1975]; Crowninshield, Pope and Johnson [1976] and Wismans [1980].

The present dynamic model also predicts that the medial and lateral collateral ligaments offer very little resistance in the flexion-extension motion of the knee joint. The major role of these ligaments is to offer varus-valgus and partial internal-external rotational stability. The model shows that as the knee joint is extended under influence of a dynamic load the lateral collateral and medial collateral ligaments elongate at different magnitudes. This prediction is in general agreement with the experimental results of Smillie [1970]; Edwards, Lafferty and Lange [1970]; and Wang, Walker and Wolf [1973].

The model shows good agreement with the quasi-static experimental investigations reported in the literature. It is important to note that the dynamic model presented in this report is an idealized representation of a very complex anatomical structure; thus, static experimental studies may not support some of the predictions of the model. Additional disagreements may also be due to approximate locations of the attachment sites of the ligaments in particular, and two-dimensional nature of the model in general.

In Figures 41 and 42, a few representative plots of forces in the anterior cruciate and lateral collateral ligaments are plotted as a function of time for two different forcing functions with varying pulse durations. Although not presented here, similar curves may be obtained for other pulse durations and pulse magnitudes. Generally, the shorter the pulse duration, for a fixed amplitude, the sooner the tibia

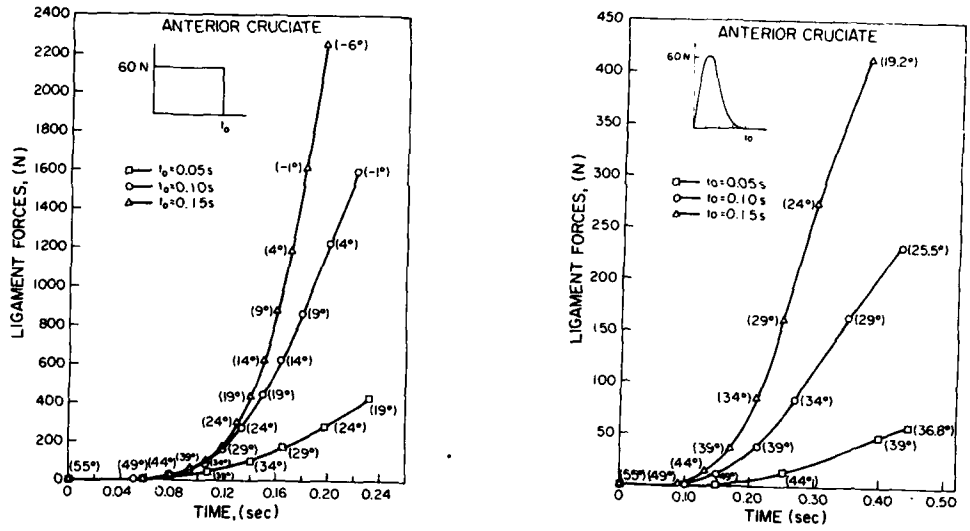

Figure 41. Anterior cruciate ligament force as a function of time for externally applied (a) rectangular and (b) exponentially decaying sinusoidal pulses, of 60 N amplitude and durations of 0.05, 0.10 and 0.15 second.

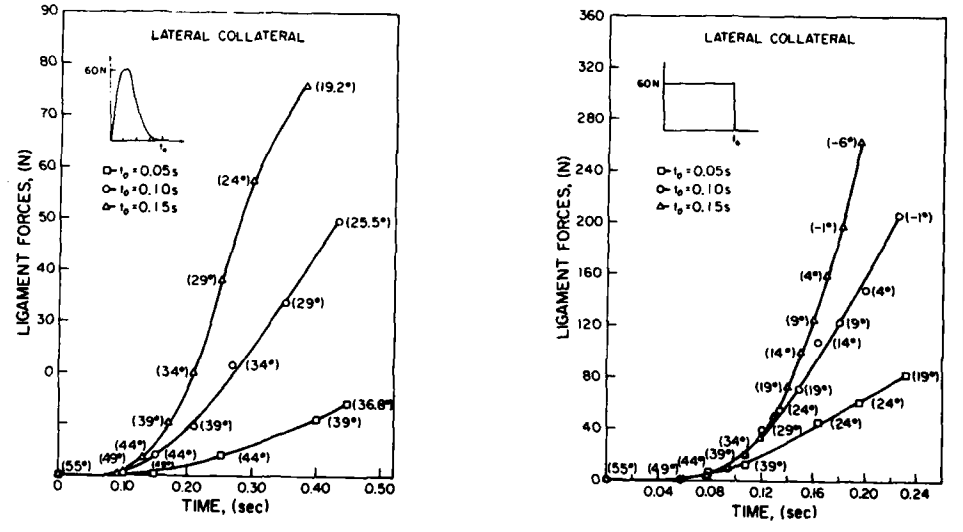

Figure 42. Lateral collateral ligament force as a function of time for externally applied (b) rectangular and (a) exponentially decaying sinusoidal pulses, of 60 N amplitude and durations of 0.05, 0.10 and 0.15 second.

reaches its turning point (i.e., direction of motion reverses) and for a given pulse duration, the smaller the amplitude, the sooner the turning point is reached. In Figures 44-47 the values in parentheses indicate the flexion angles at the corresponding times. Note that, for illustrative purposes up to 6° of hyperextension was allowed. Generally, one expects only 1 to 3° of hyperextension to be anatomically tolerable beyond which joint failure becomes unavoidable.

In Figures 43 and 44, contact forces as a function of time are plotted. These forces are in response to the different forcing functions with varying amplitudes and pulse durations. Note that the magnitudes of the ligament and the corresponding contact forces in response to a particular forcing function are comparable.

Femoral and tibial contact point locations as a function of flexion angle are plotted in Figures 45 through 50. In these figures the values in the parentheses indicate the total elapsed time of the motion since its initiation. As the flexion angle decreases, it can be seen that, the curves representing femoral contact points have a steadily increasing positive slope, while the curves of tibial contact points change slope from positive to negative or vice-versa at various flexion positions. This phenomenon may be explained by the combined rolling and sliding motion of the tibia on the femur; that is, positive and zero slopes of the curves representing the tibial contact points can be interpreted as corresponding to the sliding motion, while negative slopes indicating the rolling motion of tibia on femur. Generally, the curves of tibial contact points have predominately negative slopes toward the end of the extension motion indicating that in this part of the motion rolling is the essential component. These results are in general agreement with the work of Walker and Hajek [1972]; Kettelkamp and Jacobs [1972]; and Wismans, et al. [1980].

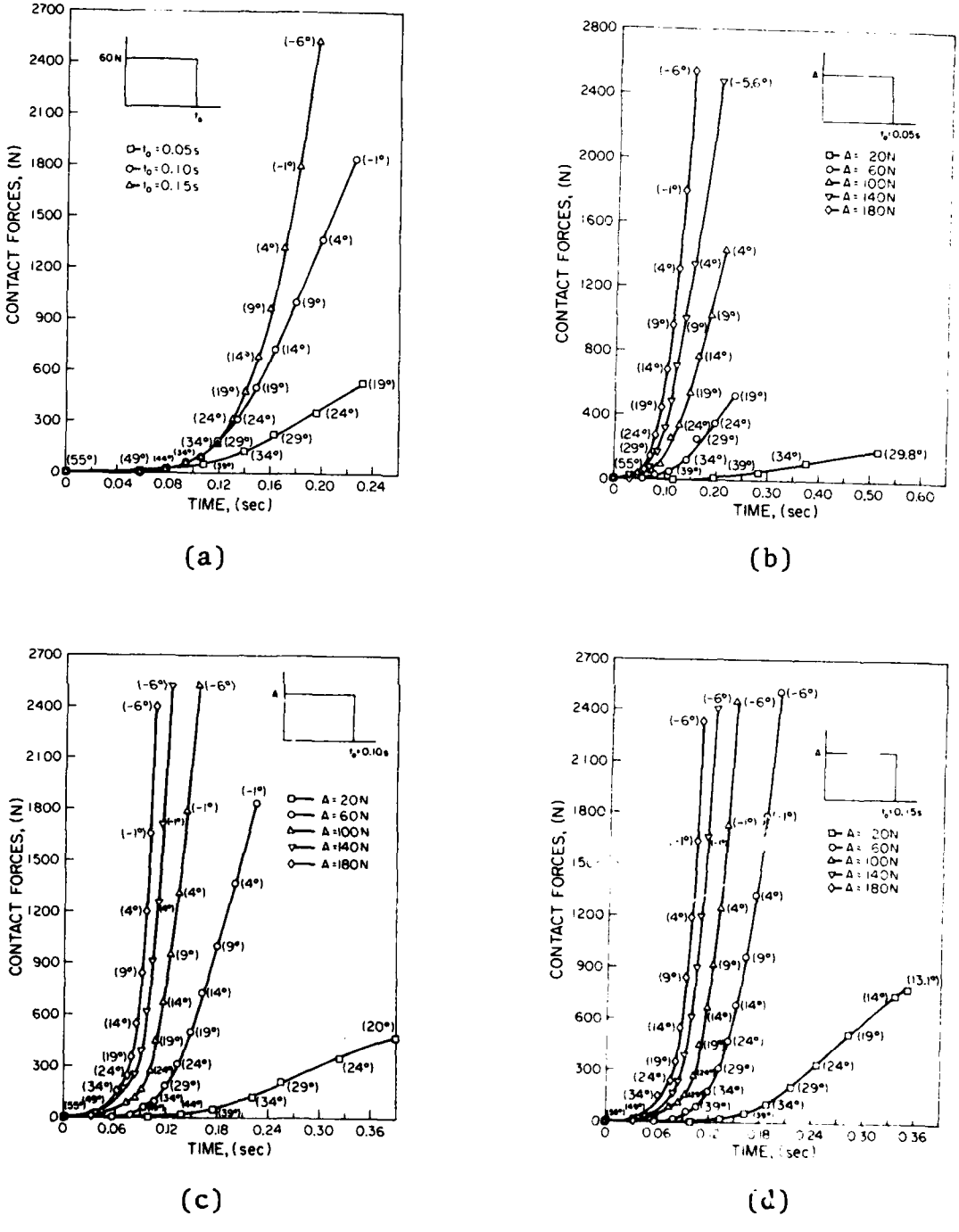

Figure 43. Contact forces as a function of time for an externally applied rectangular pulse: (a) 60 N amplitude and durations of 0.05, 0.10 and 0.15 second; 20 N, 60 N, 100 N, 140 N and 180 N amplitudes and durations of (b) 0.05 second; (c) 0.10 second and (d) 0.15 second.

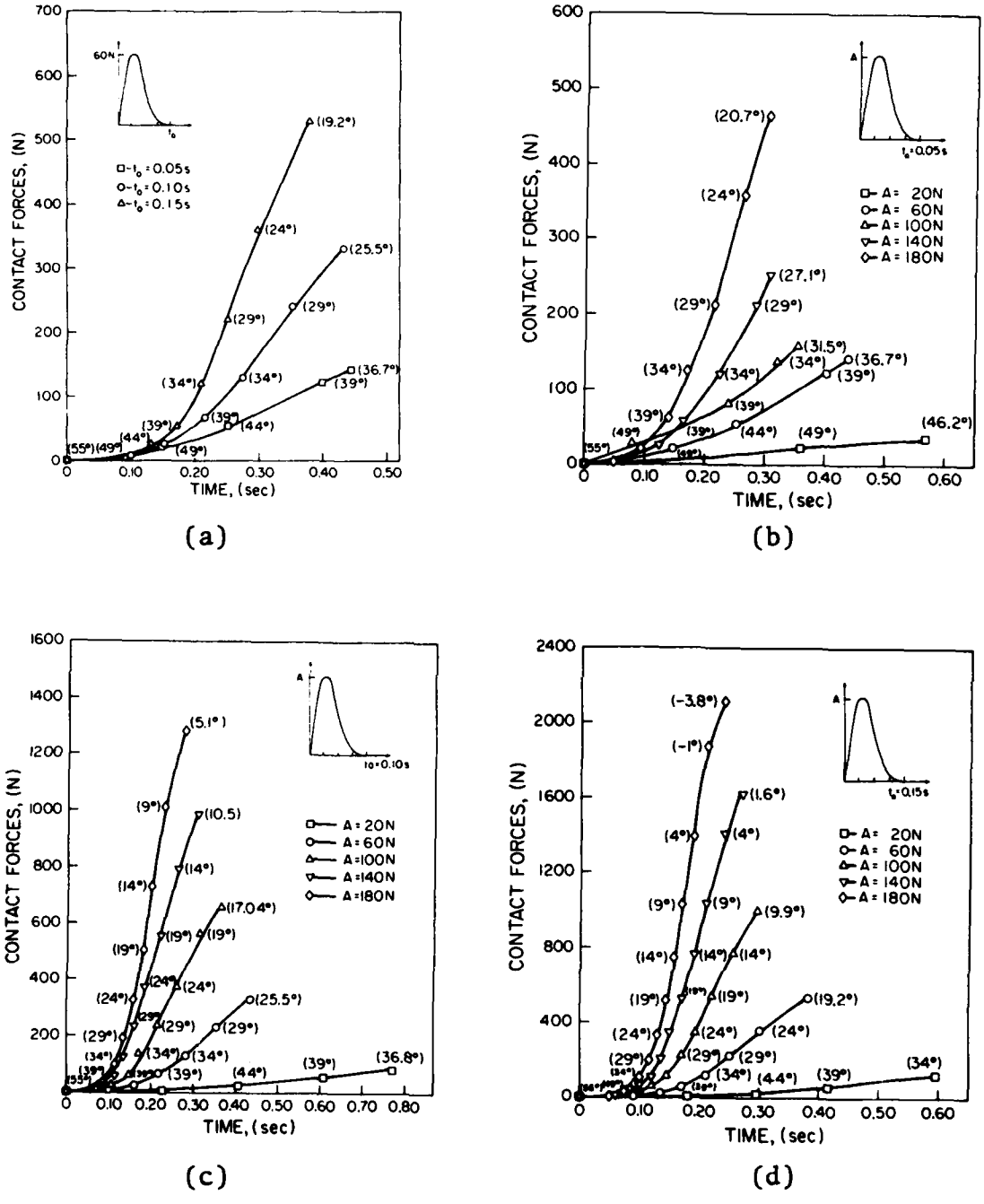

Figure 44. Contact forces as a function of time for an externally applied, exponentially decaying sinusoidal pulse; (a) 60 N amplitude and durations of 0.05, 0.10 and 0.15 second; 20 N, 60 N, 100 N, 140 N and 180 N amplitudes and durations of (b) 0.05 second, (c) 0.10 second and (d) 0.15 second.

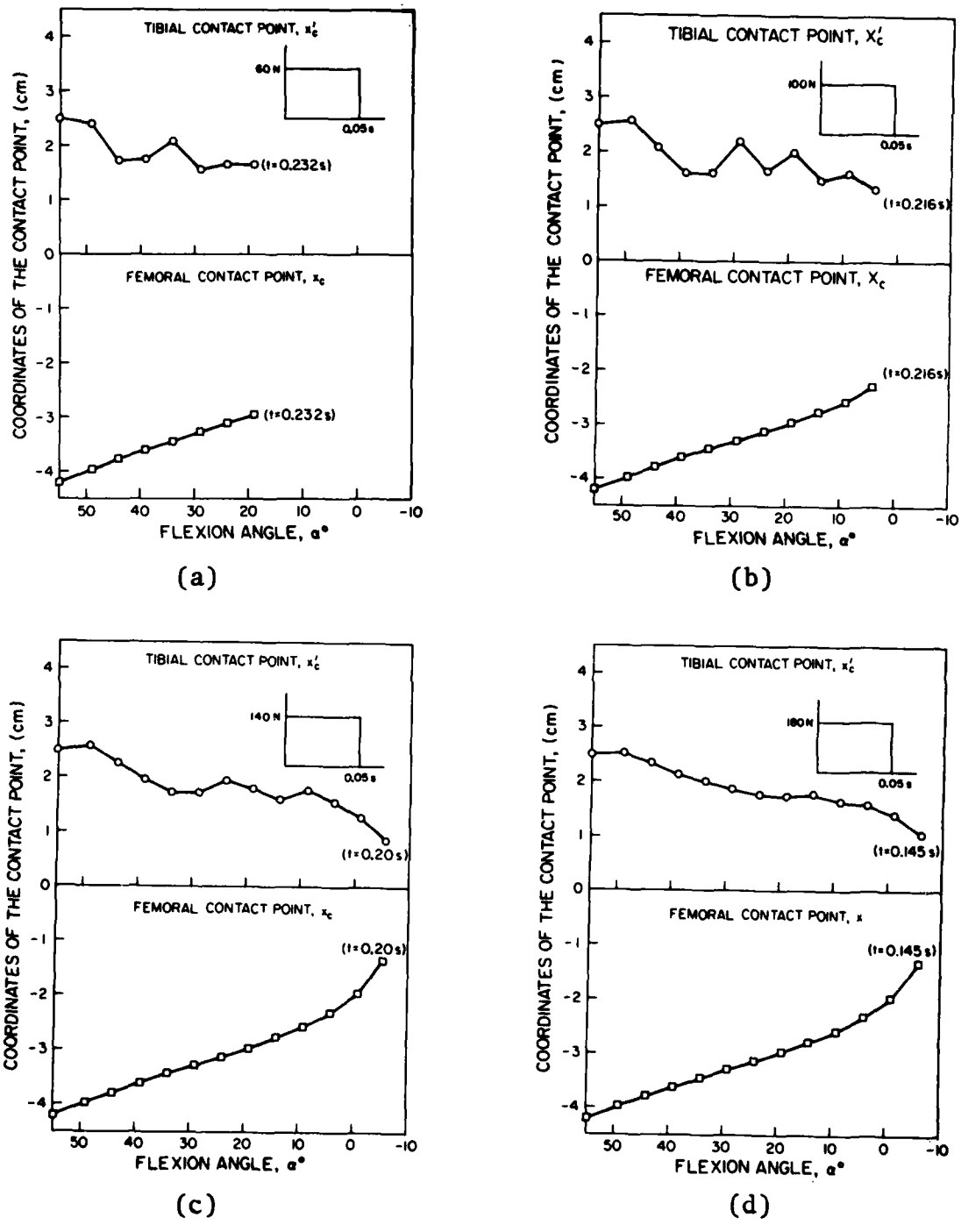

Figure 45. Femoral and tibial contact points as a function of flexion angle for an externally applied rectangular pulse of 0.05 second duration and amplitudes of (a) 60 N, (b) 100 N, (c) 140 N and (d) 180 N.

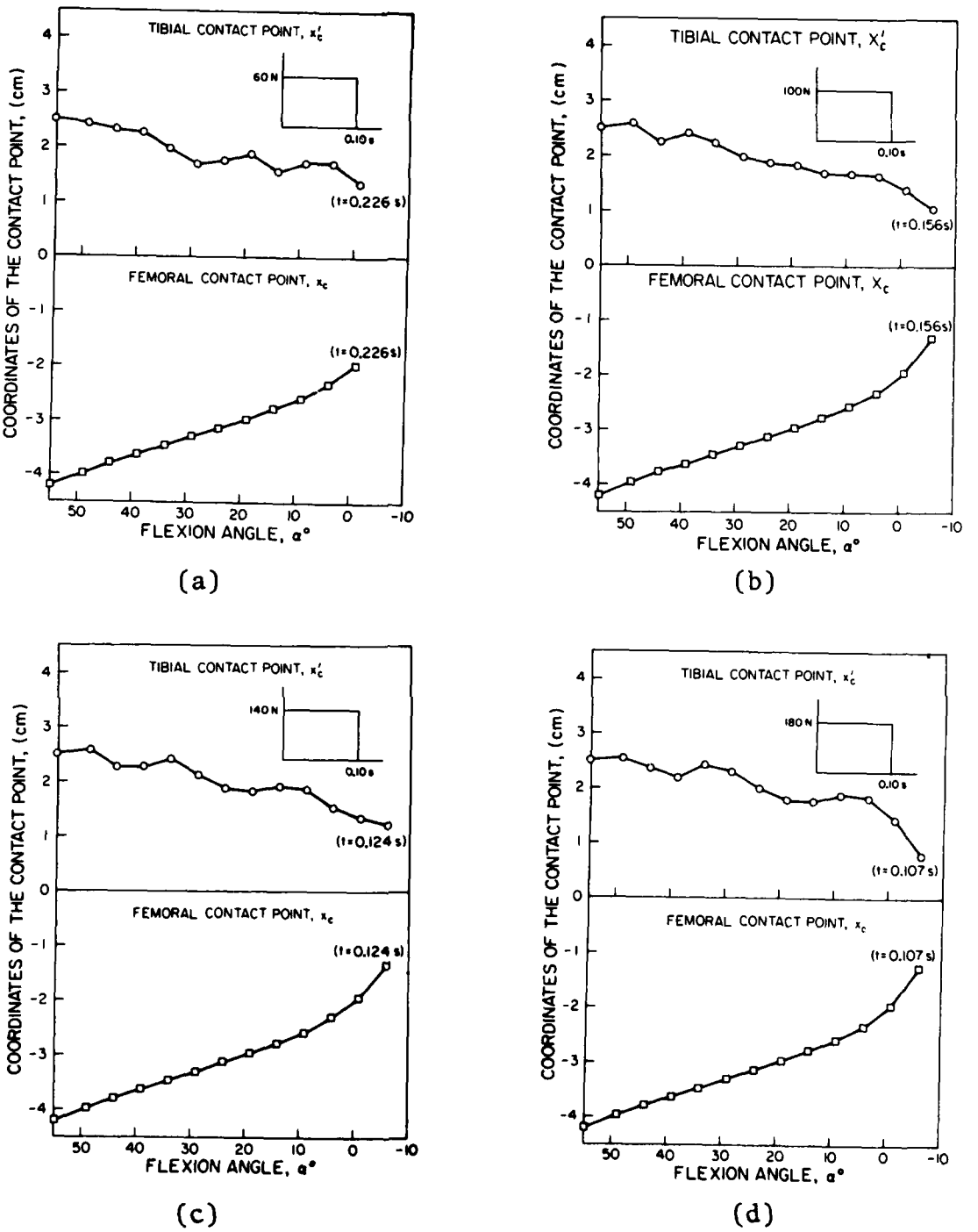

Figure 46. Femoral and tibial contact points as a function of flexion angle for an externally applied rectangular pulse of 0.10 second duration and amplitudes of (a) 60 N, (b) 100 N, (c) 140 N and (d) 180 N.

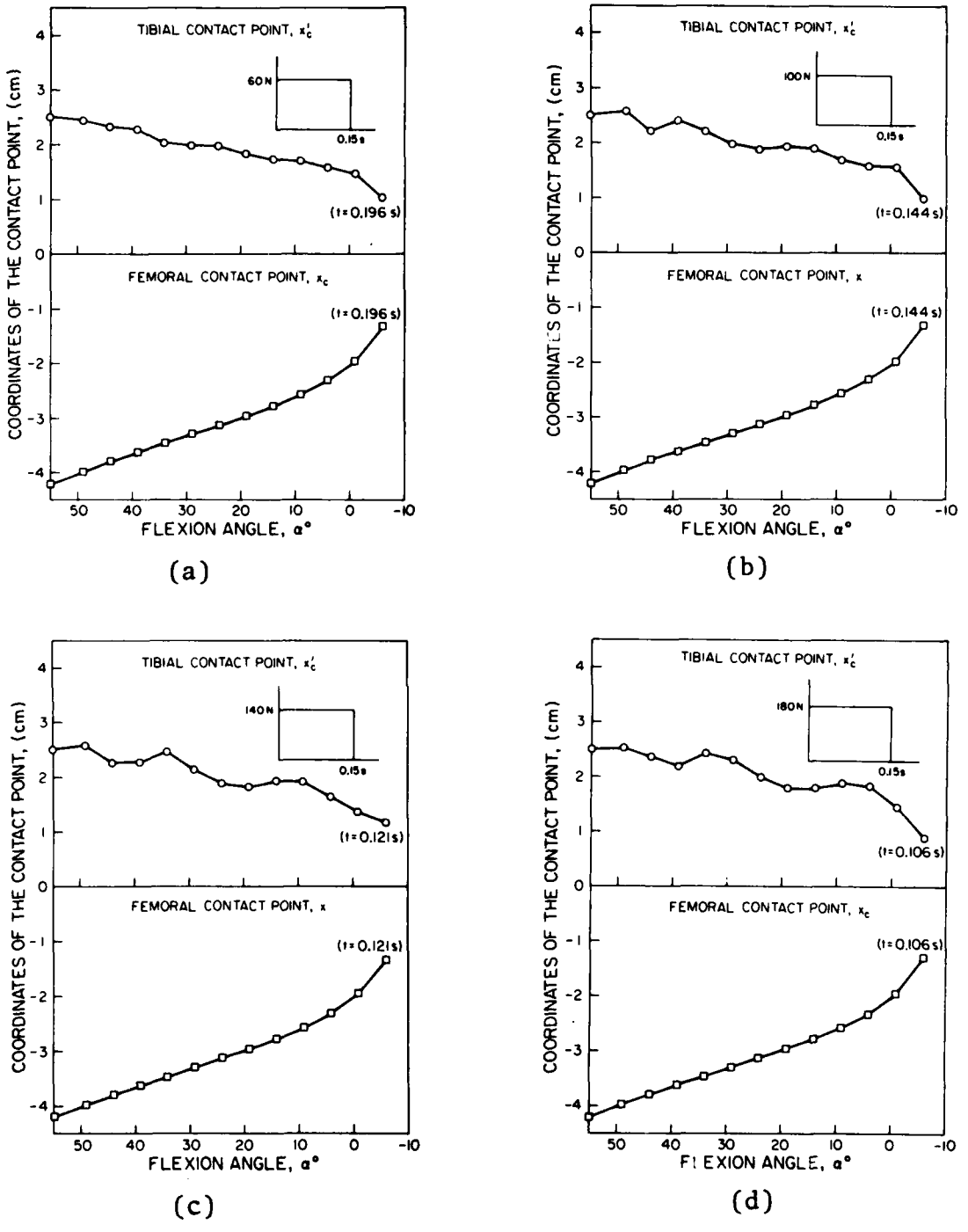

Figure 47. Femoral and tibial contact points as a function of flexion angle for an externally applied rectangular pulse of 0.15 second duration and amplitudes of (a) 60 N, (b) 100 N, (c) 140 N and (d) 180 N.

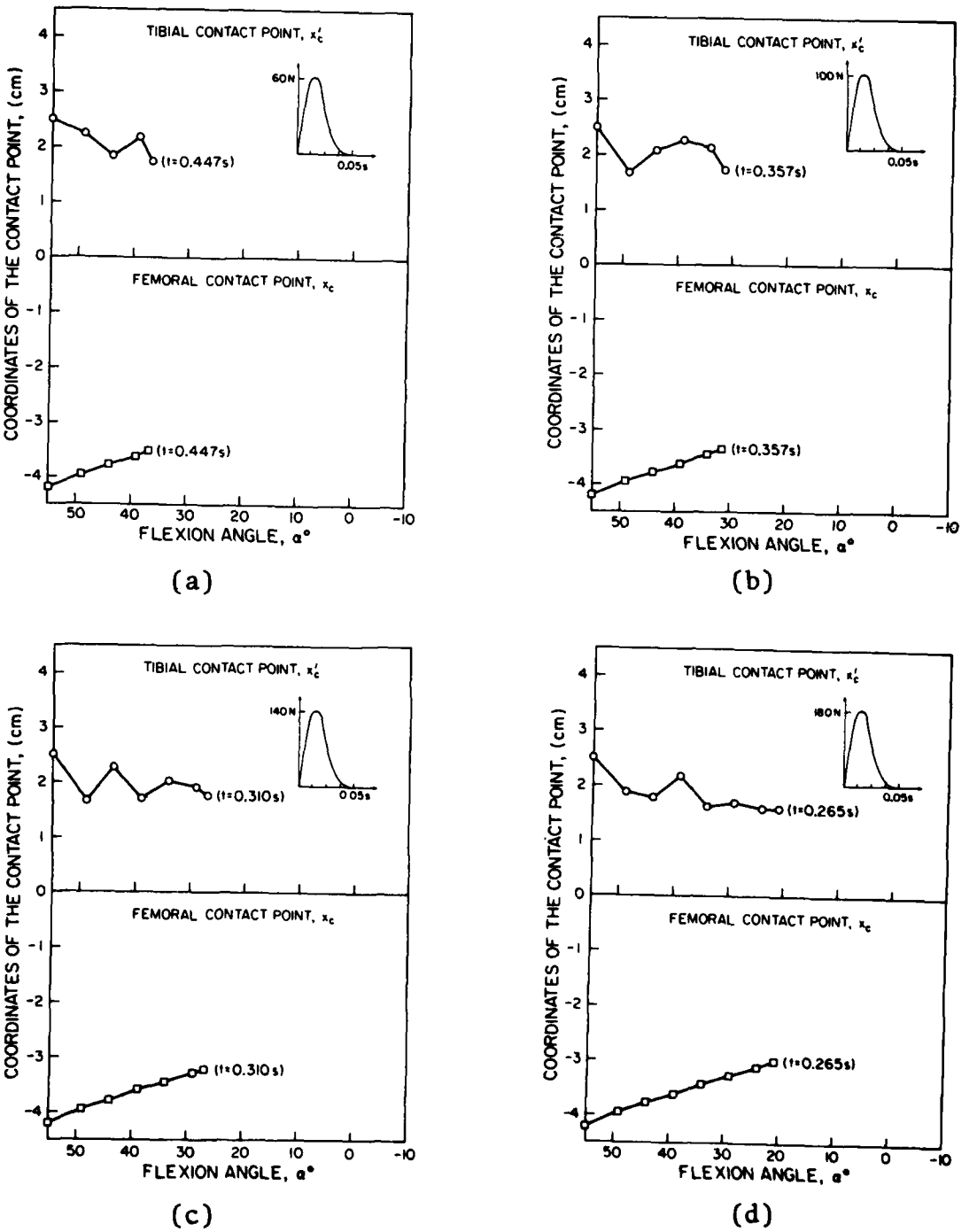

Figure 48. Femoral and tibial contact points as a function of flexion angle for an externally applied exponentially decaying sinusoidal pulse of 0.05 second duration and amplitudes of (a) 60 N, (b) 100 N, (c) 140 N and (d) 180 N.

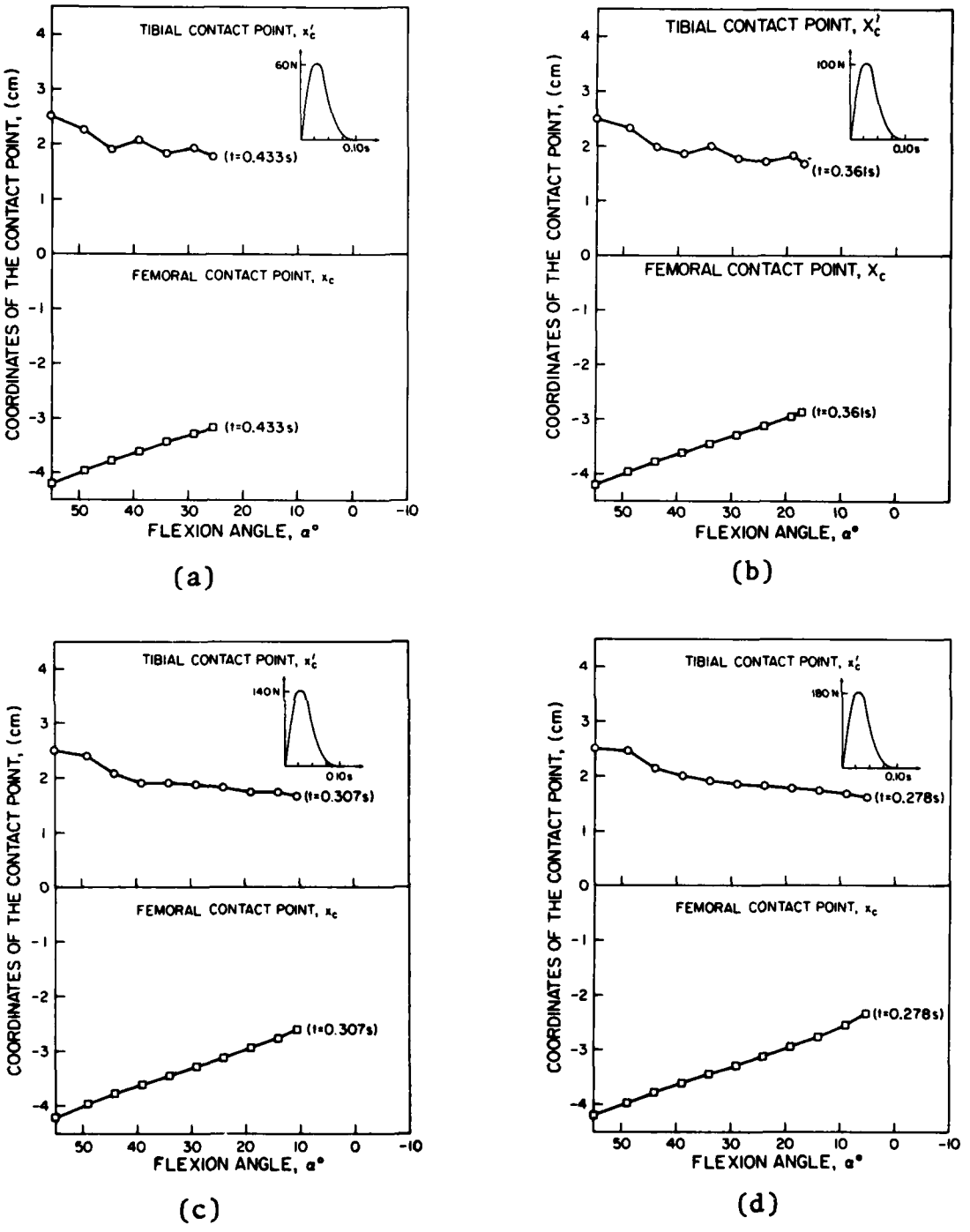

Figure 49. Femoral and tibial contact points as a function of flexion angle for an externally applied, exponentially decaying sinusoidal pulse of 0.10 second duration and amplitudes of (a) 60 N, (b) 100 N, (c) 140 N and (d) 180 N.

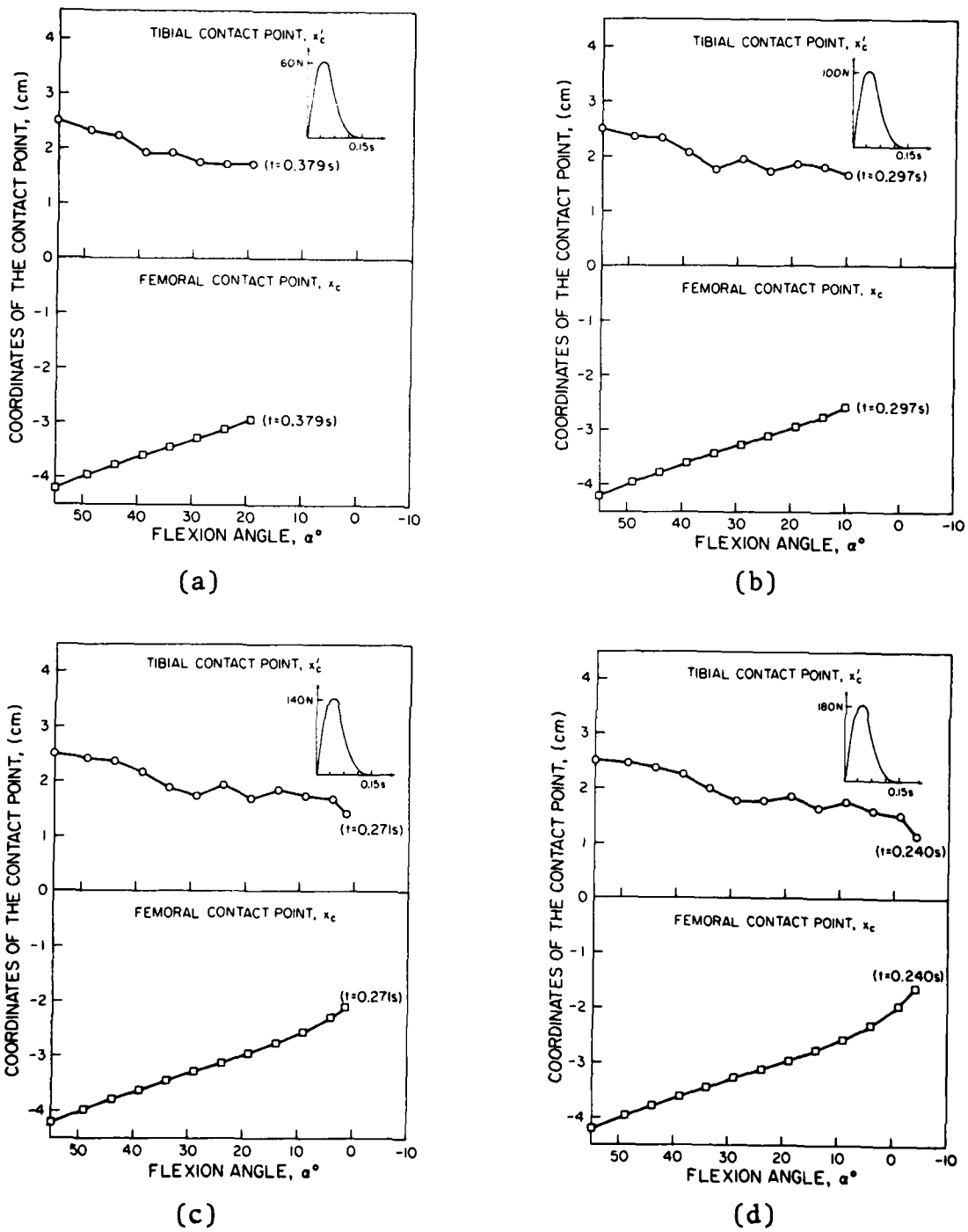

Figure 50. Femoral and tibial contact points as a function of flexion angle for an externally applied, exponentially decaying sinusoidal pulse of 0.15 second duration and amplitudes of (a) 60 N, (b) 100 N, (c) 140 N and (d) 180 N.

In Figures 51 and 52, total internal energy of the moving tibia as a function of flexion angle are plotted. This total internal energy is defined as the summation of potential energies of the nonlinear elastic springs, simulating the ligament forces, and the kinetic energy of the tibia. As it can be seen from these curves, for a given pulse shape of fixed duration, as the pulse magnitude increases, the knee joint further extended and the entire motion has a shorter response time period. External energy of the system is also calculated based on the applied external forces. Continuous plots of total internal and external energy of the system for two different pulse shapes of specified magnitude and duration are presented in Figures 53 and 54. These figures show that the total internal and external energies of the system remain the same except for the latter part of the motion, which is due to the accumulation of numerical round-off errors. Finally, for illustrative purposes, with the aid of Versatec plotter, continuous plots of x_o, y_o (coordinates of the center of mass of the tibia); x_c and x_c' (femoral and tibial contact points, respectively) and flexion angle, α, as a function of time are plotted in figures 55 and 56.

SUMMARY AND CONCLUDING REMARKS

The research work discussed and presented in this report can be summarized in the following paragraphs:

1. Detailed anatomical description and articulation of the elbow, shoulder, hip, knee and ankle joints with sufficient illustrative figures for each joint were presented and major anatomical parts have been identified using the generally applied medical terminology.

2. Mathematical descriptions of the articulating surfaces of elbow, hip, knee and ankle joints have been determined by means of a sonic digitizing technique. The attachment sites of the major ligaments of each joint were also determined and tabulated.

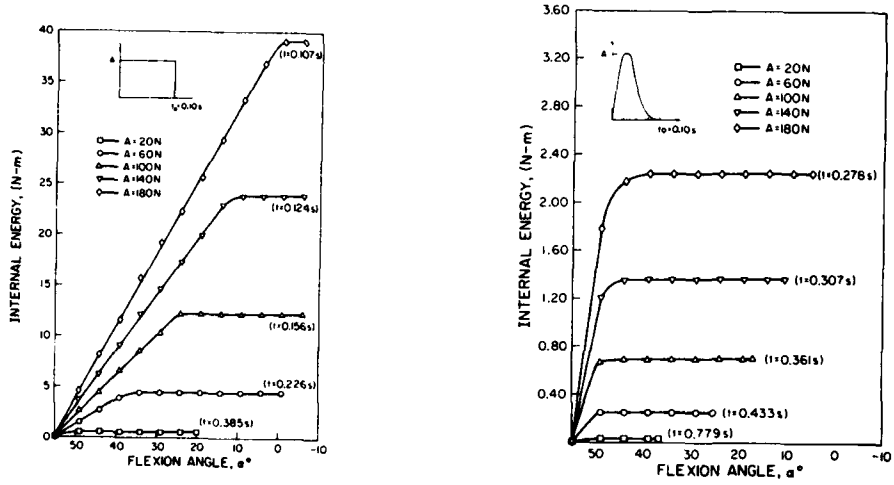

(a) (b)

Figure 51. Total internal energy of the moving tibia as a function of flexion angle for an externally applied (a) rectangular pulse and (b) exponentially decaying sinusoidal pulse of 0.10 second duration and amplitudes of 20 N, 60 N, 140 N and 180 N.

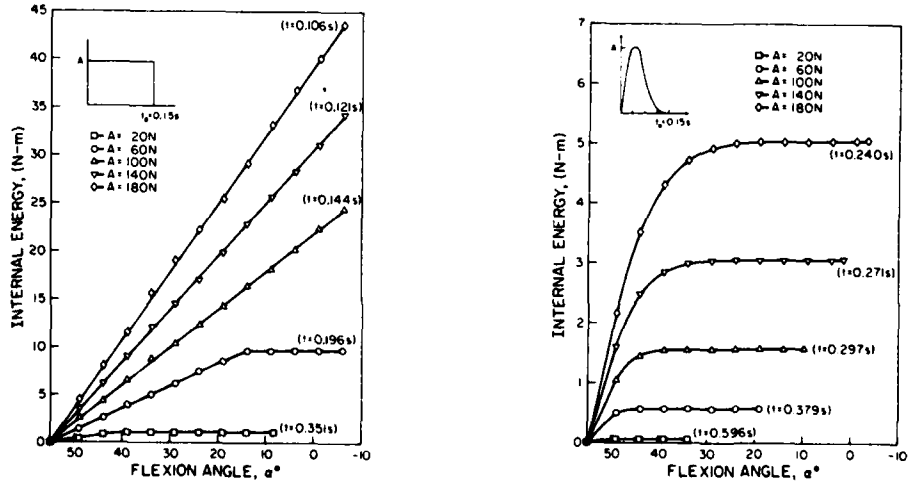

(a) (b)

Figure 52. Total internal energy of the moving tibia as a function of flexion angle for an externally applied (a) rectangular pulse and (b) exponentially decaying sinusoidal pulse of 0.15 second duration and amplitudes of 20 N, 60 N, 100 N, 140 N and 180 N.

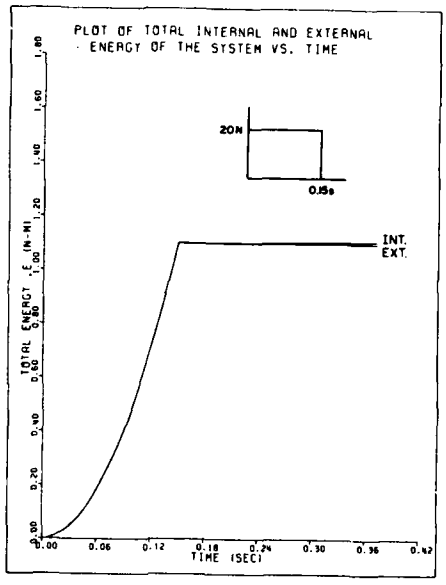

Figure 53. Continuous total internal and external energies of the joint system as a function of time for an externally applied rectangular pulse of 20 N amplitude and 0.15 second duration

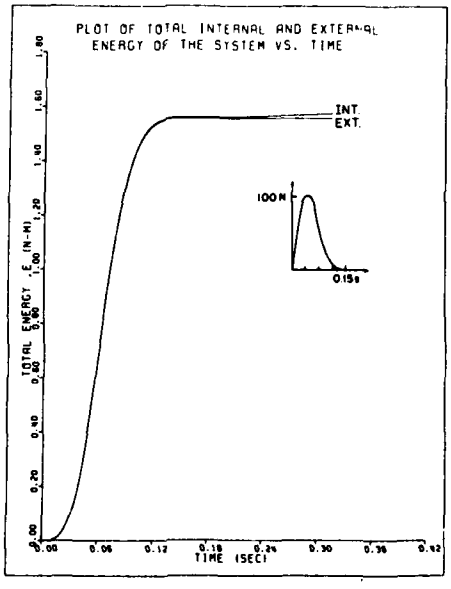

Figure 54. Continuous total internal and external energies of the joint system as a function of time for an externally applied, exponentially decaying sinusoidal pulse of 100 N amplitude and of 0.15 second duration.

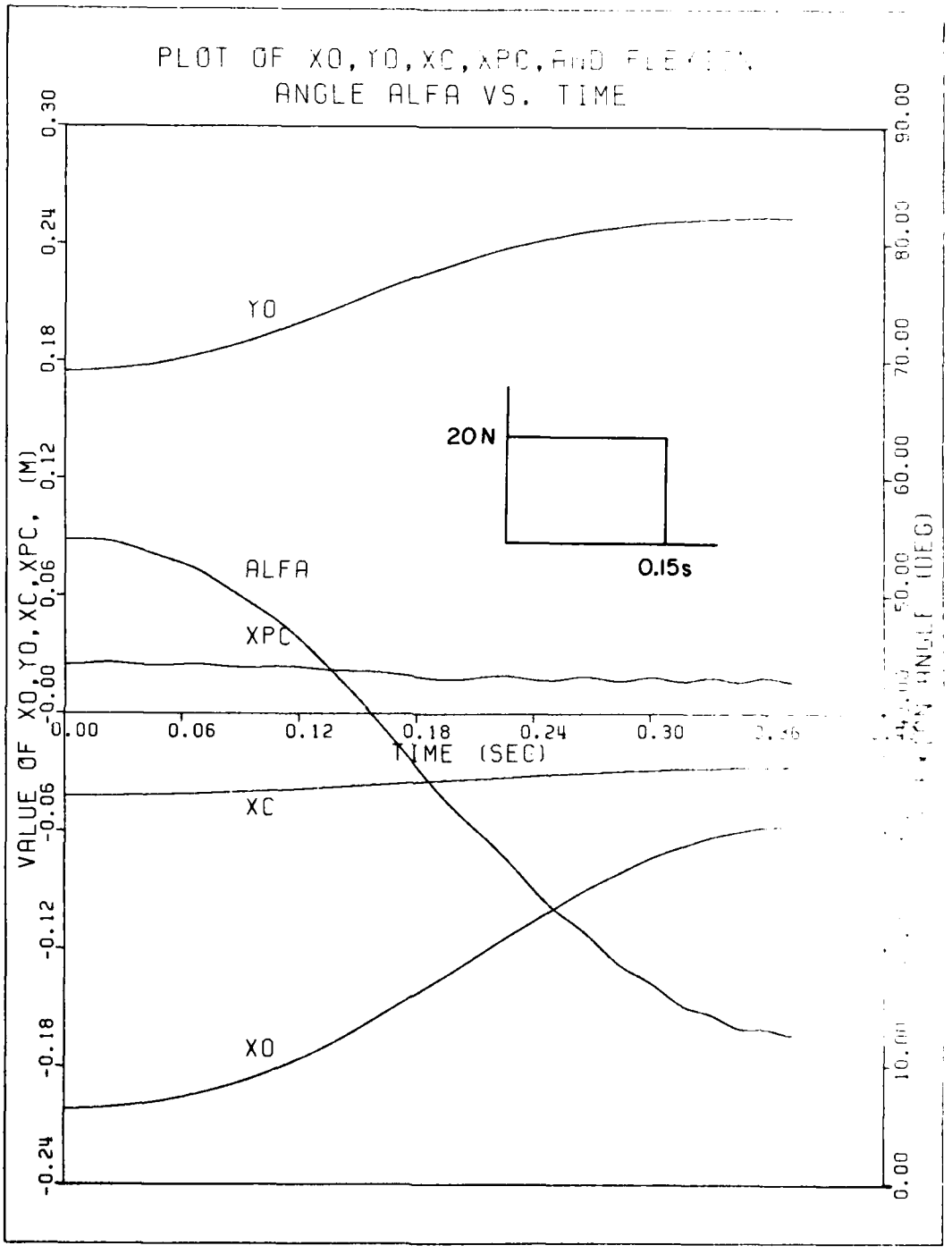

Figure 55. Continuous plots of tibial center of mass coordinates (XO,YO), femoral (XC) and tibial (XPC) contact points and the flexion angle (ALFA) as functions of time for an externally applied rectangular pulse of 20 N amplitude and of 0.15 second duration

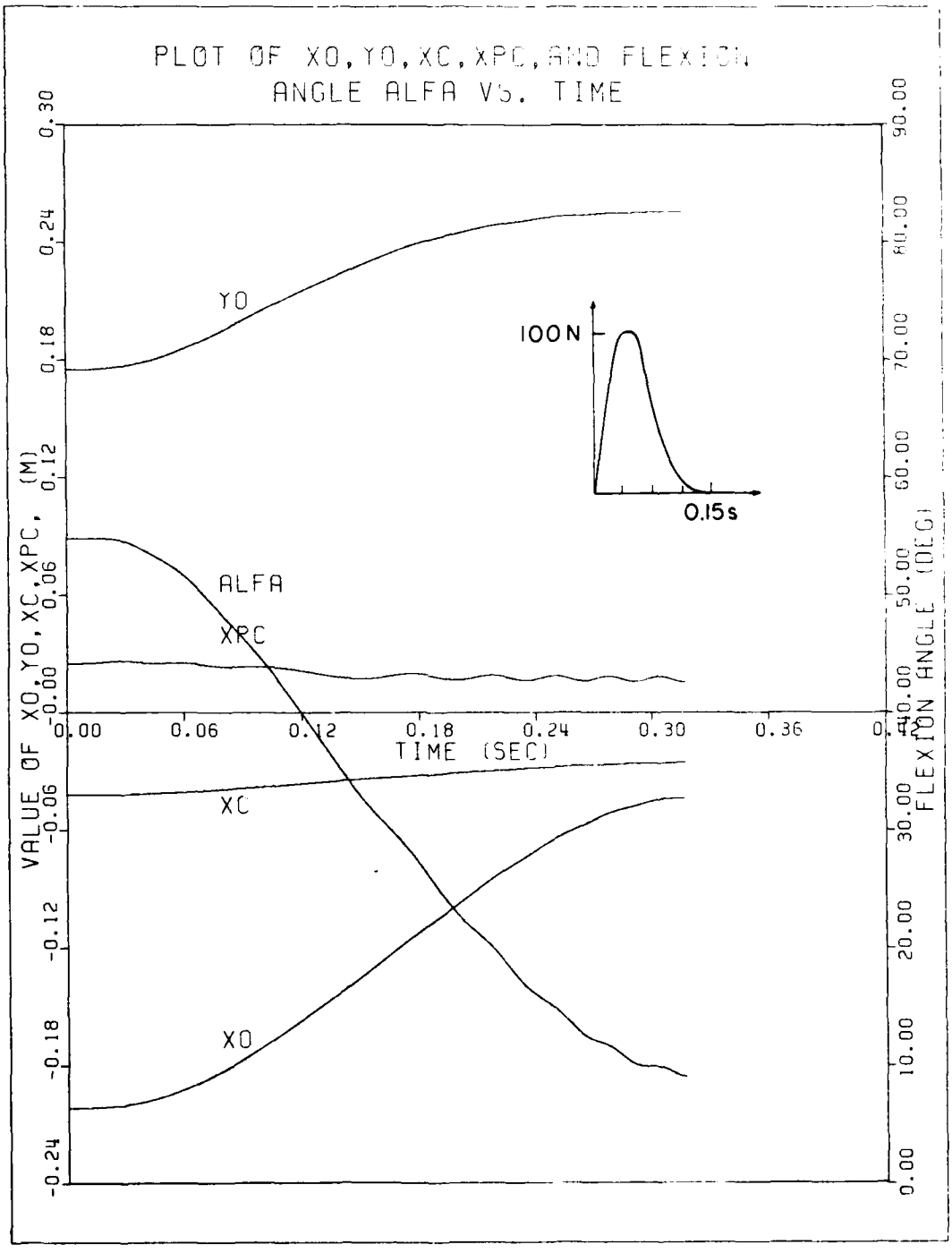

Figure 56. Continuous plots of tibial center of mass coordinates (XO,YO), femoral (XC) and tibial (XPC) contact points and the flexion angle (ALFA) as functions of time for an externally applied, exponentially decaying sinusoidal pulse of 100 N amplitude and of 0.15 second duration.

3. A review of the available literature on the biomechanical behavior of soft tissues in general and ligaments in particular was presented. An appropriate constitutive equation for the elastic behavior of the ligaments was established.

4. Two- and three-dimensional mathematical dynamic models of a general two-body-segmented articulating joint have been formulated in order to describe the relative motions between the segments and the various forces produced at the joint. The governing equations for these models are set of highly nonlinear equations and numerical solutions were discussed in some detail.

5. The two-dimensional model was applied to the knee joint and the numerical results from this model were presented to illustrate the effects of duration and shape of the dynamically applied loads on the response of the joint. Special attention has been given to the ligament and contact forces, the location of contact points, anterior-posterior displacements and the comparison between the internal and the external energy of the system. The results were compared with the available experimental data from the literature to establish the validity of the model.

It is appropriate to make several remarks on the numerical techniques tried in the course of obtaining the solution for the governing equations of the two-dimensional dynamic model (equations (45), (46) and (47), coupled with constraint equations (14) and (36)). In the first method, the second-order differential equations were transformed to a set of nonlinear algebraic equations by substituting for the differential elements, their equivalent backward difference approximations. In this case, it was impossible to obtain a converging solution due to the highly nonlinear nature of these equations.

In the second method, the flexion angle, α, of the moving tibia and contact point coordinates, x_c and x_c' were obtained from the simultaneous solution of the three nonlinear constraint equations. Knowing α, $\ddot{\alpha}$ was obtained via backward difference method and then the normal force, N, was determined from the third equation of motion. The other two second-order nonlinear differential equations which were in terms of x_o and y_o were written as a set of four first order differential equations by direct substitutions. Runge-Kutta method was applied to these equations and solutions for x_o, y_o and their time derivatives were obtained. Using the new values of x_o and y_o, a new value of α and contact point coordinates were obtained and the entire procedure was repeated for the next time step. Although mathematically all the geometric constraints and governing equations of motion were satisfied, the results obtained using this second method were not in agr ment with the actual physical geometry and the anatomy of the joint. This was concluded to be due to the solution technique which was not solving all the equations simultaneously, and during the solution process it was forcing some of the variables to accept values which were mathematically correct but physically unacceptable. Finally, the Newton-Raphson iteration process along with Newmark method of differential approximation was chosen as the method of solution which yielded accurate and stable solutions for the model. The entire numerical procedure has been explained in detail in previous sections.

The extensions of the research work presented in this report can be in several areas. One can investigate the influence of the variations of initial strain of the ligaments and their attachment sites (i.e. insertions and origins) on the response of the model. A parametric study addressing to these points may reveal the sensitivity of the model to the variations of the coordinates of the insertions and origins of the ligaments.

In a similar way the mathematical models of the other major articulating joints can be developed. However, a special attention should be given in modeling of the ligaments. Some ligaments, particularly the thick band or large cord-like ligaments, have complex behavior, with various portions behaving differently under given conditions or configurations. These are described in the literature as, in the case of the broad ligaments of the hip joint, having anterior and posterior fibers, or medial and lateral components. The mathematical model should include additional elastic elements to reflect the contributions of various fibers of the ligaments. Unfortunately proper experimental data to determine the constitutive behavior of these thick band or broad ligaments do not exist.

Finally, the numerical procedure utilized in the solution of the two-dimensional dynamic joint model equations should be applied to the three-dimensional dynamic model formulation presented in this report. Considering importance and relevance of a three-dimensional dynamic joint model to the Air Force related applications, a very serious effort should be expended in the direction of obtaining numerical solutions for this complex joint model.

APPENDIX A

COMPUTER SUBROUTINE CHEPLS: A LEAST SQUARES CURVE-FITTING ROUTINE

The calculation most commonly performed on experimental data is to fit the data with a polynomial of the form: $F(X) = A + BX + CX^2 + DX^3 + \ldots MX^N$, which is best in the least squares sense. CHEPLS routinely performs this calculation. Data input is simple enough so that no prior computer experience is required for its use.

The routine determines by means of statistical tests whether the set of data is linear or non-linear. If the data are non-linear at the 95 percent confidence level, the routine finds the lowest degree polynomial which adequately represents the data. The calculation procedure is to compare the standard deviation of the model of degree n, with the standard deviation of the $(n+1)^{th}$ degree model. If there is no significant difference at the 95 percent confidence level, then it can be said that in 19 out of 20 such sets of data, the polynomial of degree n is the lowest degree polynomial which adequately represents the data.

CHEPLS prints out the least squares coefficients for all polynomials, from the first degree through the highest degree calculated. For each polynomial, the standard deviation and the confidence bands about each coefficient at the 95 percent level are printed. Values of Y are calculated from the model for every value of X, and are compared with the observed (ie, experimental or input) values of Y. The least squares matrix is printed for reference in the event additional statistical calculations are needed. The Y values are coded by subtracting a constant to reduce round-off error. As many as 1000 data points may be submitted in each data set. CHEPLS will produce polynomials

up to degree ten. Data sets may be stacked, one behind the other for additional data sets.

RESTRICTIONS

(a) The number of data points must be less than or equal to 1000.

(b) The maximum degree polynomial is 10. Even in double-precision, round-off error may accumulate sufficiently to invalidate results for even as low as a 5^{th} degree polynomial.

(c) All numeric data must be right-justified in the field.

INPUT DATA

Each data set consists of a data header, a label and one or more data cards and a termination card. For stacked data sets, only the final data set may contain a termination card. All fixed point variables or integers are entered without a decimal. Floating point variables require a decimal in the field.

(a) Data Header

Columns 4-5	Enter the number of data points in this set.
Columns 9-10	Blank for normal use. For obtaining all polynomials up to the n^{th} degree (maximum of 10), enter n. All least squares polynomials will then be calculated for degrees 1 through n.

(b) Label

Columns 1-80	Enter any alphanumeric identification to be included on the printout for descriptive purposes.

(c) Data Cards

Columns 1-80	Enter two data pairs per card, as X, Y, X, Y. Format may be either 4E18.8 or 4F18.8. Note that for an odd number of data sets, columns 37-80 of the final data card will be blank.

(d) Termination Card

Columns 23-25	Enter END to signify the end of data entry: no further data sets.

The job control language for running this subroutine is as follows:

```
// TIME=(0,25),REGION=192K
/*JOBPARM LINES=1000,CARDS=100,DISKIO=1300
//*
//* EXECUTE THE CHEM ENG LIBRARY PROGRAM CHEPLS
//*
*//STEPB EXEC PGM=IEWL,PARM='XREF,LIST,MAP',TIME=(0,30)
//* STEPB IS LINK EDIT STEP (LOAD MODULE ASSEMBLED)
//SYSLIB DD DSNAME=SYS1.FORTLIB,DISP=SHR
//       DD DSNAME=FEA680.CHEMENGR,DISP=SHR
//       DD DSNAME=SYS2.FORTSSP,DISP=SHR
//OLDLIB DD DSNAME=FEA680.CHEMENGR,DISP=SHR
//SYSLMOD DD DSNAME=&&GO(MAIN),UNIT=SYSDA,SPACE=(CYL,(1,1,1)),        *
//             DISP=(NEW,PASS),DCB=(RECFM=U,BLKSIZE=3072)
//SYSPRINT DD SYSOUT=A
//SYSUT1 DD UNIT=SYSDA,SPACE=(CYL,(2,1))
//SYSLIN DD *
   INCLUDE OLDLIB(CHEPLS)
/*
//STEPC EXEC PGM=*.STEPB.SYSLMOD,REGION=126K,TIME=(1,00)
//* STEPC IS EXECUTION STEP
//SYSUDUMP    DD  SYSOUT=A
//FT05F001 DD DDNAME=SYSIN
//FT06F001 DD SYSOUT=A
//FT07F001 DD SYSOUT=B
//SYSIN DD *
//* REMOVE THIS CARD AND REPLACE WITH DATA DECK (BLANK CARD IF NO DATE)
/*
//
```

APPENDIX B

APPLICATION OF NEWTON-RAPHSON METHOD IN THE DERIVATION OF THE LINEARIZED GOVERNING DYNAMIC EQUATIONS OF MOTION FOR THE KNEE JOINT

EQUATIONS OF MOTION

a) From equation (45):

$$\sum_{j=1}^{4} F_{jx} + \gamma N n_{1x} + (F_e)_x = M\ddot{x}_o \tag{B1}$$

in (B1) let:

$$N = N^k + \delta_N$$

$$n_{1x} = n_{1x}^k + \delta_{n1x}$$

$$x_o = x_o^k + \delta_{x_o}$$

Then

$$\sum_{j=1}^{4} F_{jx} + \gamma(N^k + \delta_N)(n_{1x}^k + \delta_{n1x}) + (F_e)_x = M\ddot{x}_o$$

$$\sum_{j=1}^{4} F_{jx} + \gamma [N^k n_{1x}^k + N^k \delta_{n1x} + n_{1x}^k \delta_N] + (F_e)_x = M\ddot{x}_o$$

Let

$$\ddot{x}_o^t = \left\{ \frac{4}{\Delta t^2}[(x_o^k + \delta_{x_o}) - x_o^{t-\Delta t}] - \frac{4}{\Delta t}\dot{x}_o^{t-\Delta t} - \ddot{x}_o^{t-\Delta t} \right\}$$

Then

$$(\gamma n_{1x}^k)\delta_N + (\gamma N^k)\delta_{n_{1x}} - (\frac{4M}{\Delta t^2})\delta_{x_o} = -\sum_{j=1}^{4} F_{jx} - (F_e)_x$$

$$-\gamma N^k n_{1x}^k + M\left\{ \frac{4}{\Delta t^2}[x_o^k - x_o^{t-\Delta t}] - \frac{4}{\Delta t}\dot{x}_o^{t-\Delta t} - \ddot{x}_o^{t-\Delta t} \right\} \tag{B2}$$

b) From equation (46):

$$\sum_{j=1}^{4} F_{jy} + \gamma N\, n_{1y} + (F_e)_y = M\ddot{y}_o \qquad \text{(B3)}$$

in (B3) let:

$$N = N^k + \delta_N$$

$$n_{1y} = n_{1y}^k + \delta_{n1y}$$

$$y_o = y_o^k + \delta_{y_o}$$

Then

$$\sum_{j=1}^{4} F_{jy} + \gamma[(N^k + \delta_N)(n_{1y}^k + \delta_{n1y})] + (F_e)_y = M\ddot{y}_o$$

$$\sum_{j=1}^{4} F_{jy} + \gamma[N^k n_{1y}^k + N^k \delta_{n1y} + n_{1y}^k \delta_N] + (F_e)_y = M\ddot{y}_o$$

Let

$$\ddot{y}_o^{\,t} = \left\{ \frac{4}{\Delta t^2} [(y_o^k + \delta_{y_o}) - y_o^{\,t-\Delta t}] - \frac{4}{\Delta t} \dot{y}_o^{\,t-\Delta t} - \ddot{y}_o^{\,t-\Delta t} \right\}$$

Then

$$(\gamma n_{1y}^k)\delta_N + (\gamma N^k)\delta_{n1y} - \left(\frac{4M}{\Delta t^2}\right)\delta_{y_o} = -\sum_{j=1}^{4} F_{jy} - (F_e)_y$$

$$-\gamma N^k n_{1y}^k + M\left\{ \frac{4}{\Delta t^2} [y_o^k - y_o^{\,t-\Delta t}] - \frac{4}{\Delta t} \dot{y}_o^{\,t-\Delta t} - \ddot{y}_o^{\,t-\Delta t} \right\} \qquad \text{(B4)}$$

c) From equation (47):

$$\sum_{j=1}^{4} (x_j - x_o)F_{jy} - \sum_{j=1}^{4} (y_j - y_o)F_{jx} + \gamma N[(x_c - x_o)n_{1y}$$

$$-(y_c - y_o)n_{1x}] + M_e = I_z\ddot{\alpha} \qquad \text{(B5)}$$

in (B5) let:

$$x_j = x_j^k + \delta_{x_j}$$

$$y_j = y_j^k + \delta_{y_j}$$

$$N = N^k + \delta_N$$

$$x_c = x_c^k + \delta_{x_c}$$

$$y_c = y_c^k + \delta_{y_c}$$

$$n_{1x} = n_{1x}^k + \delta_{n1x}$$

$$n_{1y} = n_{1y}^k + \delta_{n1y}$$

$$x_o = x_o^k + \delta_{x_o}$$

$$y_o = y_o^k + \delta_{y_o}$$

$$\alpha = \alpha^k + \delta\alpha$$

Then

$$\sum_{j=1}^{4}[(x_j^k - x_o^k) + (\delta_{x_j} - \delta_{x_o})]F_{jy} - \sum_{j=1}^{4}[(y_j^k - y_o^k) + (\delta_{y_j} - \delta_{y_o})]F_{jx}$$
$$+ \gamma(N^k + \delta_N)\Big\{[(x_c^k - x_o^k) + (\delta_{x_c} - \delta_{x_o})][n_{1y}^k + \delta_{n1y}]$$
$$-[(y_c^k - y_o^k) + (\delta_{y_c} - \delta_{y_o})][n_{1x}^k + \delta_{n1x}]\Big\} + M_e = I_z\ddot{\alpha}$$

or

$$\sum_{j=1}^{4}(x_j^k - x_o^k)F_{jy} - \sum_{j=1}^{4}(y_j^k - y_o^k)F_{jx} + \sum_{j=1}^{4}F_{jy}\delta_{x_j} - \sum_{j=1}^{4}F_{jx}\delta_{y_j}$$
$$+ \sum_{j=1}^{4}F_{jx}\delta_{y_o} - \sum_{j=1}^{4}F_{jy}\delta x_o + \gamma(N^k + \delta_N)\Big\{[(x_c^k - x_o^k)n_{1y}^k$$

$$+ (x_c^k - x_o^k)\delta_{n1y} + n_{1y}^k \delta_{x_c} - n_{1y}^k \delta_{x_o}] - [(y_c^k - y_o^k)n_{1x}^k$$

$$+ (y_c^k - y_o^k)\delta_{n1x} + n_{1x}^k \delta_{y_c} - n_{1x}^k \delta_{y_o}]\Big\} + M_e = I_z\ddot{\alpha}$$

or

$$\sum_{j=1}^{4}(x_j^k - x_o^k)F_{jy} - \sum_{j=1}^{4}(y_j^k - y_o^k)F_{jx} + \sum_{j=1}^{4}F_{jy}\delta_{x_j}$$

$$-\sum_{j=1}^{4}F_{jx}\delta_{y_j} + \sum_{j=1}^{4}F_{jx}\delta_{y_o} - \sum_{j=1}^{4}F_{jy}\delta_{x_o} + \gamma N^k(x_c^k - x_o^k)\, n_{1y}^k$$

$$+ \gamma N^k(x_c^k - x_o^k)\delta_{n_{1y}} + (\gamma N^k n_{1y}^k)\delta_{x_c} - (\gamma N^k n_{1y}^k)\delta_{x_o}$$

$$- \gamma N^k(y_c^k - y_o^k)n_{1x}^k - \gamma N^k(y_c^k - y_o^k)\delta_{n_{1x}} - \gamma N^k n_{1x}^k \delta_{y_c}$$

$$+ \gamma N^k n_{1x}^k \delta_{y_o} + (x_c^k - x_o^k)n_{1y}^k \delta_N - (y_c^k - y_o^k)n_{1x}^k \delta_N$$

$$+ M_e = I_z\ddot{\alpha}$$

Let:

$$\ddot{\alpha}^t = \left\{\frac{4}{\Delta t^2}\left[(\alpha^k + \delta_\alpha) - \alpha^{t-\Delta t} - \frac{4}{\Delta t}\dot{\alpha}^{t-\Delta t} - \ddot{\alpha}^{t-\Delta t}\right]\right\}$$

Then

$$\sum_{j=1}^{4}F_{jy}\delta_{x_j} - [\sum_{j=1}^{4}F_{jy} + \gamma N^k n_{1y}^k]\delta_{x_o} - \sum_{j=1}^{4}F_{jx}\delta_{yj}$$

$$+ [\sum_{j=1}^{4}F_{jx} + \gamma N^k n_{1x}^k]\delta_{y_o} + [(x_c^k - x_o^k)n_{1y}^k - (y_c^k - y_o^k)n_{1x}^k]\delta_N$$

$$- [\gamma N^k(y_c^k - y_o^k)]\delta_{n_{1x}} + [\gamma N^k(x_c^k - x_o^k)]\delta_{n1y} + [\gamma N^k n_{1y}^k]\delta_{x_c}$$

$$- (\gamma N^k n_{1x}^k)\delta_{y_c} - \frac{4I_z}{\Delta t^2}\delta_\alpha = -\sum_{j=1}^{4}(x_j^k - x_o^k)F_{jy} + \sum_{j=1}^{4}(y_j^k - y_o^k)F_{jx}$$

$$-\gamma N^k[(x_c^k - x_o^k)n_{1y}^k - (y_c^k - y_o^k)n_{1x}^k] + I_z\left\{\frac{4}{\Delta t^2}(\alpha^k - \alpha^{t-\Delta t}) - \frac{4}{\Delta t}\dot{\alpha}^{t-\Delta t} - \ddot{\alpha}^{t-\Delta t}\right\} - M_e \qquad \text{(B6)}$$

CONSTRAINT EQUATIONS

From equation (8)

$$x_c = x_o + x'_c \cos\alpha - y'_c \sin\alpha \qquad \text{(B7)}$$

in (B7) let

$$x_c = x_c^k + \delta_{x_c}$$

$$x_o = x_o^k + \delta_{x_o}$$

$$x'_c = x'_c + \delta_{x'_c}$$

$$y'_c = y'_c + \delta_{y'_c}$$

$$\alpha = \alpha^k + \delta_\alpha$$

Then

$$(x_c^k + \delta_{x_c}) = (x_o^k + \delta_{x_o}) + (x'^k_c + \delta_{x'_c})\cos(\alpha^k + \delta_\alpha) - (y'^k_c + \delta_{y'_c})\sin(\alpha^k + \delta_\alpha)$$

assuming

$$\cos(\alpha^k + \delta_\alpha) = \cos\alpha^k - \delta_\alpha \sin\alpha^k$$

$$\sin(\alpha^k + \delta_\alpha) = \sin\alpha^k - \delta_\alpha \cos\alpha^k$$

then

$$(x_c^k + \delta_{x_c}) = (x_o^k + \delta_{x_o}) + (x_c'^k + \delta_{x_c'})(\cos\alpha^k - \delta_\alpha \sin\alpha^k)$$
$$- (y_c'^k + \delta_{y_c'})(\sin\alpha^k + \delta_\alpha \cos\alpha^k)$$

or

$$(x_c^k + \delta_{x_c}) = (x_o^k + \delta_{x_o}) + x_c'^k \cos\alpha^k - x_c'^k \sin\alpha^k \delta_\alpha + \cos\alpha^k \delta_{x_c'}$$
$$- y_c'^k \sin\alpha^k - y_c'^k \cos\alpha^k \delta_\alpha - \sin\alpha^k \delta_{y_c'}$$

or

$$\delta_{x_c} - \delta_{x_o} + (x_c'^k \sin\alpha^k + y_c'^k \cos\alpha^k)\delta_\alpha - \cos\alpha^k \delta_{x_c'}$$
$$+ \sin\alpha^k \delta_{y_c'} = x_o^k - x_c^k + x_c'^k \cos\alpha^k - y_c'^k \sin\alpha^k \qquad \text{(B8)}$$

Similarly from equations (8):

$$y_c = y_o + x_c' \sin\alpha + y_c' \cos\alpha \qquad \text{(B9)}$$

the variation equation is:

$$\delta_{y_c} - \delta_{y_o} - (x_c'^k \cos\alpha^k - y_c'^k \sin\alpha^k)\delta_\alpha - \sin\alpha^k \delta_{x_c'}$$
$$- \cos\alpha^k \delta_{y_c'} = y_o^k - y_c^k + x_c'^k \sin\alpha^k + y_c'^k \cos\alpha^k \qquad \text{(B10)}$$

From equation (36)

$$\sin\alpha\left(1 + \frac{df_1}{dx}\ \frac{df_2}{dx'}\right) - \cos\alpha\left(\frac{df_1}{dx} - \frac{df_2}{dx'}\right) = 0 \qquad \text{(B11)}$$

From eqs. (85), (86) and (87), equation (B11) can be written as

$$\sin\alpha[1 + (A_2 + 2A_3 x_c + 3A_4 x_c^2 + 4A_5 x_c^3)(A_2' + A_3' x_c')]$$
$$- \cos\alpha[(A_2 + 2A_3 x_c + 3A_4 x_c^2 + 4A_5 x_c^3) - (A_2' + 2A_3' x_c')] = 0 \qquad \text{(B12)}$$

in (B12) let:

$$P = A_2 + 2A_3x_c + 3A_4x_c^2 + 4A_5x_c^3$$

$$Q = A_2' + 2A_3'x_c'$$

therefore, the normal constraint equation (B12) becomes:

$$\text{Sin}\alpha[1 + PQ] - \text{Cos}\alpha[P-Q] = 0 \qquad \text{(B13)}$$

in (B13) let:

$$P = P^k + \delta_P$$

$$Q = Q^k + \delta_Q$$

$$\alpha = \alpha^k + \delta_\alpha$$

Then

$$\text{Sin}(\alpha^k + \delta_\alpha)[1 + (P^k + \delta_P)(Q^k + \delta_Q)] - \text{Cos}(\alpha^k + \delta_\alpha)[P^k + \delta_P - Q^k - \delta_Q] = 0$$

or

$$(\text{Sin}\alpha^k + \delta_\alpha\text{Cos}\alpha^k)[1 + P^kQ^k + P^k\delta_Q + Q^k\delta_P] - (\text{Cos}\alpha^k - \delta_\alpha\,\text{Sin}\alpha^k)[P^k - Q^k + \delta_P - \delta_Q] = 0$$

or

$$[\text{Sin}\alpha^k + P^kQ^k\text{Sin}\alpha^k + P^k\,\text{Sin}\alpha^k\delta_Q + Q^k\,\text{Sin}\alpha^k\,\delta_P + \text{Cos}\alpha^k\,\delta_\alpha + P^kQ^k\,\text{Cos}\alpha^k\delta_\alpha] + [-\text{Cos}\alpha^kP^k + {}^k\,\text{Sin}\alpha^k\delta_\alpha + Q^k\,\text{Cos}\alpha^k - Q^k\,\text{Sin}\alpha^k\delta_\alpha - \text{Cos}\alpha^k\delta_P + \text{Cos}\alpha^k\delta_Q] = 0$$

or

$$[P^k \sin\alpha^k + \cos\alpha^k]\delta_Q + [Q^k \sin\alpha^k - \cos\alpha^k]\delta_P$$
$$+ [\cos\alpha^k + P^k Q^k \cos\alpha^k + P^k \sin\alpha^k - Q^k \sin\alpha^k]\delta_\alpha$$
$$+ [\sin\alpha^k + P^k Q^k \sin\alpha^k - P^k \cos\alpha^k + Q^k \cos\alpha^k] = 0$$

finally:

$$[P^k \sin\alpha^k + \cos\alpha^k]\delta_Q + [Q^k \sin\alpha^k - \cos\alpha^k]\delta_P$$
$$+ [\cos\alpha^k (1 - P^k Q^k) + \sin\alpha^k (P^k - Q^k)]\delta_\alpha$$
$$= - [\sin\alpha^k (1 + P^k Q^k) - \cos\alpha^k (P^k - Q^k)] \qquad \text{(B14)}$$

For

$$P = A_2 + 2A_3 x_c + 3A_4 x_c^2 + 4A_5 x_c^3 \qquad \text{(B15)}$$

in (B15) let:

$$P = P^k + \delta_P$$
$$x_c = x_c^k + \delta_{x_c}$$

Then

$$P^k + \delta_P = A_2 + 2A_3(x_c^k + \delta_{x_c}) + 3A_4(x_c^k + \delta_{x_c})^2 + 4A_5(x_c^k + \delta_{x_c})^3$$

or

$$\delta_P - (2A_3 + 6A_4 x_c^k + 12A_5 x_c^{k^2})\delta_{x_c} = A_2 + 2A_3 x_c^k + 3A_4 x_c^{k^2}$$
$$+ 4A_5 x_c^{k^3} - P^k \qquad \text{(B16)}$$

Similarly for:

$$Q = A_2' + 2A_3' x_c'$$

Let

$$Q = Q^k + \delta_Q$$

$$x_c' = x_c'^k + \delta_{x_c'}$$

Then we have

$$\delta_Q - 2A_3' \, \delta_{x_c'} = A_2' + 2A_3' \, x_c'^k - Q^k \tag{B17}$$

COMPONENTS OF UNIT NORMALS

Equation (27) may be written as:

$$\hat{n}_1 = \frac{\gamma}{[1+P^2]^{1/2}} [- P\hat{i} + \hat{j}]$$

or:

$$n_{1x} = \frac{-\gamma P}{\sqrt{1 + P^2}} \tag{B18}$$

$$n_{1y} = \frac{\gamma}{\sqrt{1 + P^2}} \tag{B19}$$

in (B18) let:

$$n_{1x} = n_{1x}^k + \delta_{n_{1x}}$$

$$P = P^k + \delta_P$$

then:

$$n_{1x} + \delta_{n_{1x}} = \frac{-\gamma(P^k + \delta_P)}{\sqrt{1 + (P^k + \delta_P)^2}} = \frac{-\gamma(P^k + \delta_P)}{\sqrt{1 + P^{k2} + 2P^k\delta_P}}$$

or

$$n_{1x} + \delta n_{1x} = \frac{-\gamma(p^k + \delta_p)}{\sqrt{1 + p^{k^2}}\sqrt{1 + \frac{2p^k\delta_p}{1 + p^{k^2}}}}$$

using the approximation

$$\frac{1}{\sqrt{1 + x}} \simeq 1 - \frac{x}{2}$$

then

$$n_{1x} + \delta n_{1x} = \frac{-\gamma(p^k + \delta_p)}{\sqrt{1 + p^{k^2}}}\left(1 - \frac{p^k\delta_p}{1 + p^{k^2}}\right)$$

$$= \frac{-\gamma(p^k + p^{k^3} - p^{k^2}\delta_p + \delta_p + p^{k^2}\delta_p)}{(1 + p^{k^2})^{3/2}}$$

$$= \frac{-\gamma\,\delta_p}{(1 + p^{k^2})^{3/2}} - \frac{\gamma p^k}{(1 + p^{k^2})^{1/2}}$$

finally

$$\delta n_{1x} + \left[\frac{\gamma}{(1 + p^{k^2})^{3/2}}\right]\delta_p = \frac{-\gamma p^k}{(1 + p^{k^2})^{1/2}} - n_{1x}^k \qquad \text{(B20)}$$

similarly in equation (B19) let

$$n_{1y} = n_{1y}^k + \delta n_{1y}$$

$$p' = p^k + \delta_p$$

then

$$n_{1y}^k + \delta n_{1y} = \frac{\gamma}{\sqrt{1 + (p^k + \delta_p)^2}}$$

or

$$n_{1y} + \delta n_{1y} = \frac{\gamma}{\sqrt{1 + p^{k^2}}\sqrt{1 + \frac{2\, k \delta_p}{1 + p^{k^2}}}}$$

$$= \frac{\gamma}{\sqrt{1 + p^k}} \left(1 - \frac{p^k \delta p}{1 + p^{k^2}} \right)$$

and finally

$$\delta n_{1y} + \left[\frac{\gamma p^k}{(1 + p^{k^2})^{3/2}} \right] \delta p = \frac{\gamma}{\sqrt{1 + p^k}} - n_{1y}^k \qquad \text{(B21)}$$

Equation (29) may be written as:

$$\hat{n}_2' = \frac{\beta}{\sqrt{1 + Q^2}} \left[-Q\hat{i}' + \hat{j}' \right]$$

or

$$n_{2x'} = \frac{-\beta Q}{[1 + Q^2]^{1/2}} \qquad \text{(B22)}$$

$$n_{2y'} = \frac{\beta}{[1 + Q^2]^{1/2}} \qquad \text{(B23)}$$

in equation (B22) let

$$n_{2x'} = n_{2x'}^k + \delta n_{2x'}$$

$$Q = Q^k + \delta_Q$$

then

$$n_{2x'}^k + \delta n_{2x'} = \frac{-\beta (Q^k + \delta_Q)}{\sqrt{1 + (Q + \delta_Q)^2}}$$

or

$$n^k_{2x'} + \delta_{n_{2x'}} = \frac{-\beta(Q^k + \delta_Q)}{\sqrt{1 + Q^{k^2}}\sqrt{1 + \frac{2Q^k\delta_Q}{1 + Q^{k^2}}}}$$

$$= \frac{-\beta(Q^k + \delta_Q)}{\sqrt{1 + Q^{k^2}}}\left(1 - \frac{Q^k\delta_Q}{1 + Q^{k^2}}\right)$$

$$= \frac{-\beta(Q^k + Q^{k^3} - Q^{k^2}\delta_Q + \delta_Q + Q^{k^2}\delta_Q)}{(1 + Q^{k^2})^{3/2}}$$

$$= \frac{-\beta Q^k(1 + Q^{k^2})}{(1 + Q^{k^2})^{3/2}} - \frac{\beta\delta_Q}{(1 + Q^{k^2})^{3/2}}$$

and finally

$$\delta_{n_{2x'}} + \left[\frac{\beta}{(1 + Q^{k^2})^{3/2}}\right]\delta_Q = \frac{-\beta Q^k}{(1 + Q^{k^2})^{1/2}} - n^k_{2x'} \qquad \text{(B24)}$$

Similarly, in equation (B23) let

$$n_{2y'} = n^k_{2y'} + \delta_{n_{2y'}}$$

$$Q = Q^k + \delta_Q$$

then

$$n^k_{2y'} + \delta_{n_{2y'}} = \frac{\beta}{[1 + (Q^k + \delta_Q)^2]^{1/2}}$$

$$= \frac{\beta}{\sqrt{1 + Q^{k^2}}\sqrt{1 + \frac{2Q^k\delta_Q}{1 + Q^{k^2}}}}$$

or

$$n^k_{2y'} + \delta_{n_{2y'}} = \frac{\beta}{\sqrt{1 + Q^{k^2}}} \left(1 - \frac{Q^k \delta_Q}{1 + Q^{k^2}}\right)$$

$$= \frac{\beta(1 + Q^{k^2}) - \beta Q^k \delta_Q}{(1 + Q^{k^2})^{3/2}}$$

and finally

$$\delta_{n_{2y'}} + \left[\frac{\beta Q^k}{(1 + Q^{k^2})^{3/2}}\right]\delta_Q = \frac{\beta}{(1 + Q^{k^2})^{1/2}} - n^k_{2y'} \qquad \text{(B25)}$$

LIGAMENT ATTACHEMENT COORDINATES

From equation (8), the ligaments insertion coordinates are:

$$x_j = x_o + x'_j \cos\alpha - y'_j \sin\alpha \qquad \text{(B26)}$$

$$y_j = y_o + x'_j \sin\alpha + y'_j \cos\alpha \qquad \text{(B27)}$$

in equation (B26) let

$$x_j = x^k_j + \delta_{x_j}$$

$$x_o = x^k_o + \delta_{x_o}$$

$$\alpha = \alpha^k + \delta_\alpha$$

then

$$(x^k_j + \delta_{x_j}) = (x^k_o + \delta_{x_o}) + x'_j \cos(\alpha^k + \delta_\alpha) - y'_j \sin(\alpha^k + \delta_\alpha)$$

$$= (x^k_o + \delta_{x_o}) + x'_j(\cos\alpha^k - \delta_\alpha \sin\alpha^k)$$

$$+ y'_j(\sin\alpha^k + \delta_\alpha \cos\alpha^k)$$

or

$$\delta_{x_j} - \delta_{x_o} + (x_j' \, \mathrm{Sin}\alpha^k + y_j' \, \mathrm{Cos}\alpha^k)\delta_\alpha$$

$$= - x_j^k + x_o^k + x_j' \, \mathrm{Cos}\alpha^k - y_j' \, \mathrm{Sin}\alpha^k \quad (j=1,..,4) \qquad \text{(B28)}$$

similarly, in equation (B27) let:

$$y_j = y_j^k + \delta_{y_j}$$

$$y_o = y_o^k + \delta_{y_o}$$

$$\alpha = \alpha^k + \delta_\alpha$$

which, after simplification, results:

$$\delta_{y_j} - \delta_{y_o} - (x_j' \, \mathrm{Cos}\alpha^k - y_j' \, \mathrm{Sin}\alpha^k)\delta_\alpha$$

$$= - y_j^k + y_o^k + x_j' \, \mathrm{Sin}\alpha^k + y_j' \, \mathrm{Cos}\alpha^k \quad (j=1,..,4) \qquad \text{(B29)}$$

ARTICULATING CONSTRAINT SURFACES

From equations (85) and (86)

$$y_c = A_1 + A_2 x_c + A_3 x_c^{\,2} + A_4 x_c^{\,3} + A_5 x_c^{\,4} \qquad \text{(B30)}$$

in equation (B30) let:

$$x_c = x_c^k + \delta_{x_c}$$

$$y_c = y_c^k + \delta_{y_c}$$

then

$$y_c^k + \delta_{y_c} = A_1 + A_2(x_c^k + \delta_{x_c}) + A_3(x_c + \delta_{x_c})^2 + A_4(x_c + \delta_{x_c})^3 + A_5(x_c^k + \delta_{x_c})^4$$

or

$$y_c^k + \delta_{y_c} = A_1 + A_2 x_c^k + A_2\delta_{x_c} + A_3(x_c^k)^2 + 2A_3 x_c^k \delta_{x_c} + A_4(x_c^k)^3 + 3A_4(x_c^k)^2\delta_{x_c} + A_5(x_c^k)^4 + 4A_5(x_c^k)^3\delta_{x_c}$$

or

$$\delta_{y_c} - [A_2 + 2A_3x_c^k + 3A_4(x_c^k)^2 + 4A_5(x_c^k)^3]\delta_{x_c} = A_1 + A_2x_c^k + A_3(x_c^k)^2 + A_4(x_c^k)^3 + A_5(x_c^k)^4 - y_c^k \quad \text{(B31)}$$

Similarly, from equations (85) and (87)

$$y_c' = A_1' + A_2'x_c' + A_3'x_c'^2 \quad \text{(B32)}$$

in equation (B32) let:

$$x_c' = x_c'^k + \delta_{x_c'}$$

$$y_c' = y_c'^k + \delta_{y_c'}$$

which, after simplification, results:

$$\delta y_c' - (A_2' + 2A_3'x_c'^k)\delta_{x_c'} = A_1' + A_2'x_c'^k + A_3'x_c'^{k^2} - y_c'^k \quad \text{(B33)}$$

APPENDIX C

COMPUTER PROGRAM, JNTMDL

The following pages contain a listing of the computer program, JNTMDL, which follows the numerical procedures discussed in this report. JNTMDL was developed for the two-dimensional dynamic model of the knee joint and produced the results presented in its discussion.

```
C
C  ..............................................................
C
      PROGRAM JNTMDL
C
C  PURPOSE:
C      Dynamic analysis of a two-body-segmented model of the knee
C      joint, in two dimensions, in response to various dynamic
C      loading functions.
C
C  USAGE:
C      Forcing function amplitude and pulse duration must be specified.
C      Time increment, delta T, may also be varied.
C      Initial contact points between the tibia and femur must
C      be specified.
C
C  DESCRIPTION:
C      See DYNAMIC SIMULATION OF THE ARTICULATING JOINTS
C
C  REMARKS:
C      None.
C
C  SUBROUTINES AND FUNCTION SUBPROGRAMS REQUIRED:
C      SIMQ - solve a set of simultaneous linear equations
C      Various standard FORTRAN library functions.
C
C  METHOD:
C      Newton-Raphson iteration using Newmark differential
C      approximations.
```

```
C
C  AUTHOR:
C      Mannsour H. Moeinzadeh
C
C  DATE:
C      October 1980
C
C  ....................................................................
C
      IMPLICIT REAL*8(A-Z)
      INTEGER I,J,K,NUM,ITMAX,IT,KS
      DIMENSION AK(22,22),D(22),DELTA(22)
      KS=0
C
C     TIME INCREMENT  (SEC)
C
      T=0.0D0
      DELT=0.0001D0
C
C     PULSE DURATION  (SEC)  AND AMPLITUDE (N)
C
      TPULSE=0.050D0
      AMP=20.0D0
      PI=3.1415927D0
      FEXTY=0.0D0
      FEXTX=0.0D0
      SAVE=0.0D0
      ALFSAV=300.0D0
C
C     MAXIMUM SPECIFIED ITERATION NUMBER
C
      ITMAX=100
C
C     COORDINATES OF LIGAMENT INSERTIONS  (M)
C
      XP1=0.8D-2
      YP1=16.3D-2
      XP2=2.5D-2
      YP2=17.8D-2
      XP3=2.50D-2
      YP3=20.8D-2
      XP4=-0.5D-2
      YP4=21.30D-2
C
C     COORDINATES OF LIGAMENT ORIGINS  (M)
```

```
C
      X5=-2.3D-2
      Y5=1.4D-2
      X6=-2.3D-2
      Y6=1.90D-2
      X7=-3.20D-2
      Y7=2.4D-2
      X8=-2.3D-2
      Y8=1.9D-2
C
C     LIGAMENT SPRING CONSTANTS  (N/M**2)
C
      K1=15.0D6
      K2=15.0D6
      K3=35.0D6
      K4=30.0D6
C
C     SEGMENT MASS(KG),  MOMENTS OF INERTIA (N-M-SEC**2)
C
      SEGMAS=3.1479D0
      MOMINR=4.93719D-2
C
C     SURFACE EQUATIONS COEFFICIENTS
C
      A1=4.0140180D-2
      B1=-0.24762106D0
      C1=-0.06889185 6D2
      D1=-0.02704456D4
      E1=-0.008589942 1D6
      A2=21.337303D-2
      B2=-0.04560513 7D0
      C2=0.01097345 9D2
C
C     INITIAL CONTACT POINT
C
      XC=-0.0420D0
      XPC=0.0250D0
      YC=A1+B1*XC+C1*XC**2+D1*XC**3+E1*XC**4
      YPC=A2+B2*XPC+C2*XPC**2
      P=B1+2*C1*XC+3*D1*XC**2+4*E1*XC**3
      Q=B2+2*C2*XPC
      PPRIM=2*C1+6*D1*XC+12*E1*XC**2
      QPRIM=2*C2
      GAMA=PPRIM/DABS(PPRIM)
      BETA=QPRIM/DABS(QPRIM)
```

```
      N1X=-GAMA*P/DSQRT(1+P*P)
      N1Y=GAMA/DSQRT(1+P*P)
      N2XP=-BETA*Q/DSQRT(1+Q*Q)
      N2YP=BETA/DSQRT(1+Q*Q)
C
C     INITIAL FLEXION ANGLE
C
      ALFA=DATAN((P-Q)/(1+P*Q))
      ALFA=ALFA+PI
      SN=DSIN(ALFA)
      CN=DCOS(ALFA)
C
C     TIBIAL CENTER OF MASS
C
      XO=XC-XPC*CN+YPC*SN
      YO=YC-XPC*SN-YPC*CN
      FN=0.0D0
C
C     COEFFICIENT OF FRICTION
C
      MEU=0.0D0
C
C     INITIAL LINEAR AND ANGULAR VELOCITY AND ACCELERATION OF
C     TIBIAL CENTER OF MASS
C
      XOM1=XO
      XODM1=0.0D0
      XODDM1=0.0D0
      YOM1=YO
      YODM1=0.0D0
      YODDM1=0.0D0
C
      ALFM1=ALFA
      ALFDM1=0.0D0
      ALFDD1=0.0D0
C
      X1=XO+XP1*CN-YP1*SN
      X2=XO+XP2*CN-YP2*SN
      X3=XO+XP3*CN-YP3*SN
      X4=XO+XP4*CN-YP4*SN
C
      Y1=YO+XP1*SN+YP1*CN
      Y2=YO+XP2*SN+YP2*CN
      Y3=YO+XP3*SN+YP3*CN
      Y4=YO+XP4*SN+YP4*CN
```

```
C
  101 CONTINUE
      PPRIM=2*C1+6*D1*XC+12*E1*XC**2
      QPRIM=2*C2
      GAMA=PPRIM/DABS(PPRIM)
      BETA=QPRIM/DABS(QPRIM)
C
C     INITIAL LENGTHS OF LIGAMENTS
C
      L1=DSQRT((X5-X1)**2+(Y5-Y1)**2)
      L2=DSQRT((X6-X2)**2+(Y6-Y2)**2)
      L3=DSQRT((X7-X3)**2+(Y7-Y3)**2)
      L4=DSQRT((X8-X4)**2+(Y8-Y4)**2)
C
      IF(T.EQ.0.0)L1I=L1
      IF(T.EQ.0.0)L2I=L2
      IF(T.EQ.0.0)L3I=L3
      IF(T.EQ.0.0)L4I=L4
C
C     LIGAMENT FORCES
C
      IF(L1.GT.L1I) ABSF1=K1*(L1-L1I)**2
      IF(L2.GT.L2I) ABSF2=K2*(L2-L2I)**2
      IF(L3.GT.L3I) ABSF3=K3*(L3-L3I)**2
      IF(L4.GT.L4I) ABSF4=K4*(L4-L4I)**2
C
      IF(L1.LE.L1I) ABSF1=-ABSF1
      IF(L2.LE.L2I) ABSF2=-ABSF2
      IF(L3.LE.L3I) ABSF3=-ABSF3
      IF(L4.LE.L4I) ABSF4=-ABSF4
C
C
      F1X=ABSF1*(X5-X1)/L1
      F2X=ABSF2*(X6-X2)/L2
      F3X=ABSF3*(X7-X3)/L3
      F4X=ABSF4*(X8-X4)/L4
      F1Y=ABSF1*(Y5-Y1)/L1
      F2Y=ABSF2*(Y6-Y2)/L2
      F3Y=ABSF3*(Y7-Y3)/L3
      F4Y=ABSF4*(Y8-Y4)/L4
C
      ALFDEG=ALFA*180.0/PI
      IF(T.LT.0.05)GO TO 8
      IF(ALFSAV .LT. ALFDEG) GOTO 999
    8 CONTINUE
```

```
      ALFSAV=ALFDEG
C
C     MOMENT ARM
C
      MOMARM=0.0D0
C
C     TOTAL EXTERNAL ENERGY  (N-M)
C
      EXTENR=DABS(X0-TEMPX0)*FEXTX+DABS(Y0-TEMPY0)*FEXTY+
     $(FEXTX*MOMARM)*DABS(TEMALF-ALFA)
C
      TOTEXT=EXTENR+SAVE
C
      SAVE=TOTEXT
      TEMPX0=X0
      TEMPY0=Y0
      TEMALF=ALFA
C
C     TOTAL INTERNAL ENERGY
C
      POTEN1=(K1*(L1-L1I)**3)/3
      POTEN2=(K2*(L2-L2I)**3)/3
      POTEN3=(K3*(L3-L3I)**3)/3
      POTEN4=(K4*(L4-L4I)**3)/3
C
      IF(L1.LE.L1I)POTEN1=0.0D0
      IF(L2.LE.L2I)POTEN2=0.0D0
      IF(L3.LE.L3I)POTEN3=0.0D0
      IF(L4.LE.L4I)POTEN4=0.0D0
C
      POTENR=POTEN1+POTEN2+POTEN3+POTEN4
      KINENR=(MOMINR*ALFDM1**2)/2+SEGMAS*(X0DM1**2+Y0DM1**2)/2
C
      TOTINT=POTENR+KINENR
C
      YC=A1+B1*XC+C1*XC**2+D1*XC**3+E1*XC**4
      YPC=A2+B2*XPC+C2*XPC**2
C
      IF(T.GT.0.0) GO TO 102
      WRITE(6,15)
   15 FORMAT(' ',3X,'T',4X,'ALFA',5X,'ALFA:',T28,'X0',T38,'Y0',9X,'X:'
     $,9X,'Y:',T68,'XC',T78,'XPC',T88,'FN',T95,'MC.LIG',T103,'LC.LIG',
     $T111,'AC.LIG',T119,'PC.LIG',T128,'IER.$',2X,'EXT-ENR',2X,'INT-ENR
     $',6X,'YC',7X,'YPC',//)
  102 WRITE(6,16)T,ALFDEG,ALFDD1,X0,Y0,X0DDM1,Y0DDM1,XC,XPC,FN,ABSF1,
```

```
     $ABSF2,ABSF3,ABSF4,IT,TOTEXT,TOTINT,YC,YPC
  16  FORMAT(' ',F7.5,T10,F6.2,T16,F8.1,T26,F7.4,T36,F7.4,T45,F8.2,T56,
     $F8.2,T66,F8.5,T76,F7.5,T85,F8.2,T94,F7.2,T102,F7.2,T110,F7.2,T118
     $,F7.2,T128,I4,3X,F7.4,2X,F7.4,3X,F8.5,3X,F8.5)
C
      TZERO=TPULSE
C
C     APPLIED DYNAMIC FUNCTION
C
      PULSE=AMP*EXP(-4.73*(T/TZERO)**2)*DSIN(PI*T/TZERO)
C
      FEXTX=PULSE*DCOS(ALFA-PI)
      FEXTY=PULSE*DSIN(ALFA-PI)
C
      IF(T.GE.DELT. AND.T.LE.TPULSE)FEXTX=FEXTX
      IF(T.GE.DELT.AND.T.LE.TPULSE)FEXTY=FEXTY
      IF(T.GT.TPULSE)FEXTX=0.0D0
      IF(T.GT.TPULSE)FEXTY=0.0D0
C
      T=T+DELT
      IT=0.0
C
C     NEWTON-RAPHSON ITERATION PROCESS
C
    1 CONTINUE
      IT=IT+1
      IF(IT.GT.ITMAX)WRITE(6,39)
   39 FORMAT(' ',T2,'NUMBER OF ITERATIONS EXCEEDED  THE SPECIFIED
     $ ITERATION NUMBER : EXECUTION ABORTED........')
      IF(IT.GT.ITMAX)GO TO 999
C
      SN=DSIN(ALFA)
      CN=DCOS(ALFA)
C
C     INITIALIZATION OF [AK] AND [D] MATRICES
C
      DO 5 I=1,22
      D(I)=0.0
      DO 5 J=1,22
      AK(I,J)=0.0
    5 CONTINUE
C
C     COMPONENTS OF [D] MATRIX
C
      D(1)=-X1+X0+XP1*CN-YP1*SN
```

```
      D(2)=-X2+X0+XP2*CN-YP2*SN
      D(3)=-X3+X0+XP3*CN-YP3*SN
      D(4)=-X4+X0+XP4*CN-YP4*SN
C
      D(5)=-Y1+Y0+XP1*SN+YP1*CN
      D(6)=-Y2+Y0+XP2*SN+YP2*CN
      D(7)=-Y3+Y0+XP3*SN+YP3*CN
      D(8)=-Y4+Y0+XP4*SN+YP4*CN
C
      D(9)= SEGMAS*((4.0/DELT**2)*(X0-X0M1)-(4.0/DELT)*X0DM1-X0DDM1)
     $-(F1X+F2X+F3X+F4X)+FN*(MEU*N1Y-N1X)*GAMA-FEXTX
C
      D(10)=SEGMAS*((4.0/DELT**2)*(Y0-Y0M1)-(4.0/DELT)*Y0DM1-Y0DDM1)
     $-(F1Y+F2Y+F3Y+F4Y)-FN*(MEU*N1X+N1Y)*GAMA-FEXTY
C
      D(11)=-((X1-X0)*F1Y+(X2-X0)*F2Y+(X3-X0)*F3Y+(X4-X0)*F4Y-(Y1-Y0)*
     $F1X-(Y2-Y0)*F2X-(Y3-Y0)*F3X-(Y4-Y0)*F4X)-FN*GAMA*((XC-X0)*(N1Y+
     $MEU*N1X)-(YC-Y0)*(N1X-MEU*N1Y))+MOMINR*((4.0/DELT**2)*(ALFA-ALFM1
     $)-(4.0/DELT)*ALFDM1-ALFDD1)+FEXTX*MOMARM
      D(12)=X0-XC+XPC*CN-YPC*SN
      D(13)=Y0-YC+XPC*SN+YPC*CN
      D(15)=A1+B1*XC+C1*XC**2+D1*XC**3+E1*XC**4-YC
      D(16)=A2+B2*XPC+C2*XPC**2-YPC
      D(17)=B1+2*C1*XC+3*D1*XC**2+4*E1*XC**3-P
      D(18)=-(P/DSQRT(1+P**2))*GAMA-N1X
      D(19)=(1.0/DSQRT(1+P**2))*GAMA-N1Y
      D(20)=B2+2*C2*XPC-Q
      D(21)=(-Q/DSQRT(1+Q**2))*BETA-N2XP
      D(22)=(1.0/DSQRT(1+Q**2))*BETA-N2YP
C
C     COMPONENTS OF [AK] MATRIX
C
      AK(1,1)=-1.0D0
      AK(1,3)=XP1*SN+YP1*CN
      AK(1,7)=1.0D0
C
      AK(2,1)=-1.0D0
      AK(2,3)=XP2*SN+YP2*CN
      AK(2,8)=1.0D0
C
      AK(3,1)=-1.0D0
      AK(3,3)=XP3*SN+YP3*CN
      AK(3,9)=1.0D0
C
      AK(4,1)=-1.0D0
```

```
      AK(4,3)=XP4*SN+YP4*CN
      AK(4,10)=1.0D0
C
      AK(5,2)=-1.0D0
      AK(6,2)=-1.0D0
      AK(7,2)=-1.0D0
      AK(8,2)=-1.0D0
C
      AK(5,3)=-(XP1*CN-YP1*SN)
      AK(6,3)=-(XP2*CN-YP2*SN)
      AK(7,3)=-(XP3*CN-YP3*SN)
      AK(8,3)=-(XP4*CN-YP4*SN)
C
      AK(5,11)=1.0D0
      AK(6,12)=1.0D0
      AK(7,13)=1.0D0
      AK(8,14)=1.0D0
C
      AK(9 ,4)=-(MEU*N1Y-N1X)*GAMA
      AK(9 ,16)=-MEU*FN*GAMA
      AK(9 ,15)=FN*GAMA
      AK(9 ,1)=-4.0*SEGMAS/DELT**2
C
      AK(10,4)=(MEU*N1X+N1Y)*GAMA
      AK(10,16)=FN*GAMA
      AK(10,15)=MEU*FN*GAMA
      AK(10,2)=-4.0*SEGMAS/DELT**2
C
      AK(11,7)=F1Y
      AK(11,8)=F2Y
      AK(11,9)=F3Y
      AK(11,10)=F4Y
      AK(11,1)=-((F1Y+F2Y+F3Y+F4Y)+FN*(N1Y+MEU*N1X)*GAMA)
      AK(11,11)=-F1X
      AK(11,12)=-F2X
      AK(11,13)=-F3X
      AK(11,14)=-F4X
      AK(11,2)=((F1X+F2X+F3X+F4X)+FN*(N1X-MEU*N1Y)*GAMA)
      AK(11,4)=(XC-X0)*(N1Y+MEU*N1X)-(YC-Y0)*(N1X-MEU*N1Y)
      AK(11,15)=(MEU*FN*(XC-X0)-FN*(YC-Y0))*GAMA
      AK(11,16)=(FN*(XC-X0)+MEU*FN*(YC-Y0))*GAMA
      AK(11,5)=FN*(N1Y+MEU*N1X)*GAMA
      AK(11,19)=-FN*(N1X-MEU*N1Y)*GAMA
      AK(11,3)=-4.0*MOMINR/DELT**2
C
```

```
      AK(12,5)=1.0D0
      AK(12,1)=-1.0D0
      AK(12,3)=XPC*SN+YPC*CN
      AK(12,6)=-CN
      AK(12,20)=SN
C
      AK(13,2)=-1.0D0
      AK(13,3)=YPC*SN-XPC*CN
      AK(13,19)=1.0D0
      AK(13,6)=-SN
      AK(13,20)=-CN
C
      AK(14,22)=P*SN+CN
      AK(14,21)=Q*SN-CN
      AK(14,3)=CN*(1+P*Q)+SN*(P-Q)
C
      AK(15,19)=1.0D0
      AK(15,5)=-P
C
      AK(16,20)=1.0D0
      AK(16,6)=-Q
C
      AK(17,21)=1.0D0
      AK(17,5)=-(2*C1+6*D1*XC+12*E1*XC**2)
C
      AK(18,15)=1.0D0
      AK(18,21)=GAMA/(1+P*P)**1.5
C
      AK(19,16)=1.0D0
      AK(19,21)=GAMA*P/(1+P*P)**1.5
C
      AK(20,22)=1.0D0
      AK(20,6)=-2*C2
C
      AK(21,17)=1.0D0
      AK(21,22)=BETA/(1+Q*Q)**1.5
C
      AK(22,18)=1.0D0
      AK(22,22)=BETA*Q/(1+Q*Q)**1.5
C
C     CALCULATION OF COMPONENTS OF DELTA MATRIX
C
      CALL SIMQ(AK,D,22,KS)
C
      DO 44 I=1,22
```

```
      DELTA(I)=D(I)
   44 CONTINUE
C
      IF(KS.EQ.1) WRITE(6,3)
    3 FORMAT(' ','KS=1 ,SINGULAR MATRIX  :EXECUTION ABORTED .....')
      IF(KS.EQ.1) GO TO 999
C
C  NEW VALUES
C
      XO=XO+DELTA(1)
      YO=YO+DELTA(2)
      ALFA=ALFA+DELTA(3)
      FN=FN+DELTA(4)
      XC=XC+DELTA(5)
      XPC=XPC+DELTA(6)
      X1=X1+DELTA(7)
      X2=X2+DELTA(8)
      X3=X3+DELTA(9)
      X4=X4+DELTA(10)
      Y1=Y1+DELTA(11)
      Y2=Y2+DELTA(12)
      Y3=Y3+DELTA(13)
      Y4=Y4+DELTA(14)
      N1X=N1X+DELTA(15)
      N1Y=N1Y+DELTA(16)
      N2XP=N2XP+DELTA(17)
      N2YP=N2YP+DELTA(18)
      YC=YC+DELTA(19)
      YPC=YPC+DELTA(20)
      P=P+DELTA(21)
      Q=Q+DELTA(22)
C
C     CONVERGENCE TESTS
C
      OMEG=0.0001D0
C
      DO 555 I=1,22
      IF(DABS(DELTA(I)).GT.OMEG) GO TO 1
  555 CONTINUE
C
C     NEWMARK DIFFERENTIAL APPROXIMATIONS
C
C     CALCULATION OF VELOCITIES AND ACCELERATIONS AT TIME T
C
      XODDT=(4.0/DELT**2)*(XO-XOM1)-(4.0/DELT)*XODM1-XODDM1
```

```
      XODT=XODM1+(DELT/2.0)*XODDM1+(DELT/2.0)*XODDT
C
      XOM1=XO
      XODM1=XODT
      XODDM1=XODDT
C
      YODDT=(4.0/DELT**2)*(YO-YOM1)-(4.0/DELT)*YODM1-YODDM1
      YODT=YODM1+(DELT/2.0)*YODDM1+(DELT/2.0)*YODDT
C
      YOM1=YO
      YODM1=YODT
      YODDM1=YODDT
C
      ALFDDT=(4.0/DELT**2)*(ALFA-ALFM1)-(4.0/DELT)*ALFDM1-ALFDD1
      ALFDT=ALFDM1+(DELT/2.0)*ALFDD1+(DELT/2.0)*ALFDDT
C
      ALFM1=ALFA
      ALFDM1=ALFDT
      ALFDD1=ALFDDT
C
      GO TO 101
C
  999 STOP
      END
>
```

```
      SUBROUTINE SIMQ(A,B,N,KS)
C
C     ..................................................................
C
C        PURPOSE:
C           OBTAIN SOLUTION OF A SET OF SIMULTANEOUS LINEAR EQUATIONS,
C           AX=B
C
C        USAGE:
C           CALL SIMQ(A,B,N,KS)
C
C        DESCRIPTION OF PARAMETERS:
C           A - MATRIX OF COEFFICIENTS STORED COLUMNWISE.  THESE ARE
C               DESTROYED IN THE COMPUTATION.  THE SIZE OF MATRIX A IS
C               N BY N.
C           B - VECTOR OF ORIGINAL CONSTANTS (LENGTH N). THESE ARE
C               REPLACED BY FINAL SOLUTION VALUES, VECTOR X.
C           N - NUMBER OF EQUATIONS AND VARIABLES. N MUST BE .GT. ONE.
C           KS - OUTPUT DIGIT
C                0 FOR A NORMAL SOLUTION
C                1 FOR A SINGULAR SET OF EQUATIONS
C
C        REMARKS:
C           MATRIX A MUST BE GENERAL.
C           IF MATRIX IS SINGULAR, SOLUTION VALUES ARE MEANINGLESS.
C           AN ALTERNATIVE SOLUTION MAY BE OBTAINED BY USING MATRIX
C           INVERSION (MINV) AND MATRIX PRODUCT (GMPRD).
C
C        SUBROUTINES AND FUNCTION SUBPROGRAMS REQUIRED:
C           NONE
C
C        METHOD:
C           METHOD OF SOLUTION IS BY ELIMINATION USING LARGEST PIVOTAL
C           DIVISOR. EACH STAGE OF ELIMINATION CONSISTS OF INTERCHANGING
C           ROWS WHEN NECESSARY TO AVOID DIVISION BY ZERO OR SMALL
C           ELEMENTS.
C           THE FORWARD SOLUTION TO OBTAIN VARIABLE N IS DONE IN
C           N STAGES. THE BACK SOLUTION FOR THE OTHER VARIABLES IS
C           CALCULATED BY SUCCESSIVE SUBSTITUTIONS. FINAL SOLUTION
C           VALUES ARE DEVELOPED IN VECTOR B, WITH VARIABLE 1 IN B(1),
C           VARIABLE 2 IN B(2),.....,VARIABLE N IN B(N).
C           IF NO PIVOT CAN BE FOUND EXCEEDING A TOLERANCE OF 0.0,
C           THE MATRIX IS CONSIDERED SINGULAR AND KS IS SET TO 1. THIS
C           TOLERANCE CAN BE MODIFIED BY REPLACING THE FIRST STATEMENT.
```

```
C
C     ..................................................................
C
      IMPLICIT DOUBLE PRECISION (A-H,O-Z)
      DIMENSION A(1),B(1)
C
C        FORWARD SOLUTION
C
      TOL=0.0
      KS=0
      JJ=-N
      DO 65 J=1,N
      JY=J+1
      JJ=JJ+N+1
      BIGA=0
      IT=JJ-J
      DO 30 I=J,N
C
C        SEARCH FOR MAXIMUM COEFFICIENT IN COLUMN
C
      IJ=IT+I
      IF(DABS(BIGA)-DABS(A(IJ))) 20,30,30
   20 BIGA=A(IJ)
      IMAX=I
   30 CONTINUE
C
C        TEST FOR PIVOT LESS THAN TOLERANCE (SINGULAR MATRIX)
C
      IF(DABS(BIGA)-TOL) 35,35,40
   35 KS=1
      RETURN
C
C        INTERCHANGE ROWS IF NECESSARY
C
   40 I1=J+N*(J-2)
      IT=IMAX-J
      DO 50 K=J,N
      I1=I1+N
      I2=I1+IT
      SAVE=A(I1)
      A(I1)=A(I2)
      A(I2)=SAVE
C
C        DIVIDE EQUATION BY LEADING COEFFICIENT
C
```

```
   50 A(I1)=A(I1)/BIGA
      SAVE=B(IMAX)
      B(IMAX)=B(J)
      B(J)=SAVE/BIGA
C
C        ELIMINATE NEXT VARIABLE
C
      IF(J-N) 55,70,55
   55 IQS=N*(J-1)
      DO 65 IX=JY,N
      IXJ=IQS+IX
      IT=J-IX
      DO 60 JX=JY,N
      IXJX=N*(JX-1)+IX
      JJX=IXJX+IT
   60 A(IXJX)=A(IXJX)-(A(IXJ)*A(JJX))
   65 B(IX)=B(IX)-(B(J)*A(IXJ))
C
C        BACK SOLUTION
C
   70 NY=N-1
      IT=N*N
      DO 80 J=1,NY
      IA=IT-J
      IB=N-J
      IC=N
      DO 80 K=1,J
      B(IB)=B(IB)-A(IA)*B(IC)
      IA=IA-N
   80 IC=IC-1
      RETURN
      END
>
```

REFERENCES

Andriacchi, T.P., R.P. Mikosz, S.J. Hampton, and J.O. Galante, 1977, "A Statically Indeterminate Model of the Human Knee Joint", Biomechanics Symposium AMD, 23, 277.

Andriacchi, T.P., R.P. Mikosz, S.J. Hampton, and J.O. Galante, 1978, "Model Studies of the Stiffness Characteristics of the Human Knee Joint", 24th Annual Meeting Orthopaedic Research Society, Dallas, Texas.

Barnett, C.H., D.V. Davies, and M.A. Mac Conaill, 1949, Joints, Their Structure and Mechanics, Charles C. Thomas Publishers, Springfield, Illinois.

Bartel, D.L., J.L. Marshall, R.A. Schieck, and J.B. Wang, 1977, "Surgical Repositioning of the Medial Collateral Ligament", Journal of Bone and Joint Surgery, 59-A, 107.

Bartz, J.A., and F.E. Butler, 1972, "A Three-Dimensional Computer Simulation of a Motor Vehicle Crash Victim, Phase 2 Validation of the Model", Calspan Technical Report No. VJ-2978-V-2.

Bathe, K.J., and E.L. Wilson, 1976, Numerical Methods in Finite Element Analysis, Prentice-Hall, Englewood Cliffs, New Jersey.

Blacharski, P.A., J.H. Somerset, and P.G. Murray, 1975, "A Three-Dimensional Study of the Kinematics of the Human Knee", Journal of Biomechanics, 8, 375.

Blatz, P.J., B.M. Chu, and H. Wayland, 1969, "On the Mechanical Behaviour of Elastic Animal Tissue", Transactions Society of Rheology, 13, 83.

Brantigan, O.C. and A.F. Voshell, 1941, "The Mechanics of the Ligaments and Menisci of the Knee Joint", Journal of Bone and Joint Surgery, 23, 44.

Chand, R., E. Haug, and K. Rim, 1976, "Stresses in the Human Knee Joint", Journal of Biomechanics, 9, 417.

Comninou, M., and I.V. Yannas, 1976, "Dependence of Stress-Strain Non-Linearity of Connective Tissues on the Geometry of Collagen Fibers", Journal of Biomechanics, 9, 427.

Crisp, J.D.C., 1972, "Properties of tendon and Skin", In: Biomechanics: Its Foundations and Objectives, Y.C. Fung et al., eds., Prentice Hall, Englewood Cliffs, New Jersey, 141.

Crowninshield, R., M.H. Pope, and R.J. Johnson, 1976, "An Analytical Model of the Knee", Journal of Biomechanics, 9, 397.

Demiray, H., 1972: "A Note on the Elasticity of Soft Biological Tissues", Journal of Biomechanics, 5, 309.

Devens, W.E.L., 1979, "Onderzoek Naar Methoden voor de Bepalingen van de Drie-Dimensionale Geometrie van Botten", Report, Dept. WLV, Mechanical Engineering, Eindhoven University of Technology, The Netherlands.

Dijk, van R., R. Huiskes, and G. Selvik, 1979, "Roentgen Stereophotogrammetric Methods for the Evaluation of the Three-Dimensional Kinematic Behaviour and Cruciate Ligament Length Patterns of the Human Knee Joint", Journal of Biomechanics, 12, 727.

Dorlot, J.M., M. Ait Ba Sidi, G.M. Tremblay and G. Drouin, 1980, "Load Elongation Behaviour of the Canine Anterior Cruciate Ligament", Journal of Biomechanical Engineering, 102, 190.

Dowson, D., 1976, "Modes of Lubrication in Human Joints", Proceedings of the Institution of Mechanical Engineers, 181(3), 45.

Draper, N.R., and H. Smith, 1966, Applied Regression Analysis, John Wiley and Sons, New York.

Drouin, G., R. Doré, P.S. Thiry, and C. Jean-Francois, 1980, "Modeling of a Composite Prosthesis for Quasi-Cylindrical Ligaments", Journal of Biomechanical Engineering, 102, 194.

Edwards, R.G., J.F. Lafferty, and K.O. Lange, 1969, "Ligament Strain in the Human Knee Joint", Transactions ASME, Winter Annual Meeting.

Elliot, D.H., 1965, "Structure and Function of Mammalian Tendon", Biological Review, 40, 392.

Engin, A.E., and M.S. Korde, 1974, "Biomechanics of Normal and Abnormal Knee Joint", Journal of Biomechanics, 7, 325.

Engin, A.E., 1978, "Mechanics of the Knee Joint: Guidelines for Osteotomy in Osteoarthritis", Orthopaedic Mechanics, edited by D.N. Ghista and R. Roaf, Academic Press, London England, 60.

Engin, A.E., and N. Akkas, 1978, "Application of a Fluid-Filled Spherical Sandwich Shell as a Biodynamic Head Injury Model for Primates", Aviation, Space, and Environmental Medicine, 49(1), 120.

Engin, A.E., 1979a, "Measurement of Resistive Torques in Major Human Joints", AMRL Report, No. AMRL-TR-79-4.

Engin, A.E., 1979b, "Passive Resistive Torques About Long Bone Axes of Major Human Joints", Aviation, Space, and Environmental Medicine, 50(10), 1052.

Engin, A.E., I. Kaleps, R.D. Peindl, and M.H. Moeinzadeh, 1979c, "Passive Resistive Force and Moments in Human Shoulder", Proceedings of the 32nd ACEMB, 25.

Engin, A.E., 1979d, "On the Biomechanics of Major Articulating Human Joints", an INVITED CHAPTER in NATO ASI-Progress in Biomechanics, edited by N. Akkas, Sijthoff & Noordhoff Publishers, Netherlands, 157.

Engin, A.E. and I. Kaleps, 1980a, "Active Muscle Torques About Long-Bone Axes of Major Human Joints", Aviation, Space and Environmental Medicine, 51(6), 551.

Engin, A.E., 1980b, "On the Biomechanics of the Shoulder Complex", Journal of Biomechanics, 13(7), 575.

Engin, A.E. and R.D. Peindl, 1980c, "Two Devices Developed for Kinematic and Force Data Collection in Biomechanics -- Application to Human Shoulder Complex", Developments in Theoretical and Applied Mechanics, edited by J.E. Stoneking, Vol. 10, 33, The University of Tennessee Press.

Engin, A.E., N. Akkas, and I. Kaleps, 1980d, "Passive Resistive Force and Moments in Human Elbow Joint", 1980 Advances in Bioengineering, ASME Publication, 229.

Engin, A.E., 1981a, "Resistive Force and Moments in Major Human Joints", Proceedings of the Eighth Canadian Congress of Applied Mechanics, 181.

Engin, A.E., 1981b, "Response of Human Shoulder to Exteternal Forces", Proceedings of the VIIIth International Congress of Biomechanics, 189.

Engin, A.E., and M.H. Moeinzadeh, 1981c, "Dynamic Modeling of Human Articulating Joints", Proceedings of the Third International Conference on Mathematical Modeling, University of Southern California, Los Angeles, 58.

Erkman, M.J., and P.S. Walker, 1974, "A Study of Knee Geometry Applied to the Design of Condylar Prostheses", Biomedical Engineering, 14.

Fleck, J.T., 1975, "Calspan Three-Dimensional Crash Victim Simulation Program", Aircraft Crashworthiness, edited by K. Saczalski, G.T. Singley, W.D. Pilkey, and R.L. Huston, University Press of Virginia, Charlottesville, 299.

Fleck, J.T., F.E. Butler, and S.L. Vogel, 1975, "An Improved Three-Dimensional Computer Simulation of Vehicle Crash Victims", U.S. Department of Transportation, National Highway Traffic Safety Administration, Washington D.C., Report No. DOT HS-801-507.

Frisen, M., M. Mägi, L. Sonnerup, and A. Viidik, 1969, "Rheological Analysis of Soft Collagenous Tissues", Journal of Biomechanics, 2, 13.

Fung, Y.C., 1967, "Elasticity of Soft Tissue in Simple Elongation", American Journal of Physiology, 213, 1532.

Fung, Y.C., 1972, "Stress-Strain History Relations of Soft Tissues in Simple Elongation", In: Biomechanics: Its Foundations and Objectives, Y.C. Fung, et al., eds., Prentice Hall, Englewood Cliffs, New Jersey, 181.

Girgis, F.G., J.L. Marshall, and al A.R.S. Monajem, 1975, "The Cruciate Ligaments of the Knee Joint", Clinical Orthopedics and Related Research, 106, 216.

Goodnight, J.H., and W.R. Harvey, 1978, "Least Squares Means in the Fixed Effects General Model", SAS Technical Report R-103, SAS Institute Inc., Raleigh, North Carolina.

Gou, P.F., 1970, "Strain Energy Function for Biological Tissues", Journal of Biomechanics, 3, 547.

Grant, J.C.B., 1962, Grant's Atlas of Anatomy, The Williams and Wilkins Co., Baltimore.

Gray, H., 1973, Gray's Anatomy, 35th Edition, R. Warwick, and P.S. Williams, eds., Longman.

Graybill, F.A., 1961, An Introduction to Linear Statistical Models, Volume I, McGraw-Hill Inc., New York.

Green, A.E., and J.E. Adkins, 1960, Large Elastic Deformation and Non-Linear Continuum Mechanics, Oxford University Press, London.

Hallen, L.G., and O. Lindahl, 1965, "The Lateral Stability of the Knee Joint", Acta Orthopaedica Scandinavica, 36, 400.

Hallen, L.G., and O. Lindahl, 1966, "The Screw-Home Movement in the Knee Joint", Acta Orthopaedica Scandinavica, 37, 97.

Haut, R.C., and R.W. Little, 1972, "A Constitutive Equation for Collagen Fibers", Journal of Biomechanics, 5, 423.

Hildebrandt, J., H. Fukaya, and C.J. Martin, 1969, "Simple Uniaxial and Uniform Biaxial Deformation of Nearly Isotropic Incompressible Tissues", Biophysical Journal, 9, 781.

Hildebrand, F.B., 1968, Finite Difference Equations and Simulations, Prentice-Hall New Jersey.

Hughston, J.C., and A.F. Eilers, 1973, "The Role of the Posterior Oblique Ligament in Repairs of Acute Medial (Collateral) Ligament Tears of the Knee", Journal of Bone and Joint Surgery, 55-A, 923.

Huiskes, R., 1979, Some Fundamental Aspects of Human Joint Replacement, Dissertation, Eindhoven University of Technology, The Netherlands.

Huson, A., 1974, "Biomechanische Probleme des Kniegelenks", Orthopäde, 3, 119.

Huson, A., 1976, "Quelques Consequences Fonctionelles du Croisement des Ligaments Articulaires", Bulletin de l'Association des Anatomistes, 60, 71.

Huston, R.L., R.E. Hessel, and C.E. Passerello, 1974, "A Three-Dimensional Vehicle-Man Model for Collision and High Acceleration Studies", SAE Paper No. 740275.

Insall, J., W.N. Scott, and C.S. Ranawat, 1979, "The Total Condylar Knee Prosthesis", Journal of Bone and Joint Surgery, 61-A, 173.

Jacobsen, K., 1976, "Stress Radiographical Measurement of the Antero-Posterior, Medial and Lateral Stability of the Knee Joint", Acta Orthopaedica Scandinavica, 47, 335.

Jaspers, P., de A. Lange, R. Huiskes, and van Th. J.G. Rens, 1978, "The Mechanical Function of the Meniscus; Experiments on Cadaveric Pig Knee Joints", 1st Meeting European Society of Biomechanics, Brussels, Belgium.

Kao, R., 1974, "A Comparison of Newton-Raphson Methods and Incremental Procedures for Geometrically Nonlinear Analysis", Computers and Structures, 4, 1091.

Kennedy, J.C., and R.W. Grainger, 1967, "The Posterior Cruciate Ligament", Journal of Trauma, 7, 367.

Kennedy, J.C., and P.J. Fowler, 1971, "Medial and Anterior Instability of the Knee", Journal of Bone and Joint Surgery, 53-A, 1257.

Kennedy, J.C., H.W. Weinberg and A.S. Wilson, 1974, "The Anatomy and Function of the Anterior Cruciate Ligament", Journal of Bone and Joint Surgery, 56-A, 223.

Kennedy, J.C., R.J. Hawkins, R.B. Willis, and K.D. Danylchuk, 1976, "Tension Studies of Human Knee Joint Ligaments", Journal of Bone and Joint Surgery, 58-A, 350.

Kettelkamp, D.B., and E.Y. Chao, 1972, "A Method for Quantitative Analysis of Medial and Lateral Compression Forces at the Knee During Standing", Clinical Orthopedics and Related Research, 83, 202.

Kettelkamp, D.B., and A.W. Jacobs, 1972, "Tibiofemoral Contact-Area Determination and Implications", Journal of Bone and Joint Surgery, 54-A, 349.

Krause, W.R., M.H. Pope, R.J. Johnson, and D.G. Wilder, 1976, "Mechanical Changes in the Knee After Miniscectomy", Journal of Bone and Joint Surgery, 58-A, 599.

Lee, J.S., W.C. Frasher, and Y.C. Fung, 1967, "Two Dimensional Finite Deformation on Experiments on Dog's Arteries and Veins", Technical Report No. AFOSR 67-1980, University of California, San Diego.

Levens, A.S., V.T. Inman, and J.A. Blosser, 1948, "Transverse Rotation of the segments of the Lower Extremity in Locomotion", Journal of Bone and Joint Surgery, 30-A, 859.

Lotke, P.A., and M.L. Ecker, 1977, "Influence of Positioning of Prosthesis in Total Knee Replacement", Journal of Bone and Joint Surgery, 59-A, 77.

McHenry, R.R., 1965, "Analysis of the Dynamics of Automobile Passenger-Restraint System", Proceedings of the 7th Stapp Car Crash Conference, 207, (1963), Charles C. Thomas, Springfield, Illinois.

Menschik, A., 1974a, "Mechanik des Kniegelenkes, 1^{e} Teil", Z. Orthop., 112, 481.

Menschik, A., 1974b, "Mechanik des Kniegelenkes, 3^{e} Teil", F. Sailer, 1090 Wien, Porzellangasse 43, Austria.

Mooney, M., 1940, "A Theory of Large Elastic Deformation", Journal of Applied Physiology, 11, 582.

Morrison, J.B., 1967, The Forces Transmitted by the Human Knee Joint During Activity, Thesis, Univ rsity of Strathclyde, England.

Morrison, J.B., 1970, "The Mechanics of the Knee Joint in Relation to Normal Walking", Journal of Biomechanics, 3, 51.

Noyes, F.R., and E.S. Grood, 1976, "The Strength of the Anterior Cruciate Ligament in Humans and Rhesus Monkeyes", Journal of Bone and Joint Surgery, 58-A, 1074.

Perry, J., D. Antonelli, and W. Ford, 1975, "Analysis of Knee-Joint Forces During Flexed-Knee Stance", Journal of Bone and Joint Surgery, 57-A, 961.

Piziali, R.L., J.C. Rastegar, and D.A. Nagel, 1977, "Measurement of the Nonlinear Coupled Stiffness Characteristics of the Human Knee", Journal of Biomechanics, 10, 45.

Piziali, R.L., W.P. Seering, D.A. Nagel, and D.J. Schurman, 1980, "The Function of the Primary Ligaments of the Knee in Anterior-Posterior and Medial-Lateral Motions", Journal of Biomechanics, 13, 777.

Pope, M.H., R. Crowninshield, and R. Johnson, 1976, "The Static and Dynamic Behaviour of the Human Knee in Vivo", Journal of Biomechanics, 9, 449.

Pringle, J.H., 1907, "Avulsion of the Spine of the Tibia", Annals of Surgery, 46, 169.

Radin, E.L., and I.L. Paul, 1972, "A Consolidated Concept of Joint Lubrication", Journal of Bone and Joint Surgery 54-A, 607.

Ralston, A., and H.S. Wilf, 1967, Mathematical Method for Digital Computers, John Wiley and Sons Inc., New York.

Rens, van Th. J.G., and R. Huiskes, 1976, "De Operatieve Behandeling van Gonarthrosis", Ned. T. Geneesk., 120, 1322.

Rivlin, R.S., 1948, "Large Elastic Deformation of Isotropic Materials", Philisophical Transactions, A240, 459.

Robbins, D.H., R.O. Bennett, and J.M. Becker, 1977, "Validation of Human Body Modelling for Dynamic Simulation", International Automotive Engineering Congress and Exposition, Detroit, SAE No.: 770058.

Robinson, J., and C. Romero, 1968, "The Functional Anatomy of the Knee Joint with Special Reference to the Medial Collateral and Anterior Cruciate Ligaments", Canadian Journal of Surgery, 2, 36.

SAS, 1979, User's Guide, SAS Institute Inc., Cary, North Carolina.

Seedhom, B.B., D. Dowson, V. Wright, and E.B. Longton, 1972a, "A Technique for the Study of Geometry and Contact in Normal and Artificial Knee Joints", Wear, 20, 189.

Seedhom, B.B., E.B. Longton, V. Wright, and D. Dowson, 1972b, "Dimension of the Knee", Annals of the Rheumatic Diseases, 31, 54.

Seedhom, B.B., and K. Terayama, 1976, "Knee Forces During the Activity of Getting Out of a Chair With and Without the Aid of Arms", Biomedical Engineering, 278.

Seering, W.P., R.L. Piziali, D.A. Nagel and D.J. Schurman, 1980, "The Function of the Primary Ligaments of the Knee in Varus-Valgus and Axial Rotation", Journal of Biomechanics, 13, 785.

Simon, B.R., A.S. Kobayashi, D.E. Strandness, and O.A. Wiederhielm, 1970, "Large Deformation Analysis of the Arterial Cross-Section", ASME Winter Annual Meeting.

Slocum, D.B., and R.L. Larson, 1968, "Rotationary Instability of the Knee", Journal of Bone and Joint Surgery, 50-A, 211.

Smidt, G.L., 1973, "Biomechanical Analysis of Knee Flexion and Extension", Journal of Biomechanics, 6, 79.

Smillie, I.S., 1970, Injuries of the Knee Joint, Livingston, London.

Snyder, R.W., 1972, "Large Deformation of Isotropic Biological Tissue", Journal of Biomechanics, 5, 601.

Strasser, H., 1917, "Lehrbuch der Muskel--und Gelenkmechanik", Band III, Berlin, Verlag von Julius Springer, Germany.

Trent, P.S., and P.S. Walker, 1975, "The Relationship Between the Instant Centers of Rotation, the Ligament Length Patterns, and the Ligament Tensions in the Knee", Orthopedics Research Society, Paper No. 33.

Trent, P.S., P.S. Walker, and B. Wolf, 1976, "Ligament Length Patterns, Strength and Rotational Axes of the Knee Joint", Clinical Orthopedics, 117, 263.

Veronda, D.R., and R.A. Westman, 1970, "Mechanical Characteristics of Skin Finite Deformation", Journal of Biomechanics, 3, 111.

Viano, D.C., C.C. Culver, R.C. Haut, J.W. Melvin, M. Bender, R.H. Culver, and R.S. Levine, 1978, "Bolster Impacts to the Knee and Tibia of Human Cadavers and An Anthropomorphic Dummy", Proceedings of the Twenty-Second Stapp Car Crash Conference, Society of Automotive Engineers, Inc. Warrendale, Pa.

Walker, P.S., and J.V. Hajek, 1972, "The Load-bearing Area in the Knee Joint", Journal of Biomechanics, 5, 581.

Wang, C.J., P.S. Walker, and B. Wolf, 1973, "The Effects of Flexion and Rotation on the Length Patterns of the Ligaments of the Knee", Journal of Biomechanics, 6, 587.

Wang, C.J., and P.S. Walker, 1974, "Rotary Laxity of the Human Knee Joint", Journal of Bone and Joint Surgery, 56-A, 161.

Warren, L.F., J.L., Marshall, and F. Girgis, 1974, "The Prime Static Stabilizers of the Medial Side of the Knee", Journal of Bone and Joint Surgery, 56-A, 665.

Wells, K.F., 1971, Kinesiology, W.B. Saunders Co., Philadelphia.

Wismans, J., and P.J. Struben, 1977, "De Drie-Dimensionale Geometrie van een Menselijk Knie Gewricht", Report WE 77-01, Department of Applied Mechanics, Mechanical Engineering, Eindhoven University of Technology, The Netherlands.

Wisemans, J., 1980, A Three-Dimensional Mathematical Model of the Human Knee Joint, Dissertation, Eindhoven University of Technology, Eindhoven, The Netherlands.

Wismans, J., F. Veldpaus, J. Janssen, A. Huson, and P. Struben, 1980, "A Three-Dimensional Mathematical Model of the Knee-Joint", Journal of Biomechanics, 13, 677.

☆U.S GOVERNMENT PRINTING OFFICE 1982 559-007 6019